United States
Environmental Protection
Agency

Office of Water
(4601)

EPA 815-R-98-005
August 1998

EPA

Empirically Based Models for Predicting Chlorination and Ozonation By-Products: Trihalomethanes, Haloacetic Acids, Chloral Hydrate, and Bromate

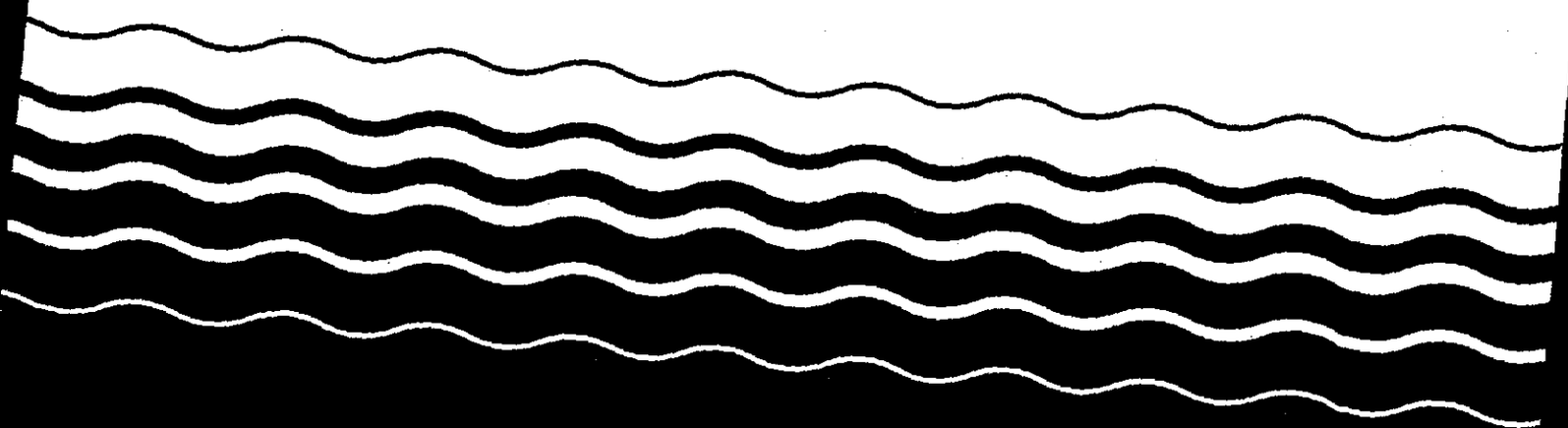

EPA-815-R-98-005
August 1998

EMPIRICALLY BASED MODELS FOR PREDICTING CHLORINATION AND OZONATION BY-PRODUCTS: TRIHALOMETHANES, HALOACETIC ACIDS, CHLORAL HYDRATE, AND BROMATE

By:

Gary Amy, Mohamed Siddiqui,
Kenan Ozekin, Hai Wei Zhu, and Charlene Wang

University of Colorado at Boulder

Number CX 819579

Project Officers:

James Westrick and Hiba Shukairy
Office of Ground Water and Drinking Water
U.S. Environmental Protection Agency
Cincinnati, Ohio

August 1998

DISCLAIMER

The information in this document has been funded wholly or in part by the United States Environmental Protection Agency under Cooperative Agreement CX 819579 with the University of Colorado. It has been subjected to the Agency's peer and administrative review, and it has been approved for publication as an EPA document. Mention of trade names or commercial products does not constitute endorsement or recommendation for use.

FORWARD

This study was initiated to help the U.S. EPA, as a regulatory agency, and U.S. water utilities, inpacted by EPA drinking water regulations, promulgate and meet new standards on disinfection by-products (DBPs). At the time of this report, new/revised regulations were being proposed for both chlorination and ozonation by-products. Most of the analytical and modeling work was performed over the 1994-1995 time frame.

ABSTRACT

This report documents a series of statistically-based empirical models for use in predicting disinfection by-products (DBPs) formed during water treatment disinfection using chlorine or ozone. The models were created and calibrated from a data base derived from bench-scale assessment of a diverse range of waters, including both surface water and groundwater sources. Each model was formulated through multiple step-wise regression analysis, and as such takes the form of a multiple regression equation. After formulation and calibration, model simulations were performed to compare predicted versus measured values, employing the same data base used in model calibration. Finally, each model was validated by using data derived from the literature. The relevant chlorination DBPs include haloacetic acids (HAAs), trihalomethanes (THMs), and chloral hydrate (CH). Bromate (BrO_3^-) served as the ozonation DBP of interest. For both chlorination and ozonation, dissolved organic carbon (DOC) has been used to represent the organic DBP precursor, while bromide ion (Br^-) represents the inorganic precursor. For the chlorination DBPs, model variables includes water quality conditions; DOC, Br^-, pH, and temperature; and treatment conditions represented by chlorine dose and reaction time. The models permit prediction of total HAAs (within the context of this report, total HAAs, THAA, corresponds to sum of six species, HAA_6), total THMs, and CH as a function of time; supplementary models permit estimates of each of the four THM species, and each of six HAA species. These models have been further adapted to apply to either raw/untreated waters or (alum or iron) coagulated waters where DBP precursor removal can be realized; of particular note is the ability of these models to account for coagulation induced changes in DBP reactivity. Bromate models permit predictions based on water quality conditions; DOC, Br^-, pH, and temperature; and treatment conditions reflected by transferred ozone dose and contact time. Supplementary models were developed to describe corresponding ozone decay as a function of time. All of these models presented herein are intended for use by both utilities and regulators. They can be used to assess the impact of changing water quality conditions on DBP formation, or to evaluate the impact of treatment modifications.

CONTENTS

FIGURES

TABLES

LIST OF ACRONYMS

BCAA	Bromochloroacetic Acid
Br^-	Bromide (Ion)
BrO_3^-	Bromate
CH	Chloral Hydrate
$CHBr_3$	Bromoform
$CHBrCl_2$	Bromodichloromethane
$CHBr_2Cl$	Dibromochloroacetic Acid
$CHCl_3$	Chloroform
Cl_2	Chlorine
DBAA	Dibromoacetic Acid
DBPs	Disinfection By-Products
DCAA	Dichloroacetic Acid
D/DBP	Disinfectants/ Disinfection By-Products (Rule)
DOC	Dissolved Organic Carbon
F	F-Statistic
HAAs	Haloacetic Acids
HAA_6	Sum of TCAA + DCAA + MCAA + DBAA + MBAA + BCAA
HAA_5	Sum of TCAA + DCAA + MCAA + DBAA + MBAA
MBAA	Monobromoacetic Acid
MCAA	Monochloroacetic Acid
MCLs	Maximum Contaminant Levels
O_3	Ozone
r	Simple Correlation Coefficient
R	Multiple Correlation Coefficient
SEE	Standards Error of Estimate
SSE	Sum Squares Error
TCAA	Trichloroacetic Acid
THAA	Total HAAs (corresponding to HAA_6 in this report)
THMs	Trihalomethanes
TOC	Total Organic Carbon
TTHM	Total THMs
UVA	UV Absorbance (@ 254 nm)
α	Significance
ϕ	Reactivity Coefficient

SECTION 1

INTRODUCTION

A number of past efforts have focused on development of predictive trihalomethane (THM) models for systems using chlorine. Most of the THM models developed have been based on raw/untreated waters as opposed to waters treated for precursor removal. Less work has been done in developing predictive models for other chlorination by-products such as haloacetic acids (HAAs) and chloral hydrate (CH), as well as ozonation by-products such as bromate (BrO_3^-) and bromoform.

The major objective of this research was to develop empirical models to define: (i) the kinetics of disinfection by-product (DBP) formation during chlorination, with additional emphasis on DBPs beyond THMs, (ii) the kinetics of chlorination DBP formation in waters subjected to treatment for DBP precursor removal, and (iii) the kinetics of brominated DBP formation during ozonation, with an emphasis on bromate.

As part of the Disinfectants/Disinfection By-Products (D/DBP) Rule Cluster, EPA regulations have been proposed with new restrictive maximum contaminant levels (MCLs) for total THMs and sum of five HAA species (HAA_5) of 80 and 60 ug/L (0.08 and 0.06 mg/L), respectively; these may be further lowered to 40 and 30 ug/L (0.04 and 0.03 mg/L) as part of a second stage of the regulations. It is possible that CH may also be regulated at a later time. Moreover, all utilities with a total organic carbon (TOC) of greater than 2 mg/L (at the point of first disinfectant application) must evaluate implementation of enhanced coagulation for precursor removal. Thus, there is a strong need for models capable of predicting THMs and HAAs, with a particular need for models relevant to coagulated waters. EPA has also proposed a MCL of 10 ug/L for bromate. Given the increasing use of ozone, there is a need for predictive models to assess potential control options such as pH depression.

BACKGROUND

Empirically-based THM prediction models have been developed (Amy, et al., 1987a; Amy et al., 1987b) which presently form the basis for EPA and AWWA sponsored efforts to develop overall DBP formation models. Whereas these original models described the chlorination of raw/untreated water, other efforts (Chadik and Amy, 1987; Moomaw et al., 1993) have attempted to address treatment effects on THM formation kinetics. Only modest progress has been made in modeling THM speciation (Chowdhury, et al., 1991). Recent work

(Siddiqui and Amy, 1993; Siddiqui et al., 1994) has focused on developing a quantitative understanding of ozonation by-products such as BrO_3^-.

Major deficiencies of existing models are: (i) there has been little work on chlorination DBPs other than THMs, (ii) only limited work has been done to describe how treatment (e.g., coagulation, adsorption, ozonation) affects THM (and other chlorination DBP) formation, and (iii) little progress has been made in modeling the kinetics of ozonation by-products.

In summary, existing empirical models can provide accurate predictions of the formation of THMs in chlorinated waters as a function of reaction time. However, these models have been largely based on raw/untreated waters; when they have been applied to treated waters, it is often assumed that the character of the precursor remaining after treatment is the same as that found in the raw water. Our knowledge of the formation kinetics of DBPs other than THMs, as well as ozonation DBPs such as BrO_3^-, is sparse. Even less is understood about THM and DBP speciation in general and, more specifically, treatment effects on speciation.

RESEARCH OBJECTIVES

The major objectives of the proposed research were to: (i) develop predictive models for haloacetic acid formation kinetics (and speciation), trihalomethane formation kinetics (and speciation), and chloral hydrate formation kinetics during free chlorination; and (ii) develop a predictive model for bromate formation kinetics during ozonation. A secondary objective is to ascertain how DBP precursor removal, with an emphasis on coagulation, affects the formation kinetics of haloacetic acids, trihalomethanes, and chloral hydrate, and the speciation of haloacetic acids and trihalomethanes.

DATA BASE AND MODELS

A range of natural waters was selected to reflect a diversity of sources, including surface waters and groundwaters. These waters were studied within bench-scale assessments of chlorination and ozonation; chlorination studies were augmented by coagulation studies to appraise DBP precursor removal. A large and robust data base was developed for statistical analysis and modeling.

In this report, we present statistically-based predictive models for predicting bromate formation kinetics during the ozonation of bromide-containing waters. Using the selected source waters, a bench-scale

parametric study was performed. The resultant data were statistically analyzed by multiple regression, yielding equations for use in predicting BrO_3^- as a function of ozone dose, bromide, dissolved organic carbon (DOC), pH, temperature, and reaction time; other variables investigated included ozone residual, ammonia, and alkalinity. Ozone residuals and corresponding ozone demands were also determined, with these data also analyzed to develop models of ozone decay.

We also present empirical models for predicting the formation of haloacetic acids (HAAs), trihalomethanes (THMs), and chloral hydrate (CH) in chlorinated drinking water, based on water quality parameters (DOC, pH, Br^-, temperature) and treatment parameters (Cl_2 dose, reaction time). (At the time of this research, the measurement of only six HAA species (HAA_6) out of a possible nine (HAA_9) was analytically possible; hence, models presented for total HAAs (THAA) actually correspond to HAA_6). These models were supplemented with models to predict HAA and THM speciation, with a particular emphasis on the influence of Br^- and DOC. Finally, the models were adapted to the arena of (alum or iron) coagulation, and its effects on chlorination DBP formation and speciation.

INTENDED MODEL USERS

The models developed through this work are intended to be used by utilities and regulators. The models have relevance in assessing how both water quality and treatment conditions affect the kinetics and extent of DBP formation. Users can assess the influence of changes in water quality conditions (e.g., DOC and/or bromide (Br^-)), and evaluate the effectiveness of changes in treatment conditions in reducing DBP formation. For chlorination DBPs, one can assess chlorine dose and contact time as treatment variables, along with coagulation for precursor removal. For ozonation DBPs (i.e., BrO_3^-), one can assess how the ozone dose and contact time associated with a contactor translate into bromate formation, and the effectiveness of potential control options such as pH depression and ammonia addition.

SECTION 2

EXPERIMENTAL METHODS AND PROCEDURES

This chapter highlights the key analytical methods and experimental procedures used in generating the chlorination by-product and ozonation by-product data bases. Emphasis is placed on measurement of DBPs, non-routine parameters affecting their formation, and protocols used in the bench-scale assessments.

ANALYTICAL METHODS

Haloacetic Acids (HAAs)

We measured HAA_6, consisting of trichloroacetic acid (TCAA), dichloroacetic acid (DCAA), monochloroacetic acid (MCAA), dibromoacetic acid (DBAA), monobromoacetic acid (MBAA), and bromochloroacetic acid (BCAA). The extraction of haloacetic acids was based on EPA method 552 which involves an acidic, salted medium extracted with ether (MTBE). The method requires that the samples be acidified to a pH of less than 0.5 prior to extraction with ether so that the HAAs are not in their dissociated form. Prior to extraction and GC analysis, the compounds were derivatized (esterified) with diazomethane to produce methyl ester derivatives which are more amenable to GC analysis. A Hewlett Packard 5890 gas chromatograph (GC) with an electron capture detector (ECD) was used with a DB-5 megabore column. A typical HAA chromatogram is shown in Figure 2.1.

Trihalomethanes (THMs)

The extraction of chloroform ($CHCl_3$), dichlorobromomethane ($CHCl_2Br$), dibromochloromethane ($CHClBr_2$), and bromoform ($CHBr_3$) was accomplished by liquid-liquid extraction with MTBE using a modification of EPA method 551. Sodium sulfate was used to decrease the solubility of ether in water and to increase the partitioning of THMs into the solvent phase. The sample bottles were filled and sealed in such a way as to ensure that there was no head space. Method 551 also permits simultaneous extraction and measurement of chloral hydrate (CH). A Hewlett Packard 5890 GC with an ECD was used with a DB-1 megabore column. A typical THM and CH chromatogram is shown in Figure 2.2.

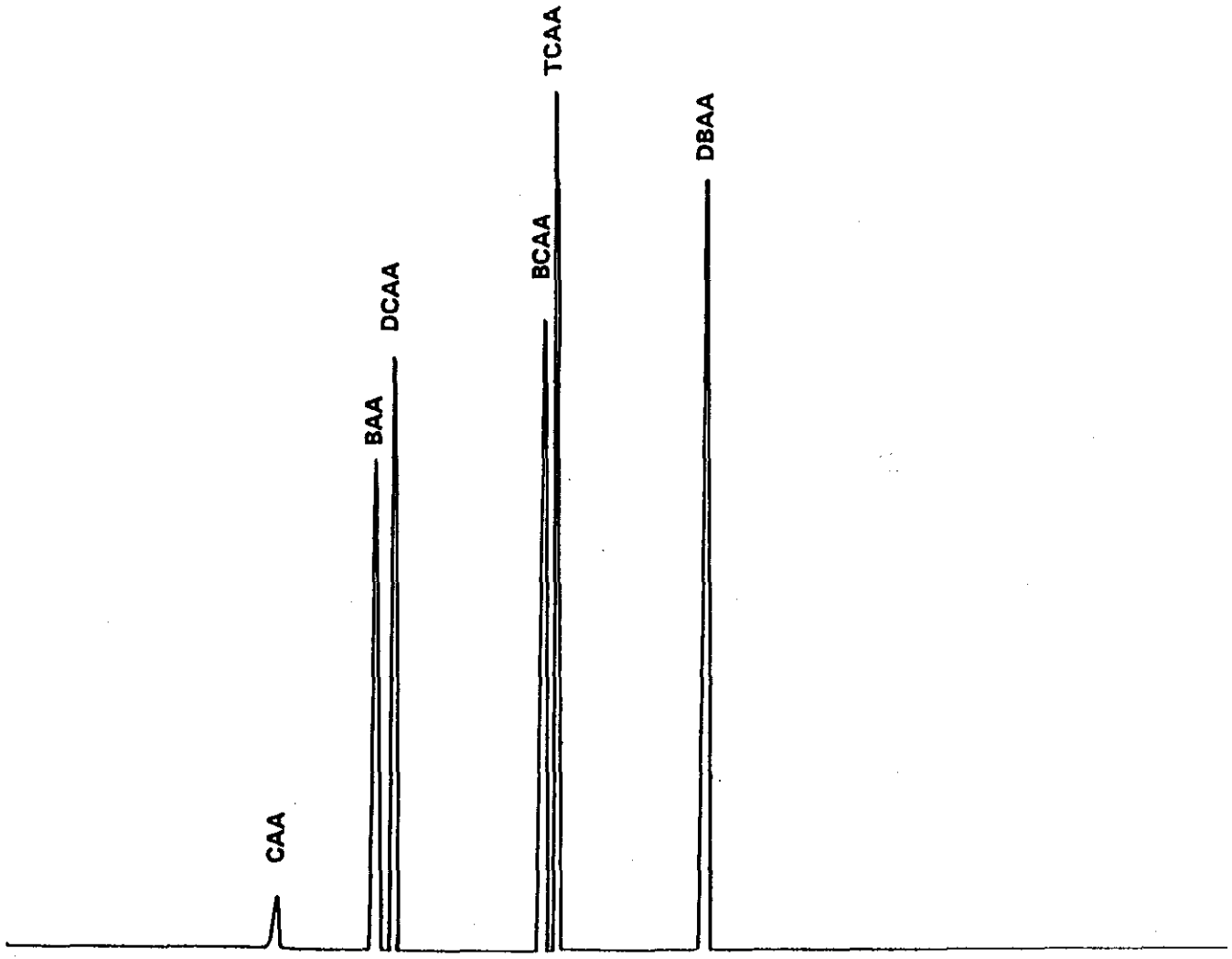

Fig. 2.1 Typical GC Chromatogram Showing HAA Species Peaks

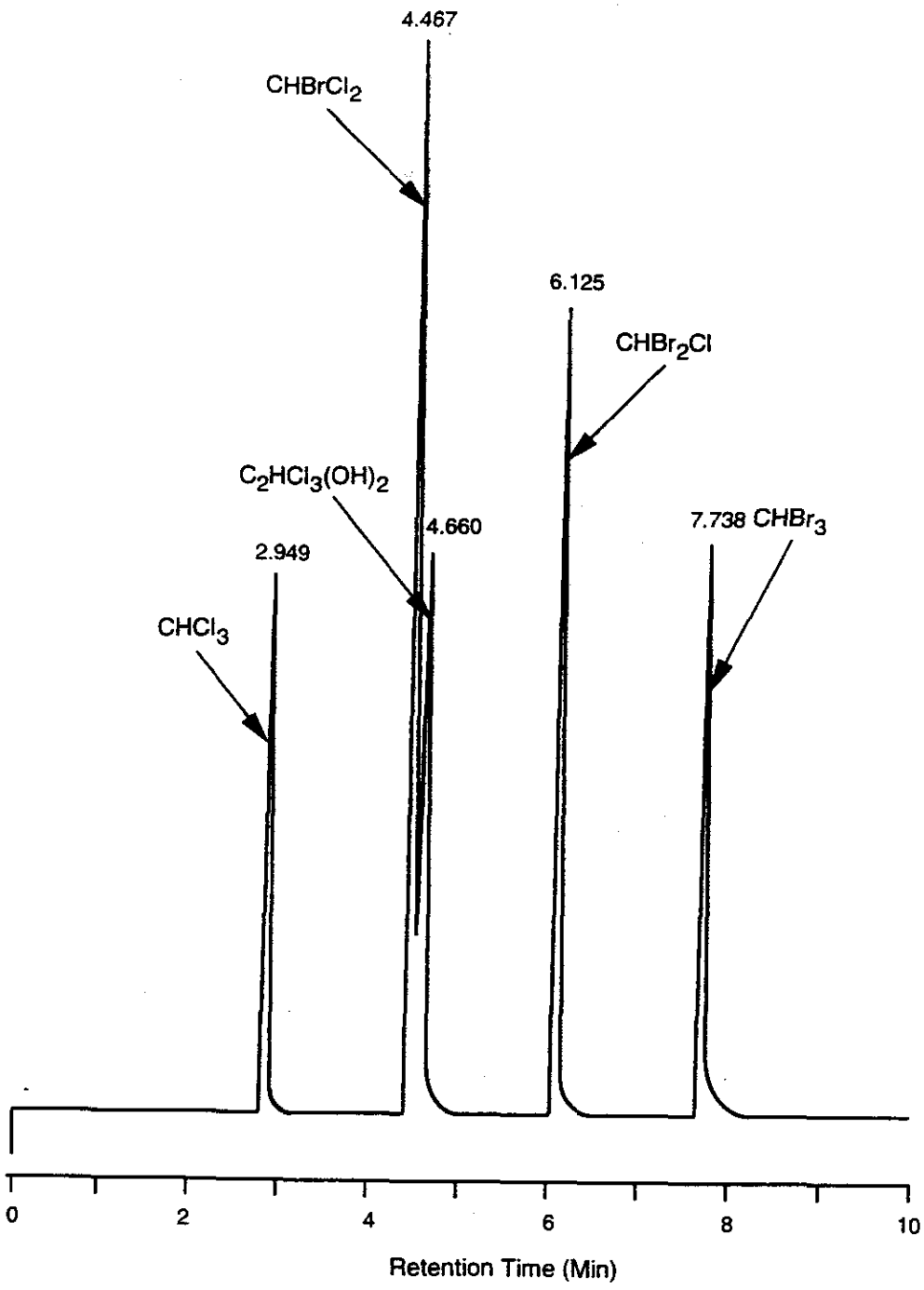

Figure 2.2 Typical GC Chromatogram Showing THM Species and Chloral Hydrate Peaks

Bromide (Br^-) and Bromate (BrO_3^-)

Br^- and BrO_3^- ion measurements were accomplished by ion chromatography (IC) using a Dionex 4500i series system coupled with A1-400 software and an IonPac AS9-SC column (EPA method 300). For bromide ion, a 2.0 mM carbonate/0.75 mM bicarbonate eluent was used in conjunction with a flow rate of 2 mL/min and a sample size (injection volume) of 100 uL. For bromate ion, a 40 mM borate/20 mM hydroxide eluent was used; the minimum detection limit at the time of this research was 2 ug/L. For samples with high chloride ion content, a silver cartridge was used to remove chloride ions prior to IC analysis for BrO_3^-. Conductivity detector response was almost perfectly linear ($r^2 \geq 0.99$) for standards ranging from 25 to 500 ug/L Br^-/L and from 5 to 50 ug/L BrO_3^-/L. Typical chromatograms for bromide and bromate are shown in Figures 2.3 and 2.4, respectively. Calibration curves for bromide and bromate are shown in Figures 2.5 and 2.6, respectively.

Total Organic Carbon (TOC) and Dissolved Organic Carbon (DOC)

TOC was measured using the combustion infrared method as described in Method 5310 B (Standard Methods) with a Shimadzu TOC-5000 analyzer fitted with an autosampler. Samples were filtered through a pre-washed 0.45 ìm nylon membrane filter in order to operationally define DOC. Samples were sparged to remove inorganic carbon after acidification to pH ≤ 2.

UV Absorbance

UV measurements at 254 nm were made using a Shimadzu UV/VIS 160 spectrophotometer and a 1-cm quartz cell. Analysis was conducted at ambient pH (typically 6 to 8). To minimize interferences caused by particulate matter, samples were filtered as described above with respect to TOC/DOC analyses.

Free Ammonia

Ammonia measurements were performed with an ammonia ion-selective electrode using Method 4500-NH_3 F (Standard Methods, 17th edition, 1989).

pH

pH was measured with a pH meter using Method 4500-H^+ as described in Standard methods, 17th Edition (1989).

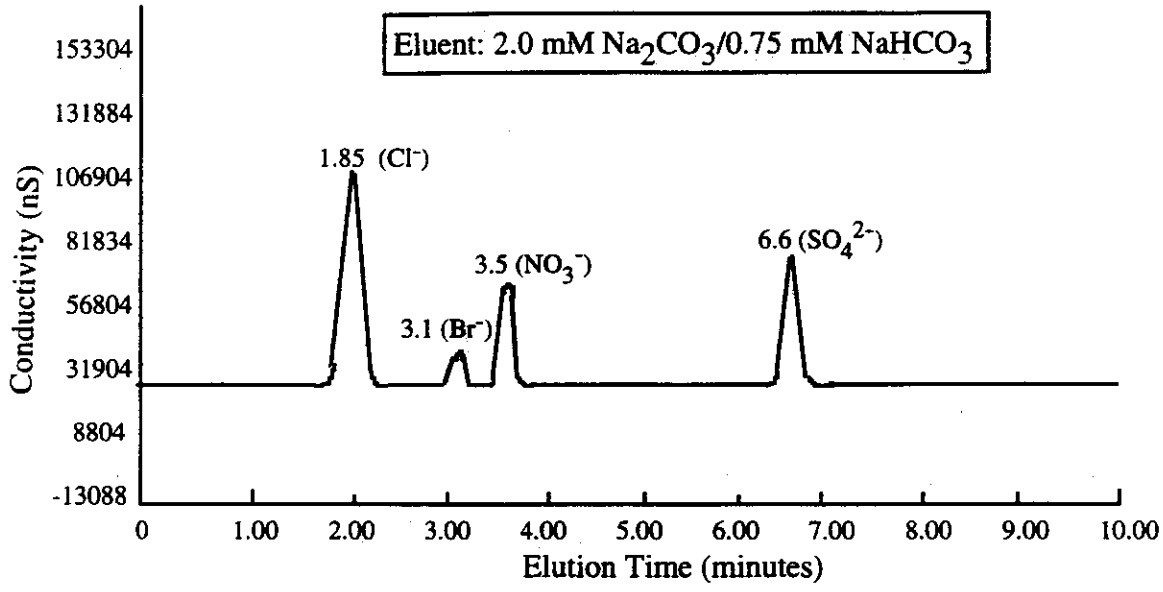

Figure 2.3. Typical IC Ion Chromatogram for Bromide Ion (Br^-).

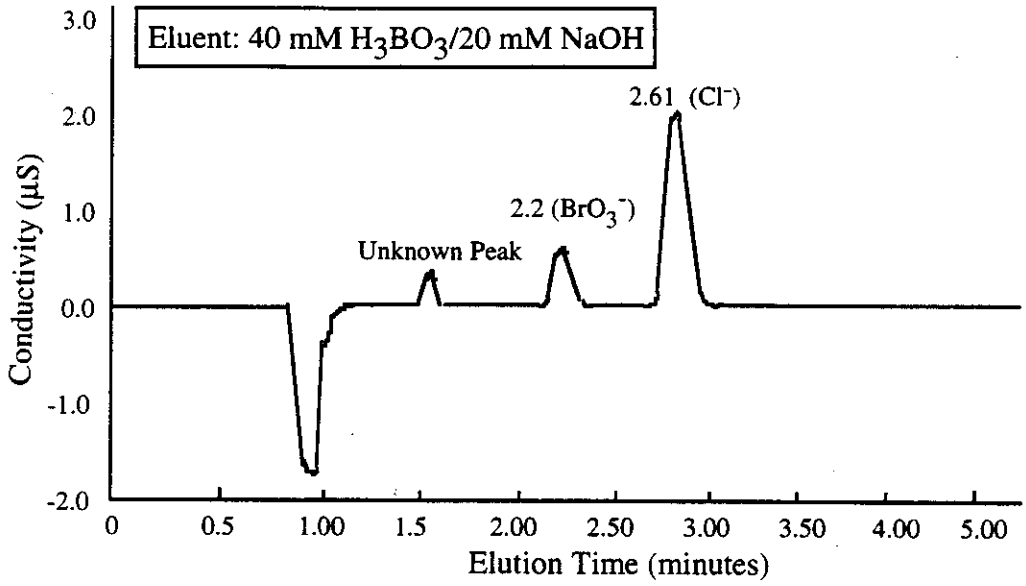

Figure 2.4. Typical IC Ion Chromatogram for Bromate Ion (BrO_3^-).

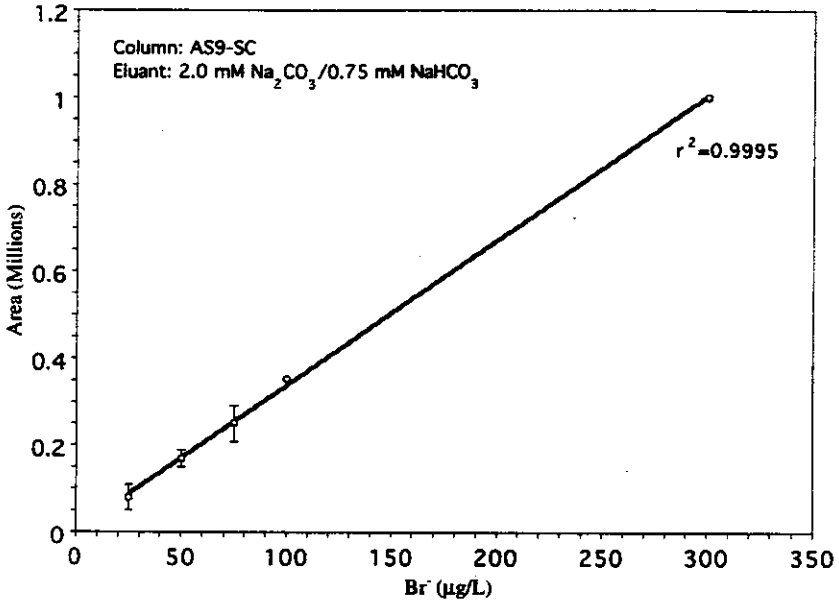

Figure 2.5. Calibration Curve for Bromide Ion.

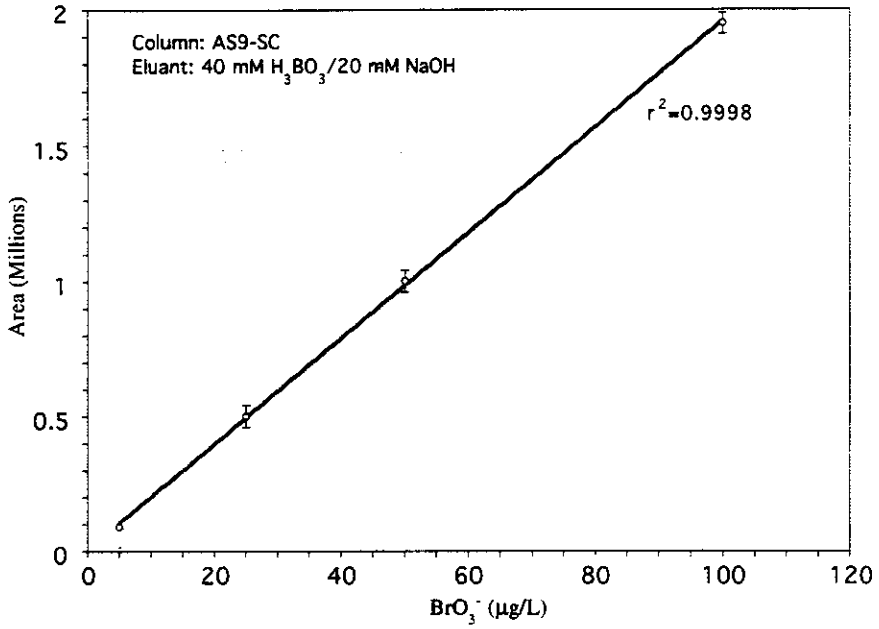

Figure 2.6. Calibration Curve For Bromate Ion.

Alkalinity

Alkalinity analyses were conducted by titration using method 2320 as described in Standard Methods, 17th edition (1989).

Turbidity

Turbidity was measured with a turbidity meter using method 2130 as described in Standard Methods, 17th edition (1989).

Residual Ozone

Ozone residuals were measured using Method 4500-03 A, the indigo trisulfonate method, as described in Standards Methods, 17th Edition (1989).

Free and Total Chlorine

Both free and total chlorine residuals were measured by using Method 4500-Cl, the DPD method, as described in Standard Methods, 17th edition (1989). Chlorine demand was calculated by the difference between the applied dose and the measured residual.

ANALYTICAL QUALITY CONTROL

Quality assessment is the process of using external and internal quality control measures to determine the quality of the data produced in this research. It includes such items as performance evaluation samples, laboratory intercomparison samples and internal quality control samples. Internal quality control includes recovery of known additions, analysis of externally supplied standards, analysis of reagent blanks, calibration with standards, and analysis of duplicates.

Minimum detection limits or minimum reporting limits (MRLs) were determined by spiking a series of concentrations in high purity water and in source waters examined. The least concentration which was detected above the noise level was assigned as the minimum reporting level of that contaminant. This is an average of several injections. A strict preventive maintenance program was in force to reduce instrument malfunctions, maintain calibration, and to reduce downtime. The minimum reporting levels/detection limits for each of these parameters are summarized in Table 2.1.

Table 2.1 Minimum Reporting Levels (MRLs).

Analyte	MRL	Units	Method
$CHCl_3$	0.6	ug/L	EPA551
$CHCl_2Br$	0.5	ug/L	EPA551
$CHClBr_2$	0.5	ug/L	EPA551
$CHBr_3$	0.3	ug/L	EPA551
CH	0.5	ug/L	EPA551
MCAA	1.2	ug/L	EPA552
DCAA	1.0	ug/L	EPA552
TCAA	1.5	ug/L	EPA552
MBAA	0.5	ug/L	EPA552
DBAA	0.7	ug/L	EPA552
BCAA	1.5	ug/L	EPA553
Cl_2	0.1	mg/L	4500-Cl*
Br^-	5.0	ug/L	EPA300
BrO_3^-	2.0	ug/L	EPA300
O_3	0.05	mg/L	4500-O3*
Alkalinity	10	mg/L	2320
Ammonia	0.1	mg/L	4500-NH3*

*Standard Methods

As a minimum, four different dilutions of the standards were measured when an analysis was initiated. Reportable analytical results are those within the range of the standard dilutions used. A minimum of 3-4 replicate analyses of an independently prepared sample having a concentration of between 5 and 50 times the method detection limit was used.

When most samples were found to have measurable levels of constituents being measured, selected analysis of duplicate samples was employed for determining precision; 10% or more of the samples were analyzed in duplicate. Precision, reported in terms of coefficients of variation (C.V.), is summarized in Table 2.2 for HAA species, Table 2.3 for THM species and chloral hydrate, and Table 2.4 for bromate (and ozone residual; simultaneous analysis of split samples).

Data reduction, validation, and reporting are the final features of a good QA program. The concentrations obtained were always adjusted for such factors as extraction efficiency, sample size, and background value. As part of the QC program, performance evaluation standards provided by the EPA were analyzed; these results are reported in Table 2.5.

BENCH-SCALE TESTING METHODS

Chlorination

The protocol for each sample aliquot involved dosing with free chlorine at a chlorine/DOC ratio (by weight) of 0.5-3.0 mg/mg and incubating for 2 to 168 hrs. A 1 mM phosphate buffer was used to maintain pH at either 6.5, 7.5, or 8.5. A water bath was used to maintain temperature at either 15, 20, or 25 °C. In the presence of ammonia, the chlorine dose was increased 7.6 times the concentration of ammonia-nitrogen to provide for breakpoint conditions.

The chlorine dosing solution was prepared from reagent-grade sodium hypochlorite and the stock chlorine solution was standardized by the DPD titrimetric method (Standard Methods, 1989). The chlorine concentration of the dosing solution was between 1.5-2.5 mg/ml, which is about 50 times the concentration needed in the samples, in order to minimize dilution errors in the reaction bottles. The chlorination experiments were conducted in glass serum bottles with teflon septa. The bottles were pre-soaked in 40% sulfuric acid for 24 hours and washed with phosphate-free detergent and rinsed with deionized water followed by NOM-free Milli-Q water. The serum vials were maintained headspace-free throughout the incubation period. After incubation, an aliquot of the sample was withdrawn for determination of chlorine residual (by DPD) and estimation of corresponding chlorine demand.

Table 2.2 Coefficients of Variation (C.V.) for HAA Species

Compound	Injection #	Area Count	s	% C.V.
CAA	1	29429		
	2	28093	668	2.3
BAA	1	326972		
	2	353867	13447	4.0
DCAA	1	803671		
	2	819567	7984	1.0
TCAA	1	2139600		
	2	2250493	55447	2.5
BCAA	1	1304154		
	2	1324020	9933	0.8
DBAA	1	867278		
	2	789652	38813	4.7
Compound	Extraction #	Area Count	s	% CV
CAA	1	8242		
	2	9150	454	5.2
BAA	1	67661		
	2	75671	4005	5.6
DCAA	1	243040		
	2	246181	1571	0.6
TCAA	1	1161904		
	2	1252530	45313	3.8
BCAA	1	516646		
	2	533885	8620	1.6
DBAA	1	311082		
	2	398810	43864	12.4

Table 2.3 Coefficients of Variation (C.V.) for THMs and Chloral Hydrate

Injection:

Compound	Injection #	Area Count	Concentration (µg/L)	s	% C.V.
$CHCl_3$	1	41842	6.697		
	2	41637	6.665	0.022627	0.339
$CHBrCl_2$	1	171257	6.911		
	2	168328	6.793	0.083438	1.218
$CHBr_2Cl$	1	136205	6.7130		
	2	137836	6.7930	0.056569	0.838
CHBr3	1	17684	2.198		
	2	17507	2.176	0.015556	0.711
CH	1	22335	0.9269		
	2	21871	0.9080	0.013364	1.46

Extraction:

Compound	Extraction #	Area Count	Concentration (µg/L)	s	% C.V.
$CHCl_3$	1	236217	41.14		
	2	248703	43.90	1.9516	4.590
$CHBrCl_2$	1	1307833	69.10		
	2	1304055	68.86	0.1697	0.246
$CHBr_2Cl$	1	191628	8.667		
	2	191758	8.673	0.004243	0.0490
CHBr3	1	8962	0.911		
	2	8874	0.902	0.006364	0.702
CH	1	203136	5.678		
	2	206052	5.759	0.057276	1.00

Table 2.4 Coefficients of Variation (C.V.)
For Bromate and Dissolved Ozone.

Analyte	Concentration	# of Measurements	C.V. (%)
Bromate	25 ug/L	2	0.91
Bromate	10 ug/L	3	1.11
Ozone*	0.50 mg/L	2	0.15
Ozone*	0.25 mg/L	3	0.25

*Based on replicate samples taken from true-batch reactor

Table 2.5. Performance Evaluation of EPA Samples (9/2/93)

Analyte	Sample #	Reported Value (ug/L)	EPA True Value (ug/L)
Trihalomethanes	1	107.1	83.8
$CHCl_3$	1	29.1	22.4
$CHBrCl_2$	1	32.9	26.4
$CHBr_2Cl$	1	22.4	17.9
$CHBr_3$	1	22.7	17.1
Chloral Hydrate	2	5.8	4.6
Haloacetic Acids	1	80.3	72.0
MCAA	1	7.4	11.8
MBAA	1	8.6	12.9
DCAA	1	17.7	15.4
DBAA	1	16.6	14.1
BCAA	1	30.4	17.8

Except THMs and BCAA, all results were found to be acceptable. All of the THM species were off by the same factor indicating a dilution error

Coagulation

The experimental plan for the coagulation experiments was designed to provide data on DOC removal using various alum ($Al_2(SO_4)_3 \cdot 18H_2O$) and ferric chloride ($FeCl_3 \cdot 6H_2O$) doses at ambient pH to remove 25-50% of the DOC. Reagent grade alum and ferric chloride were applied at different doses to each water at 20 °C. A conventional jar test apparatus was used with the following conditions: rapid mixing at 100 rpm for one minute, flocculation at 30 rpm for 30 minutes, and one hour of settling. Settled aliquots were filtered through prewashed 0.45 um filters for further analytical characterization.

Ozonation

Two modes of bench-scale ozone application were employed, semi-batch and true-batch. The general system consisted of an OREC O3V5-O (Ozone Research & Equipment Corporation) 0.25 lb/day generator and a 0.5 liter capacity glass reactor (washing bottle) with a glass frit. Ozone was generated from pure oxygen. Samples were buffered with a 1 mM phosphate buffer.

Semi-batch experiments involved continuous application of ozone and carrier gas admitted to a batch of water within the reactor. Contact time was controlled by the mass flow rate into the reactor; thus, applied dose (mg/L) was a function of mass application rate (mg/L-min) and application time (min). Applied and utilized ozone were determined by the classical iodometric method (Standard Methods, 1989). Typical transfer efficiencies were 30 to 60 %, with an average of 50 %. Dissolved ozone residuals (DO_3) present after cessation of ozone application were measured by the indigo method (APHA, 1989)

True-batch experiments were conducted by first generating a concentrated ozone stock solution (30-40 mg/L) by exhaustively ozonating Milli-Q water at 2 to 3 °C. Aliquots of the stock solution were then applied to a sample of raw water to achieve a final initial ozone concentration (typically in the range of 3 - 5 mg/L, confirmed by an initial measurement). In this procedure, the applied dose is equal to the transferred dose. Dilution of the raw water constituents by the ozone stock aliquot must be considered; dilution was generally kept to below 10 %. In contrast to the semi-batch ozonation where ozone is applied over a period of time (5 to 15 minutes) and reactions can occur during ozone application, true batch experiments involve introduction of 100% of the aqueous ozone to the system at time zero. The DO_3 measured after a designated reaction time corresponds to one point along the overall ozone decay curve.

STATISTICAL METHODS

For each of the DBP groupings; chlorination by-products including haloacetic acids, chloral hydrate, and trihalomethanes; and ozonation by-products represented by bromate; we employed a similar approach to statistical analysis. In our previous work, we used a comparable approach in both data base design and statistical analysis. It is noteworthy that our work on the development of THM prediction models (Amy, et al., 1987a; Amy et al., 1987b) presently forms the basis for EPA and AWWA sponsored efforts to develop overall DBP formation models. The following sections discuss how the data base was generated, and statistical approaches used in model development.

Data Base Design

While models and their formulations can sometimes have a theoretical basis in terms of a defined functionality (e.g., first order reaction kinetics), empirical models are often necessary if the underlying mechanisms are too complicated. When this approach is taken, caution must be exercised in terms of boundary conditions since empirical models are not intended to be severely extrapolated but rather used over limited ranges of the variables (generally corresponding to ranges within the data base). The requisite data base must be designed to reflect important variables, ranges of variables, and interactive effects among variables. Appropriate replication is needed to address experimental error so that true parameter effects can be discerned.

In developing a data base, one may choose a factorial design or an orthogonal design. A factorial design involves defining a comprehensive set of experiments within the context of a full matrix. For example, one could perform a 3 x 4 factorial design to study rats exposed to three different poisons and four different treatments. In this case, the complete matrix, without replication, would involve 12 experiments; initially, both factors would be considered of equal interest, and the possibility that the factors interact is acknowledged. In an orthogonal design, only one parameter is varied at a time while other parameters are maintained at some designated "baseline" condition. The above "rat experiment" would require only 6 experiments using this approach.

The problem with a full factorial design is the large number of experiments required. For example, in the ozonation by-product, chlorination by-product, and precursor-removal tasks being proposed herein, a full factorial design would require over ten- thousand cases (n). A compromise can be reached by

employing a partial (fractional) factorial design. An attribute of this approach is the ability to discern interactive effects.

One can argue that an orthogonal design corresponds to one version of a fractional (partial) factorial design. While an orthogonal design elucidates individual parameter effects, it does not identify interactive effects. One can argue, however, that an additional set of randomly selected experiments can help fulfill this need. On the other hand, a strictly random approach to identifying a fractional number of experiments from within a full factorial matrix leads to a "haphazard" data base in which both individual-parameter and interactive effects are difficult to discern.

We have elected to emphasize an orthogonal design with selected additional experiments performed to elucidate interactive effects; thus, in actuality, the data base reflects some movement toward a partial factorial design.

General Modeling Approach

Step-wise multiple linear and multiple nonlinear regression were used to develop models, with a given DBP (e.g., bromate) designated as the dependent variable (Y). Various independent variables (X) included both water quality (e.g., pH) and treatment variables (e.g., ozone dose).

We attempted to develop models assuming various mathematical formulations, including:

Linear Models: $Y = b_0 + b_1X_1 + \ldots$

Logarithmic Models: $\log Y = \log b_0 + b_1 \log X_1 + \ldots$
(equivalent to power function: $Y = 10^{bo}(X_1)^{b1} \ldots$)

Nonlinear Models: $Y = b_0 + b_1X_1^{b2} + \ldots$

A PC-based software package, SPSS (Statistical Package for the Social Sciences), was used for statistical analysis. Statistical fit was defined through examination of various statistical parameters, including SSE (sum squares error), SEE (standard error of estimate), the F statistic, significance (α), and R^2 (multiple coefficient of determination) for linear regression. A rigorous discussion of statistical parameters (SSE, etc.) associated with each model appears in three project-related references (Ozekin, 1994; Wang, 1994; and Zhu, 1995), representing three

dissertations/theses that evolved from, and were funded by, this cooperative EPA agreement.

Using SPSS, a correlation matrix was first developed to elucidate simple linear correlations between the dependent variable and each of the independent variables; and between the independent variables themselves. Such a matrix provides preliminary insight into the relative importance of the independent variables as well as co-linearity between them. Correlation matrices were also used to examine relationships between transformed variables (e.g., log Y vs log X).

"Step-wise" multiple regression places independent variables into the equation in order of their partial correlation coefficients with the dependent variable. Thus, the most important predictive parameters are identified in the process; this is important because it is advantageous to keep the number of predictor-parameters (each requiring an analytical measurement) to a minimum. Moreover, if two independent variables are themselves correlated, the most important parameter (based on its partial correlation coefficient) will be placed into the equation first and the partial correlation coefficient for the remaining parameter will be adjusted downward accordingly. Thus, using the stepwise approach, it is unlikely that two correlated independent parameters will be included in the final equation. A "tolerance" can be specified (e.g., ΔR^2) to dictate when stepwise inclusion ceases.

The above SPSS efforts correspond to model *calibration*. Subsequent model testing involved developing scatterplots of predicted versus measured values, as well as performing a sensitivity analysis to ascertain how predicted dependent-variable values responded to a range in specified values for each independent parameter. Model *validation* involved obtaining source waters other than those used in developing the equations to create additional data based on a random set of experimental conditions; model simulation was ascertained by comparing experimentally-derived kinetic curves (concentration versus time) versus predicted curves. We also evaluated the ability of the models to predict pertinent DBP data found in the literature. A key concern in model validation testing is the "robustness" of a model; i.e., its ability to make accurate predictions under extreme experimental conditions. In testing the "robustness" of a model, boundary conditions were also tested in terms of independent data taken from the literature.

Haloacetic Acid, Trihalomethane, and Chloral Hydrate Predictive Models

Step-wise multiple linear and multiple nonlinear regression were used to develop models with either total HAA (THAA), chloral hydrate (CH), or total THMs (TTHM) designated as the dependent variable (Y). Independent variables (X_i) included DOC (and/or UV absorbance), bromide concentration, pH, temperature, chlorine dose (and/or utilized chlorine), and reaction time. Moreover, we developed submodels to predict individual HAA species and THM species (Chowdhury, et al., 1991). As above, we examined linear models, logarithmic models, and nonlinear models.

HAA, THM, and CH Predictive Models Accounting for Precursor Removal

These "submodels" were similar in format to the raw/untreated water models discussed above for HAA and CH. Additional modeling features highlighted precursor reactivity, with delineation of a reactivity coefficient, ϕ, such that an adjustment of ϕ(DOC) can account for a different reactivity of the precursor (DOC) pool of material. A priori, it was expected that ϕ would likely range from 0 to 1.0 for coagulant-treated waters. Another important modeling consideration was the effect of an increased ratio (after coagulation) of Br^-/DOC on HAA and THM speciation. (Besides the Br^-/DOC ratio, The Br^-/Cl_2 ratio also affects speciation).

Bromate Predictive Models

As above, step-wise multiple linear and multiple nonlinear regression were used to develop models, with bromate formation designated as the dependent variable (Y). Independent variables (X) included DOC (and/or UV absorbance), bromide concentration, pH, temperature, ozone dose, and reaction time. Dissolved ozone residual (DO_3), ammonia, alkalinity, and peroxide were also considered as additional X_i parameters.

SECTION 3

SOURCE WATERS AND DATA BASE SUMMARY

The data base created through this research was derived from a broad range of natural waters acquired from throughout the United States. Single samples of twelve waters were obtained specifically as part of this EPA study. An additional four waters were obtained as part of a related study sponsored by the East Bay Municipal Utilities District (EBMUD). One additional water was obtained as part of an American Water Works Association Research Foundation (AWWARF) study. All water samples obtained (EPA and EBMUD) corresponded to raw/untreated aliquots of source waters used by operating water treatment plants under the jurisdiction of cooperating utilities. The sequence/ordering under which samples were obtained did not take into account any considerations of seasonality; thus, while they capture source-related differences, they do not reflect seasonal variations. The EPA sources included 10 surface waters and 2 groundwaters. The EBMUD sources were all surface waters while the AWWARF source was a groundwater. Of these twelve sources, eight (all surface waters) were evaluated within the coagulation part of this study. A total of thirteen waters, eight EPA waters (6 surface waters and 2 groundwaters), all four EBMUD waters, and the one AWWARF water, were evaluated as part of the ozonation part of this study. The EBMUD sources and the AWWARF source were only studied within the context of the ozonation component of the study. The specific waters evaluated and their abbreviation identifiers (used hereafter) are summarized below:

EPA Sources:

- Silver Lake (CO); SLW
- State Project Water (CA); SPW
- Brazos River (TX); BRW
- Susquehanna River (PA); SRW
- Burton Groundwater (MI); BGW
- Manhattan Groundwater (KS); MGW
- Harwood Mill Reservoir (VA); HMR
- Palm Beach Reservoir (FL); PBW
- Ilwaco Reservoir (WA); ISW
- Verde River (AZ); VRW
- Salt River (AZ); STW
- Sioux River (SD); SXW

EBMUD Sources:

- Pardee Reservoir (CA); EIS
- San Leandro Reservior (CA); ESL
- Bixler Reservoir/Mokelumne Aqueduct (CA); EWC
- San Pablo Reservoir (CA); EES

AWWARF Source:

- Teays Aquifer (IL); TYA

The geographical distribution of the source waters is portrayed in Figure 3.1. The EBMUD sources are all shown clustered in northern California. The EPA source shown in southern California actually reflects Sacramento River Delta Water transported via the California State Project to the Metropolitan Water District.

RAW/UNTREATED WATERS

Important characteristics of the raw/untreated source waters are shown in Table 3.1. It can be seen that the selected sources cover a wide range of important water quality characteristics. Here, both DOC and UVA serve as indices of (organic) DBP precursors present. The ratio of UVA/DOC, the specific absorbance, indicates the character of the precursor DBP material present; a higher ratio reflects a greater humic-substances content. Bromide, of course, represents the inorganic precursor whose collective action with the organic precursor is manifested in DBP formation. Based on a recent estimate of a national average of almost 100 ug/L (Amy et al., 1994), the ambient Br^- levels range from below to above average; it is important to note that ambient conditions represent the baseline condition for bromide within the orthogonal experimental matrix.

Background levels of ammonia are important insofar as they exert a free chlorine demand, and may impact bromate formation. The ambient pH conditions shown do nothing more than provide an indication of the actual pH levels expected under water treatment conditions; ambient pH was not part of the orthogonal matrix. Turbidity here is primarily important in terms of its effect on coagulation and its ability to remove DBP precursors. Alkalinity affects both the coagulation process as well as ozone chemistry; When water samples were adjusted to reflect the pH conditions specified in the orthogonal matrix, these adjustments were accompanied by changes in alkalinity.

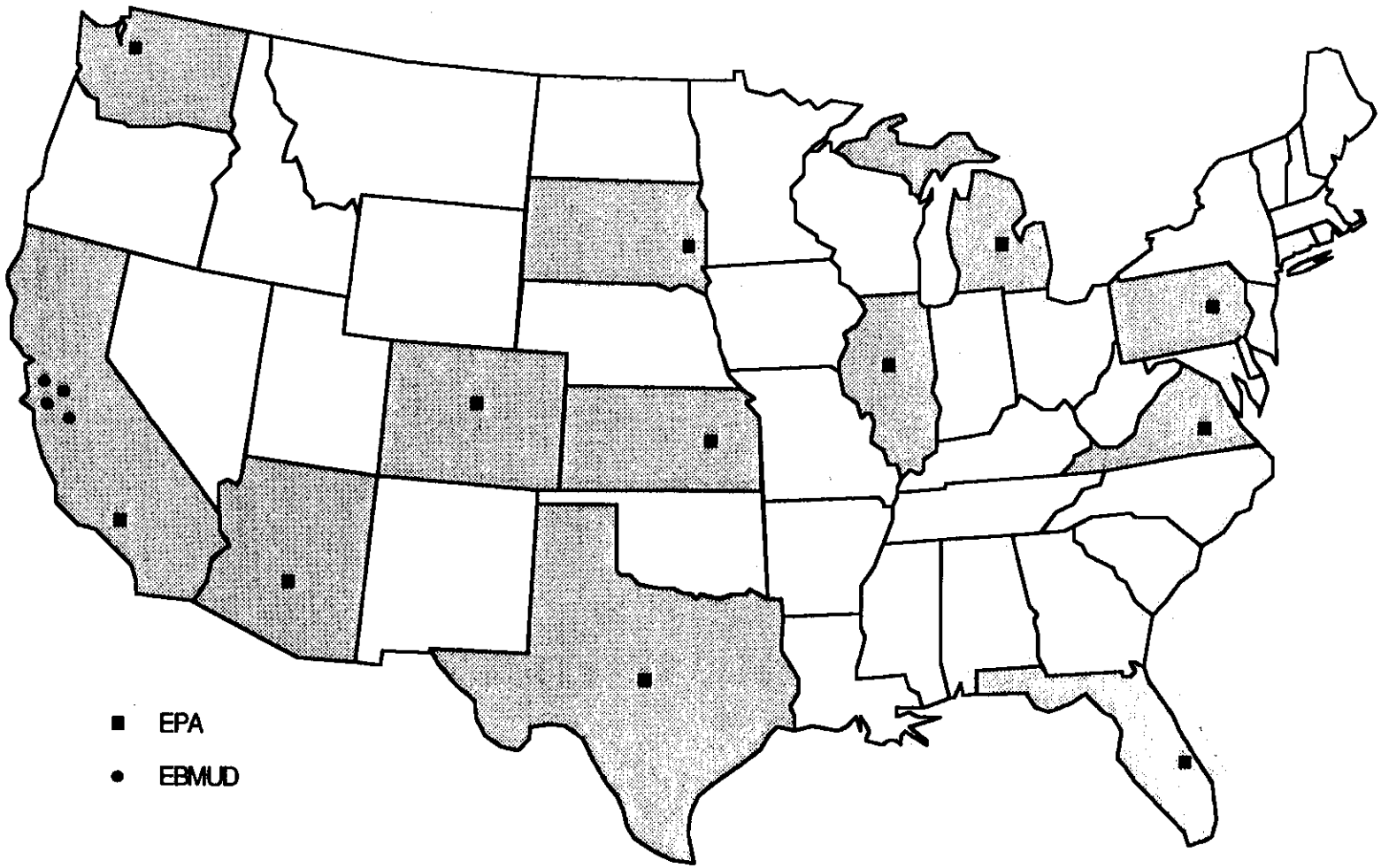

Figure 3.1 Location of Utilities/Source Waters.

Table 3.1 Source Water Characteristics: Raw/Untreated

Raw/Untreated

Water	Date	DOC (mg/L)	UVA (cm^{-1})	pH	NH_3-N (mg/L)	Alk (mg/L)	Bromide (µg/L)	Turbidity (NTU)
Sources Selected for EPA Study								
SLW	4/92	7.15	0.258	7.0	0.25	15	7	1.1
SPW	6/92	4.19	0.169	8.2	0.12	83	312	0.3
BRW	10/92	3.54	0.198	8.2	0.21	153	250	20.0
SRW	11/92	4.18	0.129	7.5	0.14	43	50	0.9
BGW	1/93	1.20	0.010	7.7	0.12	186	143	0.2
MGW	1/93	2.44	0.161	7.3	0.69	205	206	2.2
HMR	2/93	5.73	0.223	7.1	0.21	50	40	2.5
PBW	4/93	10.6	0.280	7.8	0.10	99	97	0.3
ISW	5/93	2.86	0.102	6.5	0.065	14	83	0.65
VRW	7/93	3.67	0.102	8.4	0.09	156	71	5
STW	6/93	4.36	0.099	8.2	0.145	140	54	20.0
SXW	7/28	10.55	0.318	8.1	0.25	248	68	0.94
EBMUD Sources								
EIS	3/93	6.3	0.24	6.4	0.11	142	90	6
ESL	3/93	5.1	0.14	7.8	0.05	185	28	3.1
EWC	3/93	2.1	0.04	8.6	0.00	44	7	1.3
EES	3/93	4.9	0.14	7.6	0.13	104	24	12
AWWARF Source								
TYA	2/93	3.0	0.12	8.6	0.79	330	90	1.0

The orthogonal matrices employed for the raw/untreated water, coagulated water, and ozonation work are summarized below (* = baseline condition):

Chlorination Conditions; Raw/Untreated Waters:

- DOC = ambient
- Cl_2/DOC = 0.5, 1.0*, 1.5, 2.0, and 3.0 mg/mg
- pH = 6.5, 7.5*, 8.5
- Temperature = 15, 20*, 25 °C
- Br^- = ambient*, amb. + 100 ug/L, amb. + 200 ug/L, amb. + 300 ug/L
- Time = 2, 12, 24, 48, 96, 168 hrs

Chlorination Conditions; Coagulated Waters:

- DOC = ambient
- Cl_2/DOC = 1 and 3 mg/mg
- pH = 7.5
- Temperature = 20 °C
- Br^- = ambient
- Time = 2, 12, 24, 48, 96, 168 hrs

Ozonation Conditions:

- DOC = ambient
- O_3/DOC = 0.5, 1.0*, 2.0 mg/mg (transferred)
- pH = 6.5, 7.5*, 8.5
- Temperature = 15, 20*, 25 °C
- Br^- = ambient*, amb. + 100 ug/L*, amb. + 200 ug/L
  (* = amb. or amb. + 100 ug/L for $Br^- > 80$ or ≤ 80 ug/L, respectively)
- Time = 1, 5, 10, 20, 30, 60 min
- NH_3/O_3 = 0*, 0.35, 0.50 mg/mg (addition)

COAGULATED WATERS

Screening experiments were performed to evaluate the removal of DBP precursors by alum or iron coagulation; experiments were done at ambient pH, with pH allowed to drift upon coagulant addition. The major objective was to determine a coagulant dose that would provide a targeted DOC reduction within the range of 25 to 50 %. Upon defining an appropriate dose, a larger batch of coagulated water was produced for assessment of chlorination by-products.

This targeted range was selected because it approximately encompasses the range of DOC removal expected at plants either optimized for turbidity removal as opposed to plants which practice enhanced coagulation. Draft Stage 1 of the D/DBP Rule specifies that plants with a TOC of greater than 2 mg/L must evaluate enhanced coagulation (EC). Required removals are specified as a function of initial TOC and alkalinity (a 3 x 3 matrix), with TOC removals ranging from 15 to 50 % (Step 1). If these removals are not attained, enhanced coagulation is defined by a "point of diminishing returns" corresponding to a ΔTOC/alum of 0.3 mg/L/10 mg/L (Step 2).

Figures 3.2 and 3.3 summarize the results of coagulation screening experiments. The graphs show DOC versus dose, DOC removal (%) versus dose, ΔDOC versus dose, and ΔDOC/Δdose versus dose. For comparative purposes, it can be seen that DOC removals observed in four of the eight waters reflected the attainment of enhanced coagulation by alum, based on the slope criterion and the assumption that DOC ≈ TOC.

In several cases, the targeted DOC reductions (% removal or point of diminishing returns) were not achieved over the range of doses evaluated, 0 to 100 mg/L. In these cases, a pragmatic selection of targeted dose was made. The final characteristics of coagulated waters are shown in Table 3.2 Selected coagulant doses ranged from 25 to 100 mg/L; iron provided slightly better DOC removal than alum. It is noteworthy that bromide was virtually conservative through the coagulation process.

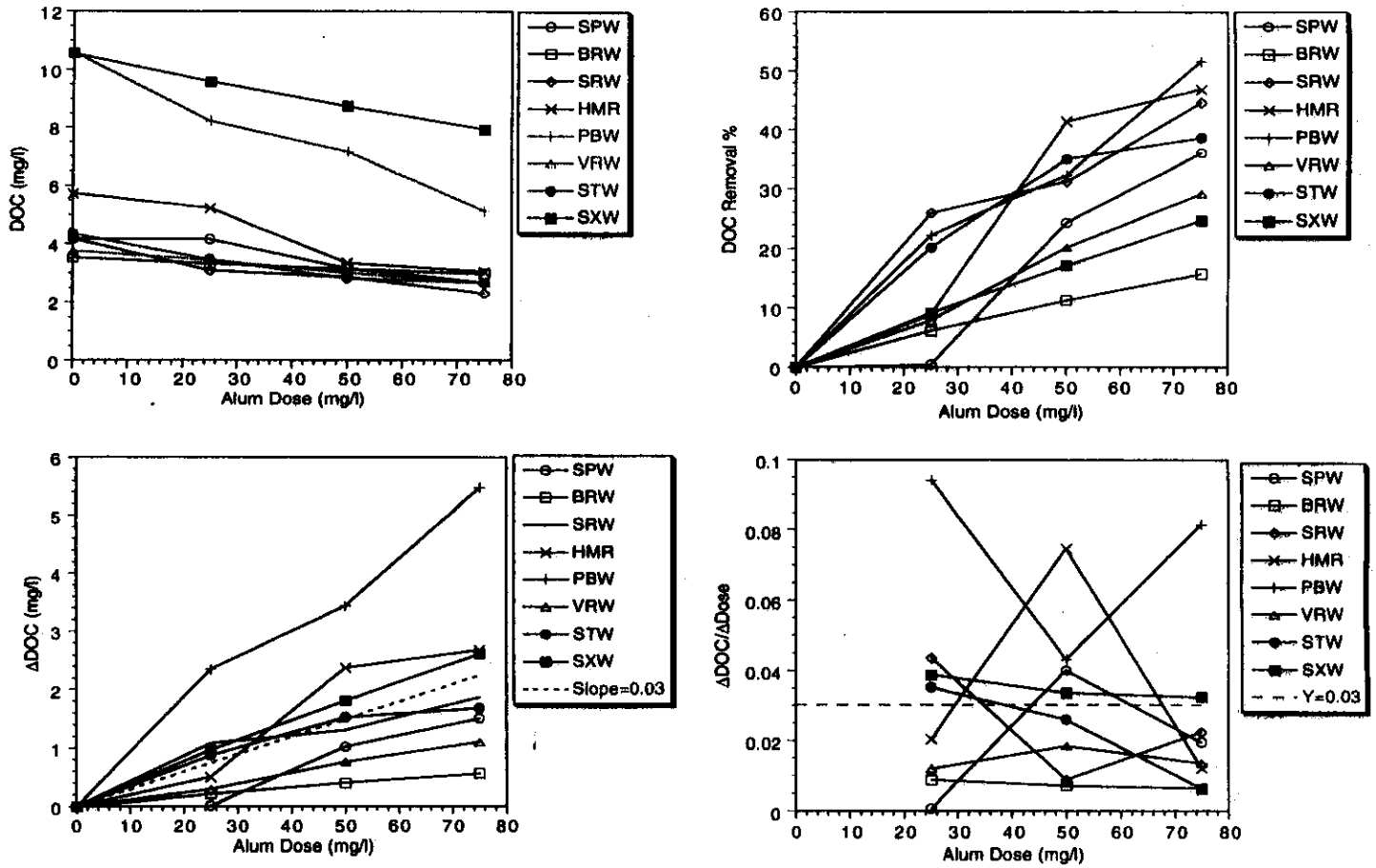

Figure 3.2 Result of Alum Coagulation Screening Experiments

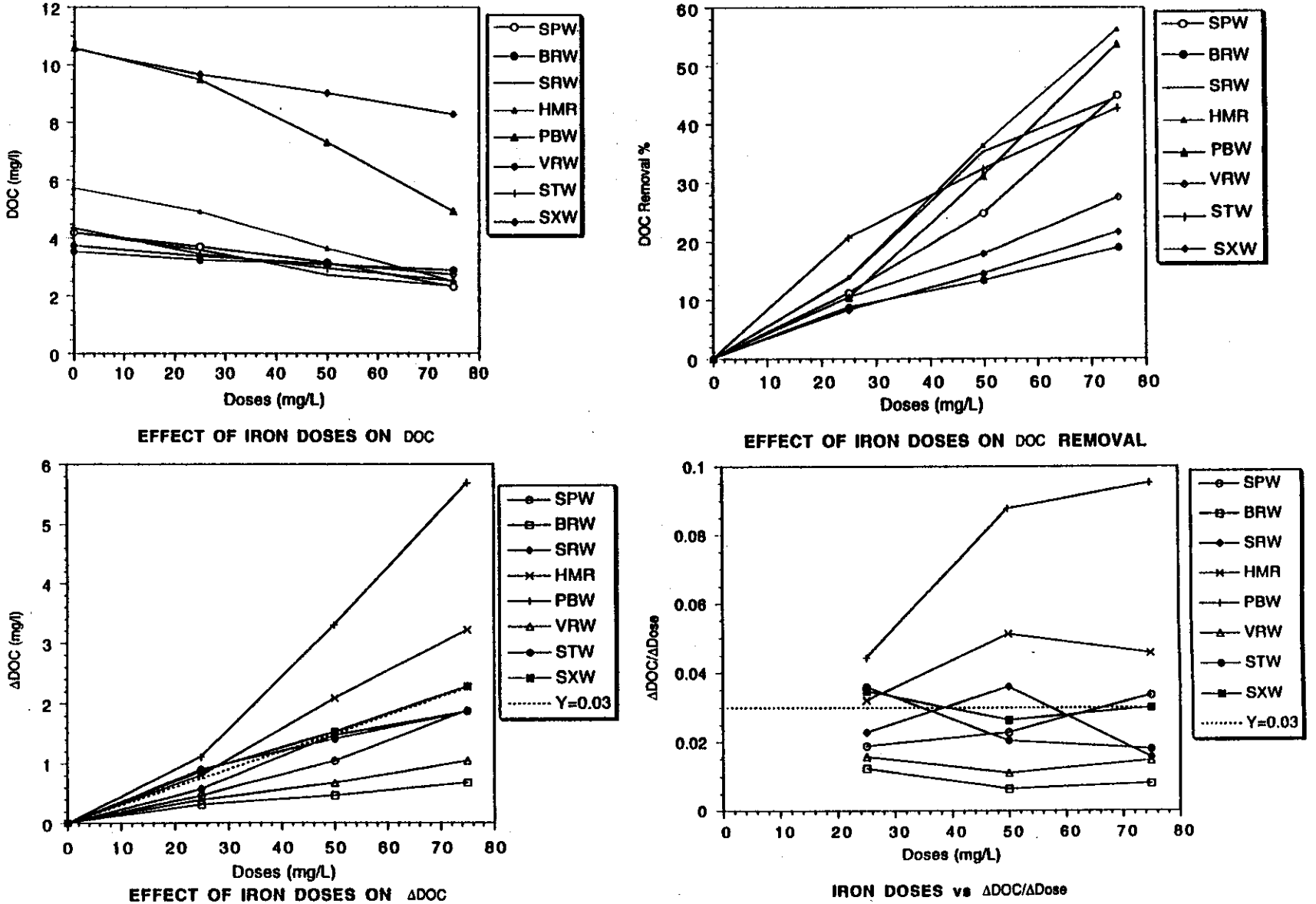

Figure 3.3. Results of Iron Coagulation Screening Experiments

Table 3.2. Coagulated Waters – Water Quality

After Coagulation

Water	Coagulant	Dose*	pH	DOC (mg/L)	NH_3-N (mg/L)	UVA (cm^{-1})	Bromide (µg/L)
SPW	Alum	70	7.4	2.61	0.05	0.115	306
	Iron	60	7.8	2.58	0.07	0.104	308
BRW	Alum	100	7.2	2.72	0.01	0.039	245
	Iron	100	7.2	2.63	0.01	0.055	245
SRW	Alum	65	6.8	2.56	0.03	0.030	45
	Iron	65	6.2	2.55	0.01	0.021	44
HMR	Alum	45	7.1	4.29	0.08	0.078	36
	Iron	45	7.0	4.23	0.10	0.108	37
PBW	Alum	100	7.8	4.60	0.05	0.075	n/a
	Iron	100	7.7	4.20	0.02	0.073	n/a
ISW	Alum	25	5.5	1.0	0.015	0.016	n/a
	Iron	25	4.8	1.03	0.055	0.039	n/a
VRW	Alum	75	7.4	2.56	0.06	0.051	n/a
	Iron	75	7.3	2.35	0.03	0.043	n/a
STW	Alum	50	7.5	2.91	0.11	0.080	n/a
	Iron	50	7.4	2.76	0.07	0.078	n/a
SXW	Alum	100	7.4	7.77	0.19	0.215	n/a
	Iron	100	7.5	7.63	0.21	0.196	n/a

* mg/L as $Al_2(SO_4)_3 \cdot 18H_2O$ or $FeCl_3 \cdot 6H_2O$.
n/a: not available.

SECTION 4

HALOACETIC ACID MODELS

There is a need to model both the formation of total haloactic acids (THAA) as well as that of haloacetic acid (HAA) species. (As previously mentioned, THAA corresponds to HAA_6 in this report). In addition, the effects of treatment (e.g., coagulation) on subsequent HAA formation after chlorination need to be elucidated through a model. The primary purpose of this chapter is to develop and present a modeling scenario for assessing the formation and control of HAAs when free chlorine is used as a disinfectant.

PARAMETERS AFFECTING HALOACETIC ACID FORMATION

Various water quality (pH, temperature, DOC, Br^-) and treatment conditions (Cl_2) affect the total yield, formation kinetics, and speciation of HAAs (Figures 4.1 and 4.2, 24-hour reaction time). Results of the effects of various parameters on the formation of total haloacetic acids (HAA_6) and individual HAA species are discussed under the following separate headings. Experiments were conducted to evaluate the effect of pH, temperature, bromide, DOC, chlorine dose, and reaction time on the formation of THAA and HAA species. These were later augmented by experiments to assess the effects of coagulant type and dose on HAA formation. Lower levels of HAAs were observed in the BGW source, a result attributable to the relatively low DOC and UV absorbance which represent HAA precursors. The highest levels of HAAs were generally found in the SXW source, a result attributable to the relatively high DOC, and the highest UV absorbance observed.

Effect of pH

Figure 4.1 shows pH effects on THAA formation for two source waters (HMR and MGW). For one source, a trend of decreasing THAA with increasing pH is seen; for another source, pH-dependent variations appear to be minor. These differences can be attributed to the effects of pH on individual HAA species (Figure 4.2). TCAA was found to strongly decrease on increasing the pH from 6.5 to 8.5 while DCAA and CAA (not shown in figure) were relatively insensitive to pH. Brominated species, BCAA, DBAA and BAA, all slightly increased with pH. Reckhow and Singer (1984) observed a decrease in TCAA and DCAA with increasing pH. There is little information in the literature on pH effects on brominated HAA species. Since TCAA and DCAA are the dominant species, a model which captured their behavior will also likely do well in simulating THAA (i.e., HAA_6).

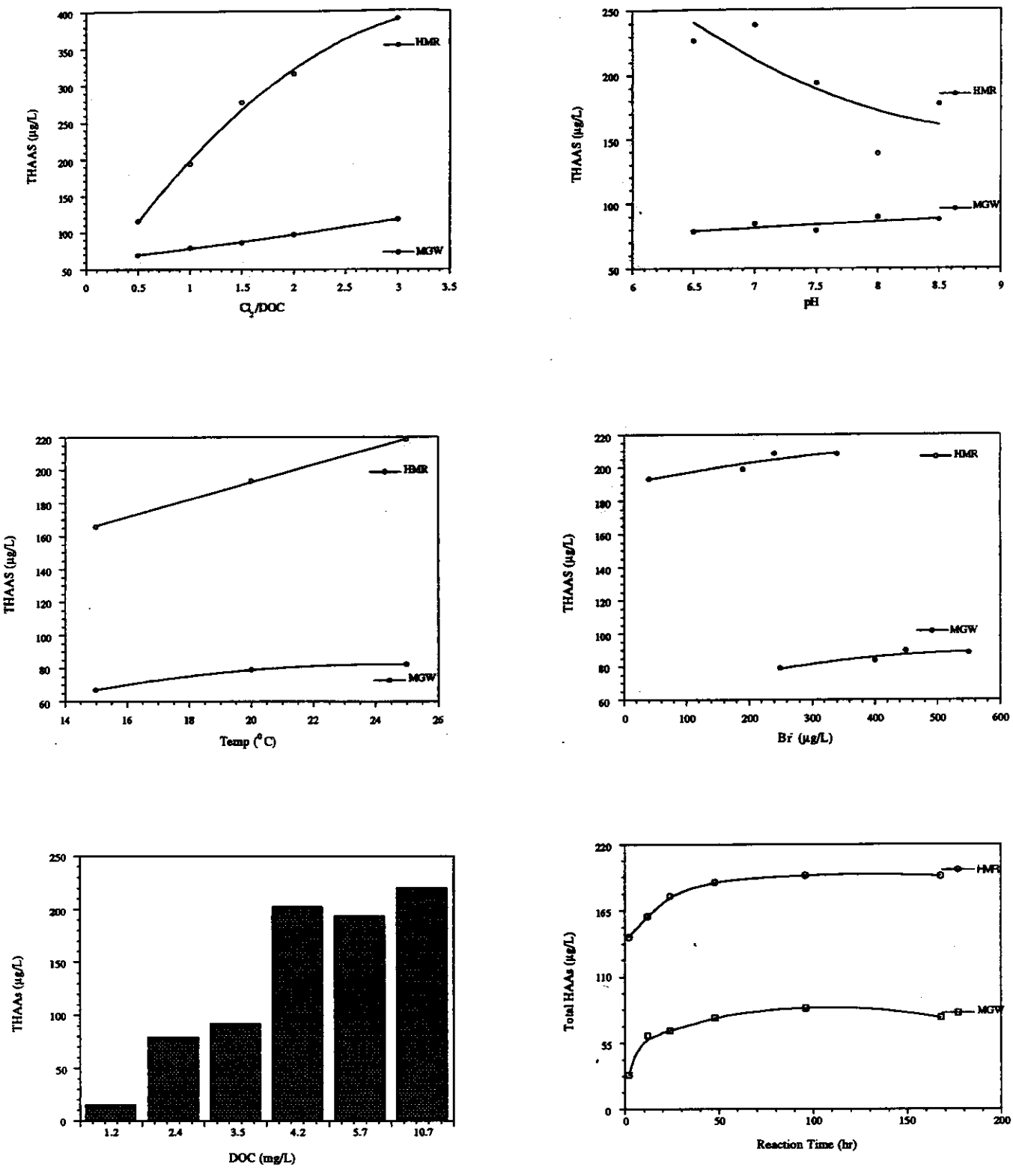

Fig. 4.1 Individual Parameters Effects on THAA Formation: Effects of Chlorine, pH, Temperature, Bromide, DOC, and Reaction Time (all other parameters held at baseline conditions).

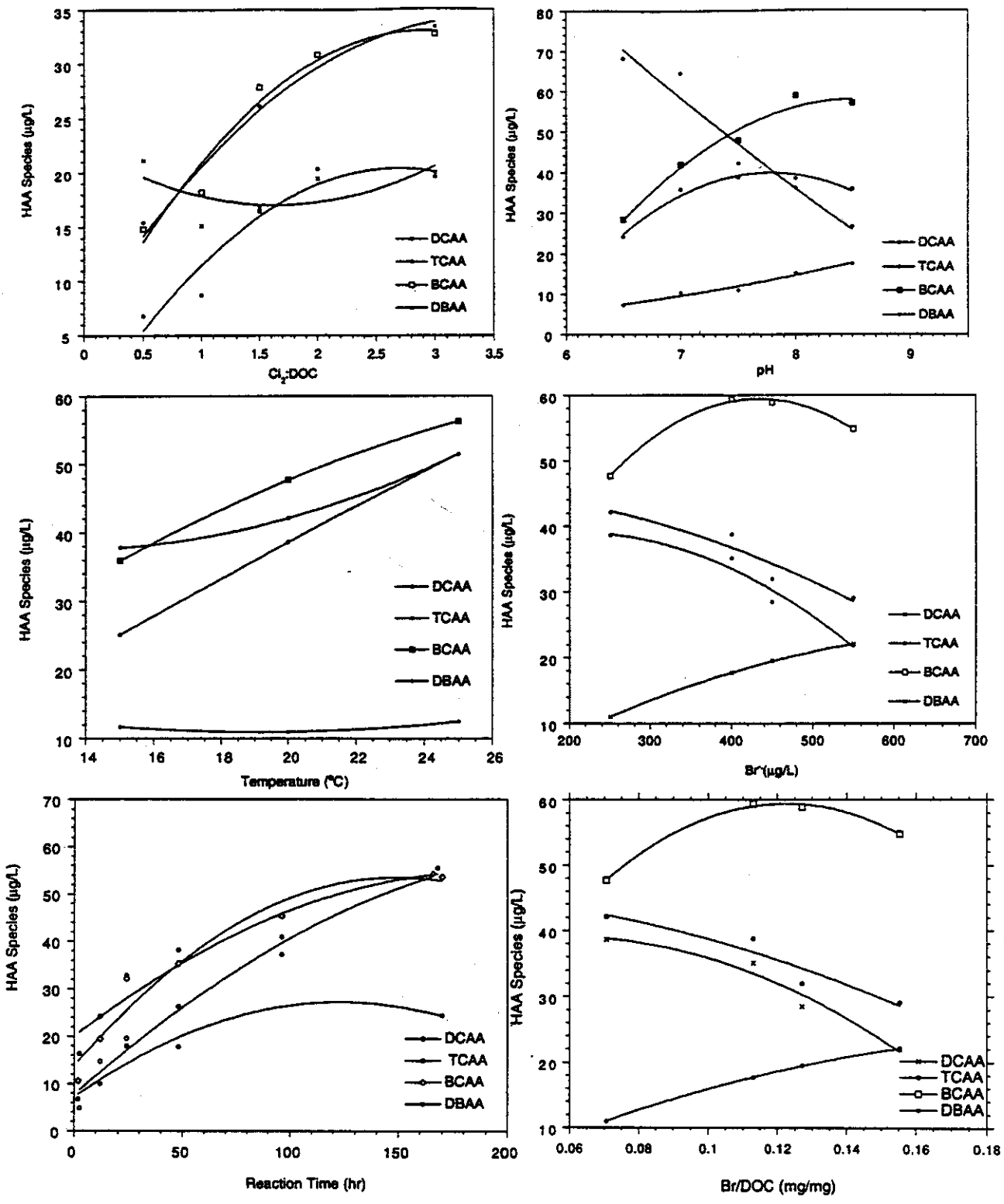

Fig. 4.2. Individual Parameter Effects on HAA Species Formation in BRW Sources: Effects of Chlorine, pH, Temperature, Bromide and Reaction Time (All other Parameters held at Baseline Conditions)

Effect of Bromide Concentration

The concentration of bromide ion (Br^-) in raw water is a significant factor in the formation of chlorination by-products such as HAAs and THMs. Br^- influences both the total HAA (and THM) yield as well as the species distribution of chlorine and bromine-containing species when chlorine oxidizes the bromide to hypobromous acid (HOBr), which behaves in a manner analogous to hypochlorous acid (HOCl). Generally, HOBr is a more effective substitution agent than HOCl, while HOCl is a better oxidant (reduced to Cl^-). HOCl is typically present in great abundance relative to HOBr. Bromine substitution is favored over chlorine, even when chlorine is present in large excess compared with the Br^- concentration. Any bromide present will immediately be oxidized by $HOCl/OCl^-$ to $HOBr/OBr^-$. Therefore, if the $HOBr/OBr^-$ is involved in an oxidation/reduction reaction and Br^+ is reduced to Br^-, it would be rapidly reoxidized to Br^+ with an excess of $HOCl/OCl^-$.

Increased amounts of BCAA and DBAA were generally observed at higher levels of bromide; TCAA and DCAA decreased with an increase in bromide concentration (Figure 4.2). The net effect was generally a slight increase in THAA with increasing Br^-, as shown in Figure 4.1.

The ratio of Br^-/DOC for raw and treated waters is the parameter most influential in controlling HAA speciation basis (the ratio of an individual species to THAA). As the ratio increases, a shift to the more bromo-substituted species occurs (Figure 4.2). The ratio of Br^-/Cl_2 also influences speciation.

Effect of Chlorine Dose

The specific chlorination conditions affect both THAA and HAA species formation. In our work, we have elected to represent chlorination conditions through the use of the Cl_2/DOC ratio, whereby chlorine dose is normalized to precursor (DOC) concentration.

Figure 4.1 shows the results of changing the chlorine to DOC ratio on THAA formation for two source waters. Figure 4.2 shows effects on individual HAA species. The results are supported by the concept that an increase in the chlorine dose results in a decrease in the total bromide to chlorine ratio (Br^-/Cl_2), and as the chlorine dose increases, speciation shifts to the chloro-substituted species, THAA-Cl.

Effect of Temperature

Figure 4.1 shows the impact of temperature on THAA formation. The formation of TCAA, DCAA, and BCAA increased with temperature (Figure 4.2); for DBAA, however, temperature had little effect.

Effect of DOC

A clear correlation was found between THAA and DOC (Figure 4.1). Speciation effects were manifested through the Br^-/DOC ratio. UVA provided poorer precursor-related prediction capabilities than DOC; because of the colinearity between DOC and UVA, UVA was excluded from the HAA models.

Effect of Reaction Time

The kinetic response of THAAs is a composite effect of the effects of reaction time on individual HAA species. Figure 4.1 shows the results of THAAs formation for two source waters, at varying chlorination reaction times. These THAA kinetic curves show the composite effects of individual HAA species which form at different rates (Figure 4.2). Generally, DBAA increases to a plateau after about 24 hours and then remains relatively unchanged thereafter. TCAA, DCAA, and BCAA all increase continuously with increasing reaction time up to about 168 hours. The formation of the bromo-substituted DBPs (THAA-Br) is generally faster than the chloro-substituted (THAA-Cl). Thus, for the first 24 hours, the molar ratio of the THAA-Br to the THAA-Cl increases with increasing reaction time. After 24 hours, there is a decrease in this ratio, indicating a shift to the chloro-substituted species at longer reaction times.

GENERAL MODELING APPROACH

When the various parameters are considered, either molar or weight based THAAs could theoretically serve as the dependent variable whereas the other variables, in either their arithmetic or transformed state, represent candidate independent variables. The general strategy adopted in formulating each model was to include single terms to describe the roles of precursor, chlorine, temperature, pH, bromide, and reaction time in the formation of THAAs. In keeping with the philosophy of developing chemically rational models, both molar based as well as weight based THAAs were used as the dependent variable THAA. However, as will be shown, little difference was observed between statistical correlations based on molar versus weight basis THAAs.

TOTAL HALOACETIC ACIDS; RAW/UNTREATED WATERS

This section focuses on models which can predict the formation of haloacetic acids in untreated source waters subjected to chlorination. Their relevance is severalfold: (i) they can be used to assess pre-chlorination; (ii) they can be used to describe the behavior of treated waters where little precursor removal has taken place (e.g., direct filtration); (iii) they can be used to predict treated-water response if treated-water precursor levels are input, even though treatment affects both the amount and type of precursor; and (iv) they provide a framework for further modeling efforts where changes in the amount and *type* of precursor can be incorporated.

As part of the model building (formulation) process, the individual effects of independent parameters on total HAAs were evaluated singularly. Selected results were previously discussed and shown in Figure 4.1. Such evaluations were used to help define individual parameter effects, linear versus nonlinear effects, and positive versus inverse effects. Positive effects were exerted by Cl_2 dose, temperature, Br^- concentration, DOC (or UVA), and reaction time. The effects of pH were generally mixed, presenting additional modeling challenges.

Engerholm and Amy (1983) found that formation of chloroform from humic acid under different conditions of pH, temperature, precursor concentration, and chlorine-to-DOC ratio could be accurately modeled by transforming both dependent and independent variables into logarithmic forms. This approach was later modified to account for bromide effects (Amy et al., 1987). These previously successful modeling approaches were applied to the entire data base (738 cases). Ordinary step-wise multiple-regression modeling efforts highlighted the logarithmic (power-function) formulation shown below:

$$Y = 10^{bo}(X_1)^{b1}(X_2)^{b2} \qquad (4.1)$$

where Y = dependent variable,

X_i= independent variable(s), and b_i= regression coefficient(s)

The power-function models, expressed on both a weight and molar basis, derived from the above approach are shown in Table 4.1. (The THAA models correspond to HAA_6; HAA_5 predictions can be based on summation of predictions for each of the five relevant individual species). Perusal of the model exponents indicates the positive influence of chlorine dose, temperature, reaction time and DOC (DOC was selected over UVA because UVA did not provide better correlations), inverse influence of pH, and the mixed influence of bromide. These trends are generally consistent with the results shown in Figure 4.1. While pH affects individual species differently, its effects on

Table 4.1 PREDICTIVE RAW-WATER MODELS FOR HALOACETIC ACIDS (HAA): TOTAL HAAS (THAA) AND HAA SPECIES

Weight-Based (μg/L) Models:

$[CAA] = 0.45\ t^{0.009}\ [Temp]^{0.573}\ pH^{-0.279}\ [Cl_2]^{0.397}\ [DOC]^{0.173}\ [Br^-]^{0.029}$
$R^2 = 0.14 \quad F = 18 \quad \alpha \leq 0.0001 \quad N = 738$

$[BAA] = 6.21 \times 10^{-5}\ t^{0.090}\ [Temp]^{0.707}\ pH^{0.604}\ [Cl_2]^{0.754}\ [DOC]^{-0.584}\ [Br^-]^{1.100}$
$R^2 = 0.43 \quad F = 83 \quad \alpha \leq 0.0001 \quad N = 738$

$[DCAA] = 0.30\ t^{0.218}\ [Temp]^{0.465}\ pH^{0.200}\ [Cl_2]^{0.379}\ [DOC]^{1.396}\ [Br^-]^{-0.149}$
$R^2 = 0.83 \quad F = 589 \quad \alpha \leq 0.0001 \quad N = 738$

$[TCAA] = 92.68\ t^{0.180}\ [Temp]^{0.299}\ pH^{-1.627}\ [Cl_2]^{0.331}\ [DOC]^{1.152}\ [Br^-]^{-0.229}$
$R^2 = 0.87 \quad F = 821 \quad \alpha \leq 0.0001 \quad N = 738$

$[BCAA] = 5.51 \times 10^{-3}\ t^{0.220}\ [Temp]^{0.379}\ pH^{0.581}\ [Cl_2]^{0.522}\ [DOC]^{0.463}\ [Br^-]^{0.667}$
$R^2 = 0.76 \quad F = 360 \quad \alpha \leq 0.0001 \quad N = 738$

$[DBAA] = 3.59 \times 10^{-5}\ t^{0.095}\ [Temp]^{0.380}\ pH^{-0.001}\ [Cl_2]^{0.673}\ [DOC]^{-1.086}\ [Br^-]^{2.052}$
$R^2 = 0.77 \quad F = 370 \quad \alpha \leq 0.0001 \quad N = 738$

$[THAA] = 9.98\ t^{0.178}\ [Temp]^{0.387}\ pH^{-0.655}\ [Cl_2]^{0.443}\ [DOC]^{0.935}\ [Br^-]^{-0.031}$
$R^2 = 0.87 \quad F = 831 \quad \alpha \leq 0.0001 \quad N = 738$

Molar-Based (μmoles/L) Model:

$[THAA] = 4.58\ t^{0.156}\ [Temp]^{0.431}\ pH^{-0.613}\ [Cl_2]^{0.665}\ [DOC]^{0.639}\ [Br^-]^{-0.062}$
$R^2 = 0.80 \quad F = 490 \quad \alpha \leq 0.0001 \quad N = 738$

Symbols are defined below:
[CAA]; [BAA]; [DCAA]; [TCAA]; [BCAA]; [DBAA]: Individual HAA Species (μg/L);
[THAA]: Total Haloacetic Acids (μg/L or μmoles/L);
t: Reaction Time (hr); $2 \leq t \leq 168$
[Temp]: Temperature (°C); $15 \leq [Temp] \leq 25$
pH: $6.5 \leq pH \leq 8.5$
$[Cl_2]$: Applied Chlorine Dose (mg/L), $2.11 < [Cl_2] < 26.4$
[DOC]: Dissolved Organic Carbon (mg/L; $1.2 < [DOC] < 10.7$
$[Br^-]$: Concentration of Br^- (μg/L); $7 \leq [Br^-] \leq 560$
$[Cl_2]$:[DOC]: $0.5 \leq [Cl_2]:[DOC] \leq 3$ (mg/mg)

*Source Waters: SLW, SPW, BRW, SRW, BRW, MGW, BGW. PBW,ISW, STW, and SXW

THAAs was generally inverse for most source waters (MGW being an exception). Other researchers (Miller and Uden, 1983) have shown that pH, chlorine dose, and reaction time have similar effects on TCAA and DCAA formation similar to those observed herein. With a few exceptions, the model exponents generally reflect the expected effects of individual parameters. Expressed in this form, the log-log model cannot yield a negative prediction. Moreover, if t (reaction time), DOC, Cl_2 dose, pH, Temp, or Br^- are zero, the multiple-parameter power function predicts a THAA of zero. For the parameters t, DOC, Cl_2, these zero predictions strictly conform to theoretical expectations. For pH and temperature, it is also reasonable to expect that, as these conditions approach zero, THAA formation should likewise approach zero. On the other hand, the presence of bromide is not absolutely necessary for TCAA, DCAA, and CAA formation; other modelers have used a (Br + 1) term, which reduces to unity, to compensate for this limitation. On the other hand, vitually all natural waters contain some level of bromide (Amy et al., 1994). If necessary, the user can simply input a very low value (5 ug/L) near the detection limit to represent a zero level for bromide.

Internal Data Simulation

Each of the models has been subjected to a model testing procedure by plotting predicted versus measured values, employing the same data base used in model calibration. These data simulations (internal validations) are summarized in Figures 4.3, 4.4 and 4.5. Figures 4.3 and 4.5 describe weight and molar based THAA models, respectively. Figure 4.4 is an elaboration of Figure 4.3 whereby individual-source data sets are shown. A perfect model simulation would be represented by a plot with an intercept of zero, a slope of 1.0, and a r^2 of 1.0; a positive intercept suggests overprediction at lower concentrations while a slope of less than 1.0 generally suggests underprediction. With the entire data base (738 cases), regressions of predicted versus measured THAAs were conducted for the log-log models on both a weight and molar basis, yielding r^2 values of 0.90 and 0.91, respectively; intercepts of 2.57 and 0.056, respectively; and slopes of 0.97 and 0.98, respectively. These results are portrayed in Figure 4.3 and 4.5. Although correlations between measured and predicted values are very good, the intercepts and slopes of the above regression equations indicate that all of the models showed a tendency to overpredict at low THAA levels and underpredict at high THAA levels. Thus, the models tend to overpredict for conditions least conducive to THAA formation and underpredict for conditions most conducive to THAA formation. Figure 4.4 shows the identification of individual-source data points used in the testing of the weight basis model, allowing observation of sources which conform to or diverge from predictions.

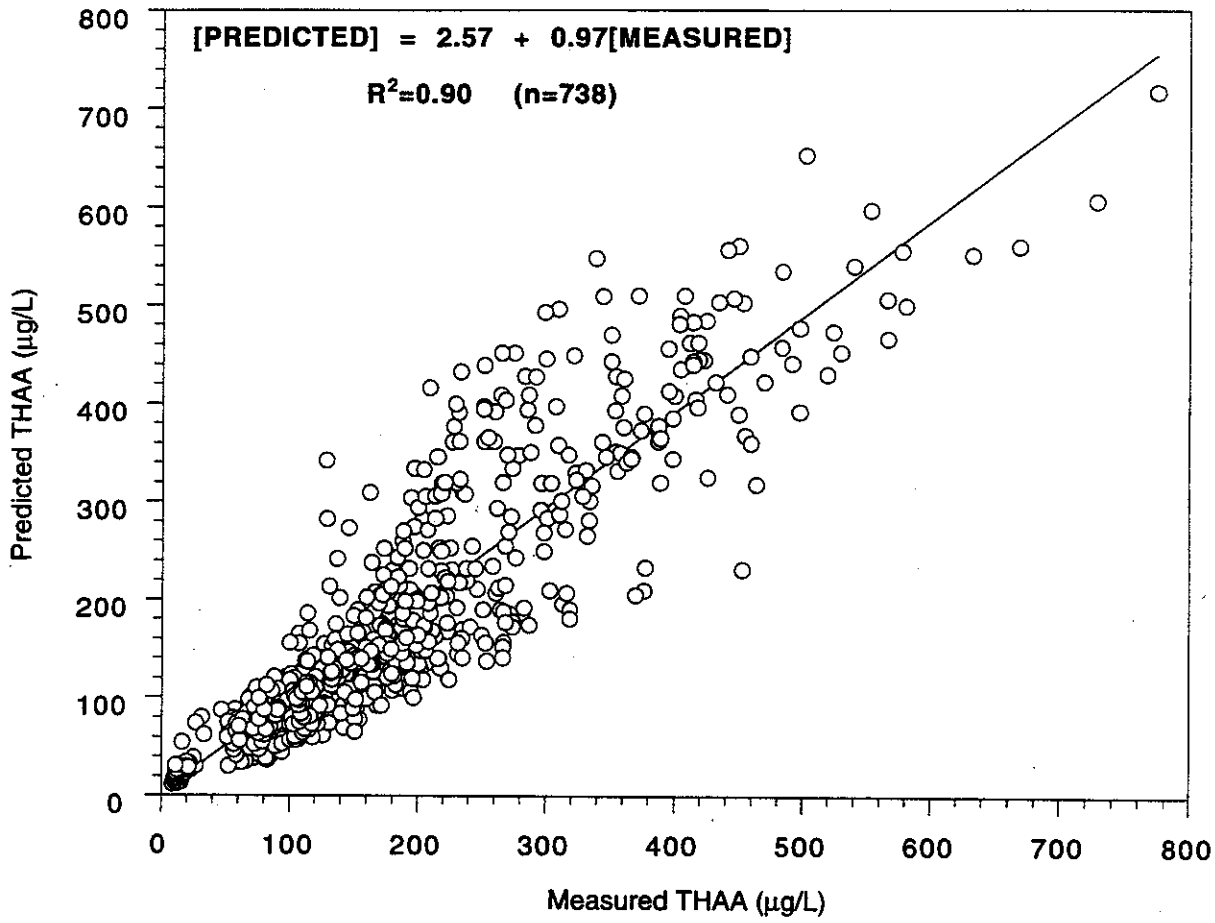

Figure 4.3. Predicted versus Measured Values for Raw/Untreated Weight-Based (µg/L) Model

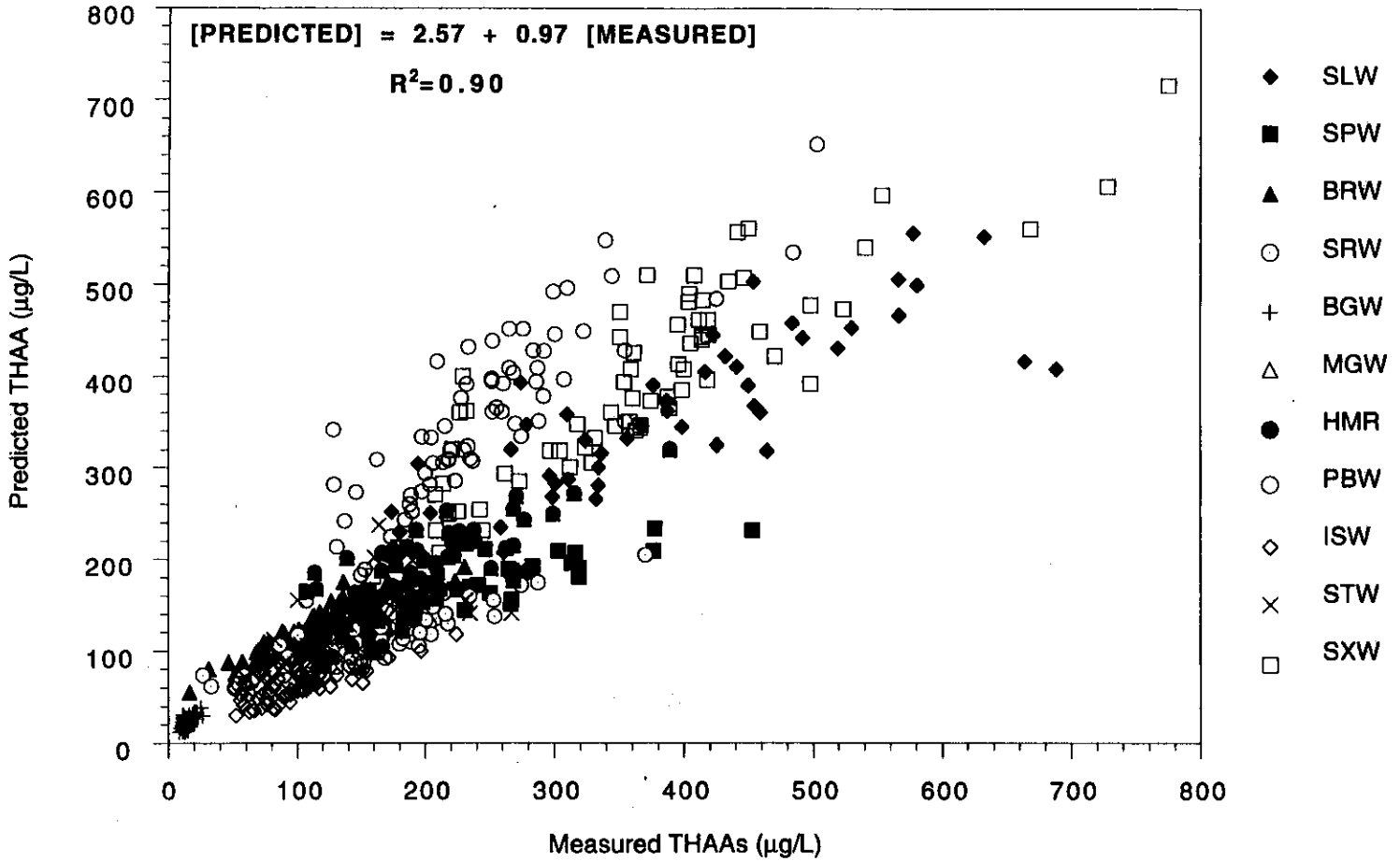

Figure 4.4. Predicted versus Measured Values for Raw/Untreated Water THAAs; Identification of Individual Sources.

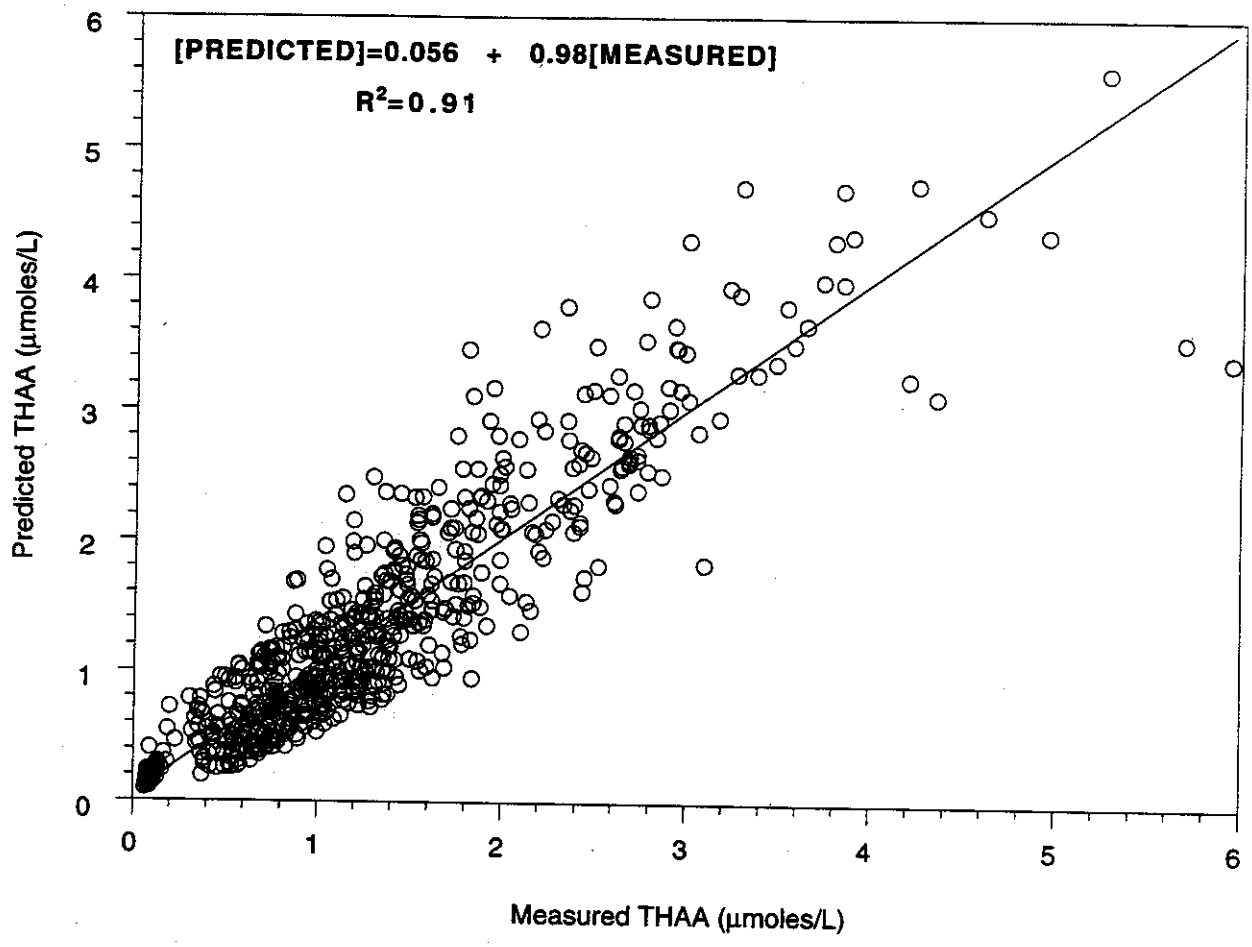

Figure 4.5. Predicted versus Measured Values for Raw/Untreated Water THAAs: Molar-Based (µmoles/L) Model.

External Data Validation

The next step in model validation was external validation with data not used in the calibration of the model. Selected data were taken from the literature (James M. Montgomery Engineers, 1991 to test and validate the original model (Figure 4.6). The symbols shown in Figure 4.6 represent actual data from a range of utility source waters; the line shown represents the correlation between our predictions (Table 4.1; THAA weight-basis equation) and their measurements. This attempt at model validation indicated that the model overpredicted at lower levels and underpredicted at higher levels. Thus, the model appears to be most applicable to chlorination of waters with a propensity to form THAAs at levels in the general vicinity of the USEPA proposed primary drinking water standard (60 ug/L), although there is a trend toward modest overpredictions.

A similar validation of the model's ability to capture reaction kinetics is shown in Figure 4.7. Divergence between measured and predicted values was more apparent at higher HAA levels.

HAA SPECIES; RAW/UNTREATED WATERS

As part of the total HAA measurements, the concentrations of six individual species were measured: trichloroacetic acid (TCAA); dichloroacetic acid (DCAA), monochloroacetic acid (CAA); bromochloroacetic acid (BCAA); dibromoacetic acid (DBAA); and monobromoacetic acid (BAA). In low bromide waters, the only significant species were TCAA and DCAA; in waters with moderate bromide, BCAA was also significant; DBAA was only an important constituent in experiments involving spiked levels of bromide. In almost all experiments, CAA and BAA were trace constituents present near detection limits. Individual parameter effects were highlighted in Figure 4.2 as part of the model building process. Table 4.1 also shows the individual HAA species models. For the various models, higher values of R^2 were obtained for DCAA, TCAA, BCAA, and DBAA than CAA and BAA because CAA and BAA were only minor (present at very low concentration) constituents in all cases.

Predicted versus measured values for TCAA, DCAA and BCAA are plotted in Figure 4.8. Several outliers for both TCAA and DCAA in the figures were identified as being from SLW, one of the first source waters evaluated which involved a higher Cl_2/DOC baseline (3:1) than the other waters. Near the beginning of the research, we elected to lower the baseline condition from 3:1 to 1:1 mg/mg.

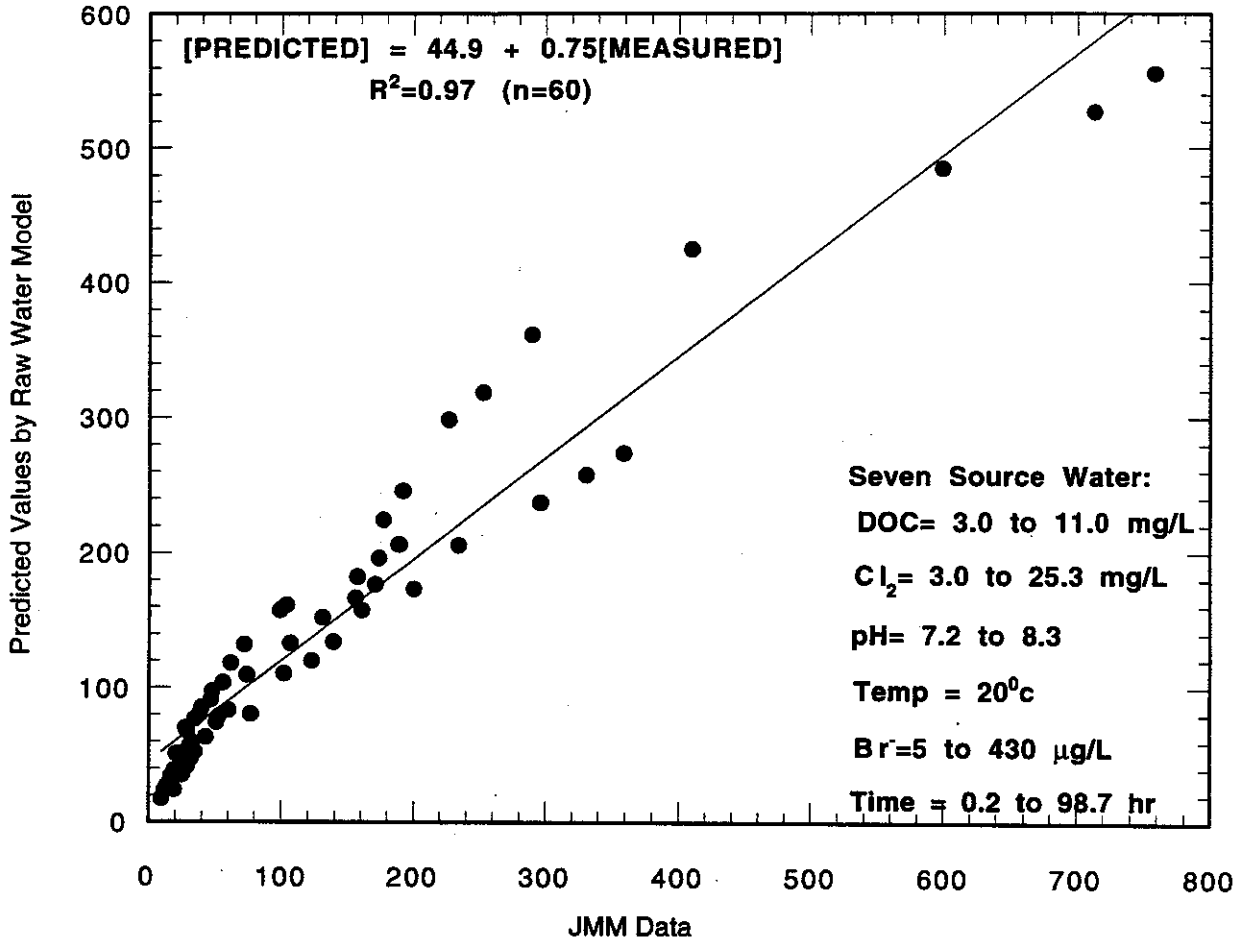

Figure 4.6. Overall External Validation Using JMM Data with Raw Water Model (Final Report: Disinfection By-Products Database and Model Project, 1991)

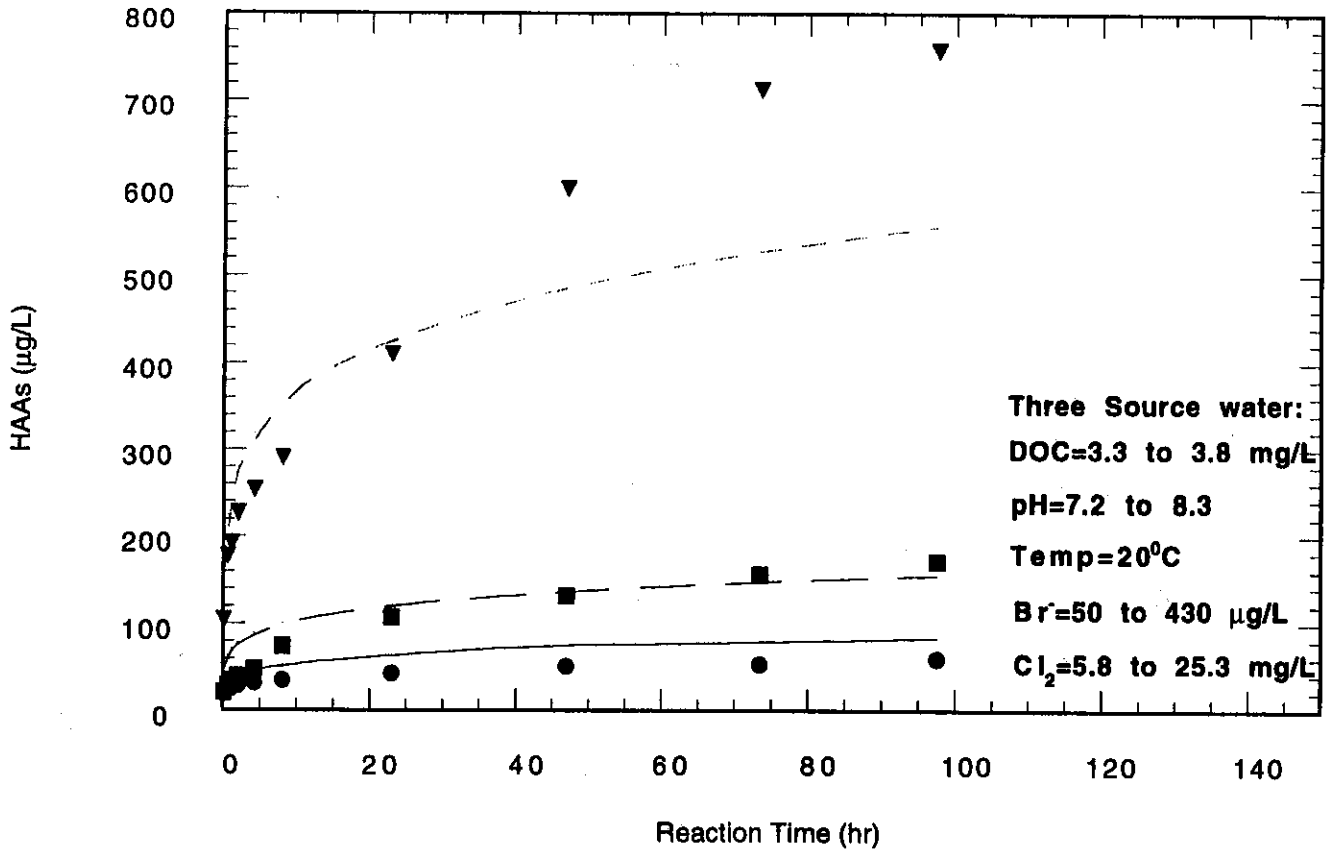

Figure 4.7. External Evaluation of Kinetics Using JMM Data with Raw Water Model (JMM Final Report to AWWA, 1991) (Lines=Model; Symbols=Data)

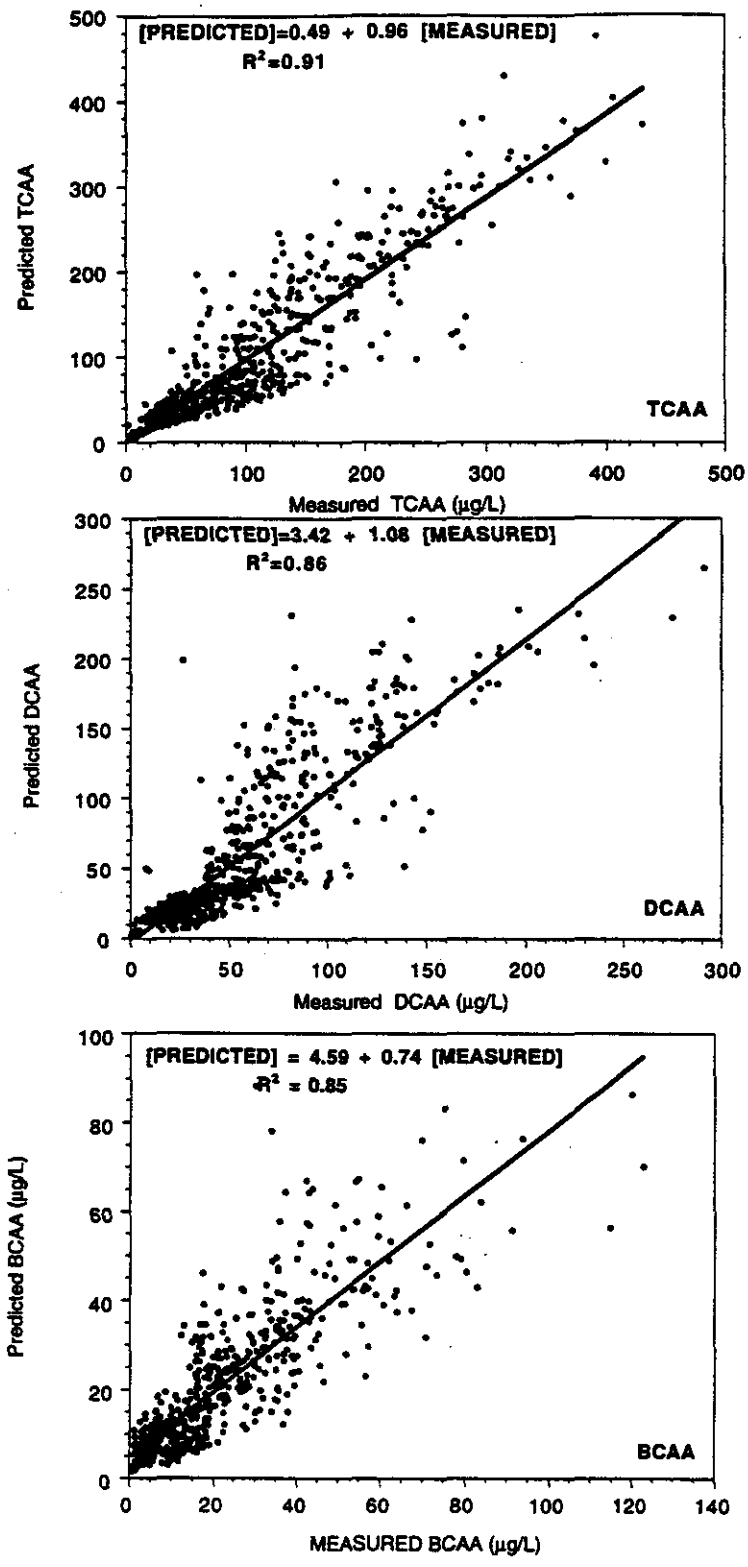

Figure 4.8. Predicted versus Measured Values for Raw-Water TCAA, DCAA and BCAA

Theoretically, predictions derived from the individual HAA-species models should be consistent with total THAA model predictions; in other words, the summation of predicted values of individual HAA species should be equal to the measured and/or predicted values of total THAAs. Figure 4.9 shows the relationship between the summation of predicted individual species (from the respective individual species models) versus directly predicted THAA values (from the overall model). As can be seen, a good relationship was observed. This suggests two alternative approaches for predicting THAA: either directly (with the THAA model) or indirectly (with summation of predictions from individual species models).

COAGULATED-WATER MODELS

Precursor (DOC) removal influences both the kinetics and yield of HAAs formed. Some precursor removal processes such as coagulation, adsorption, and membrane separation remove precursor molecules intact; others such as ozonation transform (partially oxidize) precursor molecules. The precursor remaining after treatment may be less (or possibly more) reactive in forming DBPs.

While removing precursors, coagulation has little effect on bromide ion, Br^- (Amy et al., 1991); thus, coagulated waters have a greater amount of bromide ion relative to organic precursor. Ultimately, HAA speciation is affected by both precursor and bromide levels; as the ratio of Br^-/DOC (or Br^-/Cl_2) increases, the formation of brominated species is favored.

These "submodels" are generally similar in format to the raw/untreated water models discussed above. However, since pH and temperature were maintained constant at their baseline conditions, these parameters do not *appear in the coagulated-water models, a model limitation. The THAA and HAAs* models for alum and iron coagulated waters are shown in Tables 4.2 and 4.3, respectively. There are 144 cases (n = 144) for each coagulant-specific data base. As can be seen, both sets of models have similar functionalities associated with each parameter; moreover, model simulations by each provided comparable results. Thus, a decision was made to combine the data bases together for development of a combined *alum plus iron* set of models. The corresponding total HAA models, on both a weight and molar basis, and HAA species models for all of the treated waters are listed in Table 4.4. As discussed before, more accurate models were found for DCAA, TCAA, BCAA, and DBAA than for CAA and BAA. Little difference was observed between weight and molar basis models for THAAs.

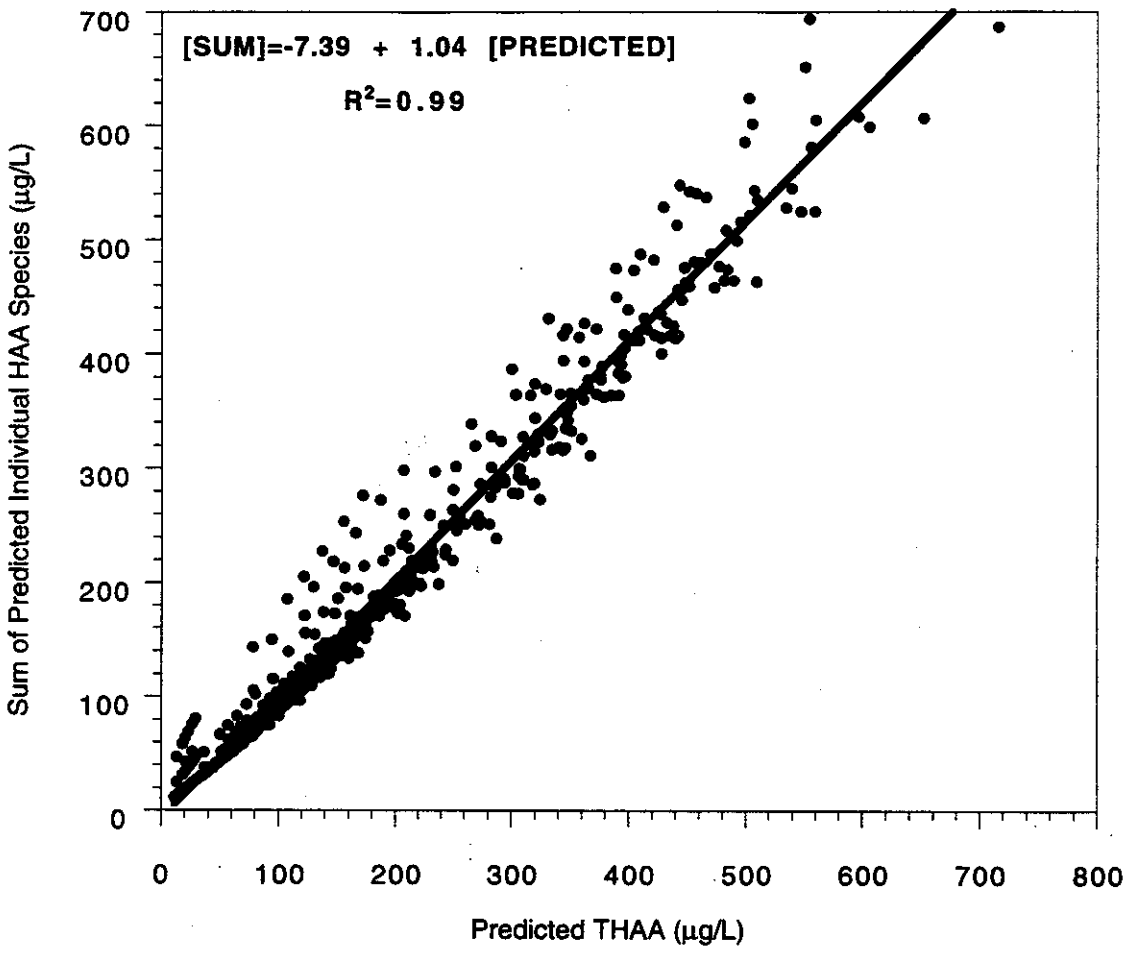

Figure 4.9. Summation of Predicted Individual HAA Species vs. Predicted Raw-Water THAAs; Weight-Based Models (µg/L)

TABLE 4.2 PREDICTIVE COAGULATED-WATER MODELS FOR THAA AND HAA SPECIES: ALUM MODELS*

Alum Coagulated Water Models:

$[HAA] = 7.05\ t^{0.159}\ [DOC]^{0.581}\ [Br^-]^{0.080}\ [Cl_2]^{0.529}$

$R^2 = 0.90 \quad F = 313 \quad \alpha \leq 0.0001 \quad N = 144$

$[CAA] = 12.82\ t^{-0.066}\ [DOC]^{-0.377}\ [Br^-]^{-0.303}\ [Cl_2]^{0.671}$

$R^2 = 0.30 \quad F = 15 \quad \alpha \leq 0.0001 \quad N = 144$

$[BAA] = 3.97 \times 10^{-3}\ t^{0.132}\ [DOC]^{0.409}\ [Br^-]^{0.834}\ [Cl_2]^{0.095}$

$R^2 = 0.33 \quad F = 17 \quad \alpha \leq 0.0001 \quad N = 144$

$[DCAA] = 10.96\ t^{0.230}\ [DOC]^{0.704}\ [Br^-]^{-0.514}\ [Cl_2]^{0.751}$

$R^2 = 0.84 \quad F = 178 \quad \alpha \leq 0.0001 \quad N = 144$

$[TCAA] = 6.22\ t^{0.164}\ [DOC]^{0.900}\ [Br^-]^{-0.267}\ [Cl_2]^{0.697}$

$R^2 = 0.93 \quad F = 460 \quad \alpha \leq 0.0001 \quad N = 144$

$[BCAA] = 0.13\ t^{0.193}\ [DOC]^{0.286}\ [Br^-]^{0.675}\ [Cl_2]^{0.251}$

$R^2 = 0.86 \quad F = 204 \quad \alpha \leq 0.0001 \quad N = 144$

$[DBAA] = 4.84 \times 10^{-5}\ t^{0.077}\ [DOC]^{-0.424}\ [Br^-]^{2.222}\ [Cl_2]^{0.379}$

$R^2 = 0.85 \quad F = 188 \quad \alpha \leq 0.0001 \quad N = 144$

Symbols are defined below:

[HAA]: Total Concentration of Haloacetic Acids (µg/L); Sum of Six Species

[DCAA]; [TCAA]; [BCAA]: Individual Haloacetic Acid Species

t: Reaction Time (hr); $2 \leq t \leq 168$

$[Cl_2]$: Applied Chlorine Dose (mg/L), $1.11 < [Cl_2] < 14.19$

[DOC]: Dissolved Organic Carbon (mg/L); $1 < [DOC] < 4.6$

$[Br^-]$: Concentration of Br^- (µg/L); $36 \leq [Br^-] \leq 308$

$[Cl_2]$:[DOC]: $1 \leq [Cl_2]:[DOC] \leq 3$ (mg/mg)

*Source Waters: SPW, BRW, SRW, HMR, PBW, ISW, STW and SXW

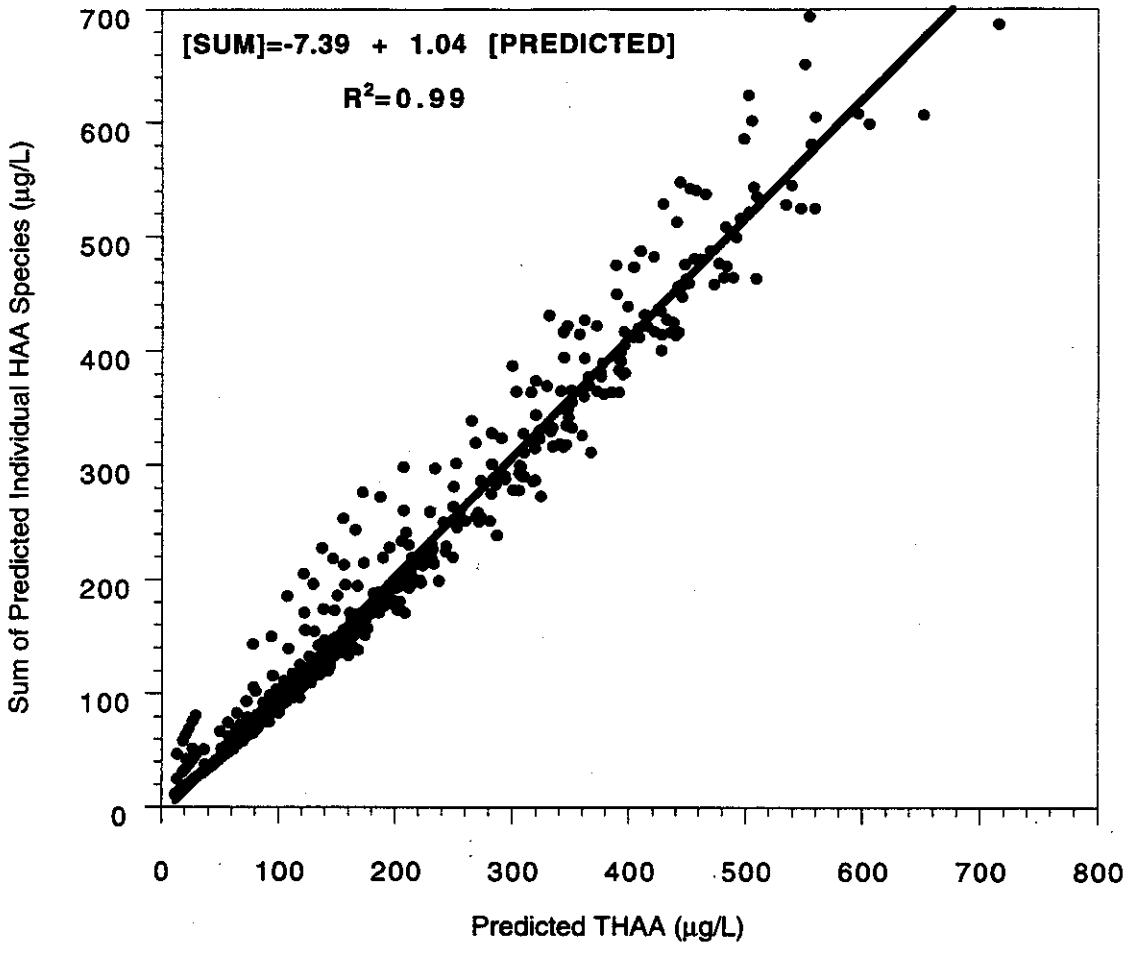

Figure 4.9. Summation of Predicted Individual HAA Species vs. Predicted Raw-Water THAAs; Weight-Based Models (µg/L)

TABLE 4.2 PREDICTIVE COAGULATED-WATER MODELS FOR THAA AND HAA SPECIES: ALUM MODELS*

Alum Coagulated Water Models:

$[HAA] = 7.05\ t^{0.159}\ [DOC]^{0.581}\ [Br^-]^{0.080}\ [Cl_2]^{0.529}$

$R^2 = 0.90 \quad F = 313 \quad \alpha \leq 0.0001 \quad N = 144$

$[CAA] = 12.82\ t^{-0.066}\ [DOC]^{-0.377}\ [Br^-]^{-0.303}\ [Cl_2]^{0.671}$

$R^2 = 0.30 \quad F = 15 \quad \alpha \leq 0.0001 \quad N = 144$

$[BAA] = 3.97 \times 10^{-3}\ t^{0.132}\ [DOC]^{0.409}\ [Br^-]^{0.834}\ [Cl_2]^{0.095}$

$R^2 = 0.33 \quad F = 17 \quad \alpha \leq 0.0001 \quad N = 144$

$[DCAA] = 10.96\ t^{0.230}\ [DOC]^{0.704}\ [Br^-]^{-0.514}\ [Cl_2]^{0.751}$

$R^2 = 0.84 \quad F = 178 \quad \alpha \leq 0.0001 \quad N = 144$

$[TCAA] = 6.22\ t^{0.164}\ [DOC]^{0.900}\ [Br^-]^{-0.267}\ [Cl_2]^{0.697}$

$R^2 = 0.93 \quad F = 460 \quad \alpha \leq 0.0001 \quad N = 144$

$[BCAA] = 0.13\ t^{0.193}\ [DOC]^{0.286}\ [Br^-]^{0.675}\ [Cl_2]^{0.251}$

$R^2 = 0.86 \quad F = 204 \quad \alpha \leq 0.0001 \quad N = 144$

$[DBAA] = 4.84 \times 10^{-5}\ t^{0.077}\ [DOC]^{-0.424}\ [Br^-]^{2.222}\ [Cl_2]^{0.379}$

$R^2 = 0.85 \quad F = 188 \quad \alpha \leq 0.0001 \quad N = 144$

Symbols are defined below:

[HAA]: Total Concentration of Haloacetic Acids (µg/L); Sum of Six Species

[DCAA]; [TCAA]; [BCAA]: Individual Haloacetic Acid Species

t: Reaction Time (hr); $2 \leq t \leq 168$

$[Cl_2]$: Applied Chlorine Dose (mg/L), $1.11 < [Cl_2] < 14.19$

[DOC]: Dissolved Organic Carbon (mg/L); $1 < [DOC] < 4.6$

$[Br^-]$: Concentration of Br^- (µg/L); $36 \leq [Br^-] \leq 308$

$[Cl_2]$:[DOC]: $1 \leq [Cl_2]:[DOC] \leq 3$ (mg/mg)

*Source Waters: SPW, BRW, SRW, HMR, PBW, ISW, STW and SXW

TABLE 4.3 PREDICTIVE COAGULATED-WATER MODELS FOR THAA AND HAA SPECIES: IRON MODELS*

Iron Coagulated Water Models:

$[THAA] = 3.84\ t^{0.163}\ [DOC]^{0.682}\ [Br^-]^{0.170}\ [Cl_2]^{0.551}$
$R^2 = 0.94 \quad F = 525 \quad \alpha \leq 0.0001 \quad N = 144$

$[CAA] = 11.94\ t^{-0.021}\ [DOC]^{-0.668}\ [Br^-]^{-0.415}\ [Cl_2]^{1.061}$
$R^2 = 0.44 \quad F = 27 \quad \alpha \leq 0.0001 \quad N = 144$

$[BAA] = 3.33 \times 10^{-3}\ t^{-0.020}\ [DOC]^{0.211}\ [Br^-]^{0.925}\ [Cl_2]^{0.313}$
$R^2 = 0.39 \quad F = 22 \quad \alpha \leq 0.0001 \quad N = 144$

$[DCAA] = 6.31\ t^{0.213}\ [DOC]^{0.846}\ [Br^-]^{0.416}\ [Cl_2]^{0.742}$
$R^2 = 0.90 \quad F = 329 \quad \alpha \leq 0.0001 \quad N = 144$

$[TCAA] = 3.97\ t^{0.163}\ [DOC]^{1.063}\ [Br^-]^{-0.215}\ [Cl_2]^{0.680}$
$R^2 = 0.94 \quad F = 523 \quad \alpha \leq 0.0001 \quad N = 144$

$[BCAA] = 0.075\ t^{0.209}\ [DOC]^{0.444}\ [Br^-]^{0.752}\ [Cl_2]^{0.199}$
$R^2 = 0.90 \quad F = 301 \quad \alpha \leq 0.0001 \quad N = 144$

$[DBAA] = 3.92 \times 10^{-5}\ t^{0.068}\ [DOC]^{0.318}\ [Br^-]^{2.256}\ [Cl_2]^{0.397}$
$R^2 = 0.92 \quad F = 189 \quad \alpha \leq 0.0001 \quad N = 144$

Symbols are defined below:

[HAA]: Total Concentration of Haloacetic Acids (µg/L); Sum of Six Species

[DCAA]; [TCAA]; [BCAA]: Individual Haloacetic Acid Species

t: Reaction Time (hr); $2 \leq t \leq 168$

$[Cl_2]$: Applied Chlorine Dose (mg/L), $5 < [Cl_2] < 24$

[DOC]: Dissolved Organic Carbon (mg/L); $1.03 < [DOC] < 4.20$

$[Br^-]$: Concentration of Br^- (µg/L); $37 \leq [Br^-] \leq 308$

$[Cl_2]$:[DOC]: $1 \leq [Cl_2]:[DOC] \leq 3$ (mg/mg)

*Source Waters: SPW, BRW, SRW, HMR, PBW, ISW, STW and SXW

TABLE 4.4 PREDICTIVE COAGULATED-WATER MODELS FOR THAA AND HAA SPECIES: COMBINED ALUM PLUS IRON MODELS*

Weight-Based (μg/L) Models:

$[THAA] = 5.22\ t^{0.153}\ [DOC]^{0.585}\ [Br^-]^{0.031}\ [Cl_2]^{0.565}$

$R^2 = 0.92 \quad F = 771 \quad \alpha \leq 0.001 \quad N = 288$

$[CAA] = 12.30\ t^{-0.043}\ [DOC]^{-0.522}\ [Br^-]^{-0.355}\ [Cl_2]^{0.859}$

$R^2 = 0.36 \quad F = 40 \quad \alpha \leq 0.0001 \quad N = 288$

$[BAA] = 3.68 \times 10^{-3}\ t^{0.077}\ [DOC]^{0.299}\ [Br^-]^{0.877}\ [Cl_2]^{0.206}$

$R^2 = 0.35 \quad F = 37 \quad \alpha \leq 0.0001 \quad N = 288$

$[DCAA] = 8.38\ t^{0.222}\ [DOC]^{0.777}\ [Br^-]^{-0.466}\ [Cl_2]^{0.744}$

$R^2 = 0.88 \quad F = 461 \quad \alpha \leq 0.0001 \quad N = 288$

$[TCAA] = 4.98\ t^{0.163}\ [DOC]^{0.988}\ [Br^-]^{-0.240}\ [Cl_2]^{0.683}$

$R^2 = 0.93 \quad F = 460 \quad \alpha \leq 0.0001 \quad N = 288$

$[BCAA] = 0.098\ t^{0.201}\ [DOC]^{0.369}\ [Br^-]^{0.713}\ [Cl_2]^{0.221}$

$R^2 = 0.87 \quad F = 485 \quad \alpha \leq 0.0001 \quad N = 288$

$[DBAA] = 4.41 \times 10^{-5}\ t^{0.072}\ [DOC]^{-0.374}\ [Br^-]^{2.237}\ [Cl_2]^{0.387}$

$R^2 = 0.84 \quad F = 382 \quad \alpha \leq 0.0001 \quad N = 288$

Molar-Based (μmoles/L) Models:

$[THAA] = 3.03\ t^{0.153}\ [DOC]^{0.585}\ [Br^-]^{0.031}\ [Cl_2]^{0.565}$

$R^2 = 0.92 \quad F = 771 \quad \alpha \leq 0.001 \quad N = 288$

Symbols are defined below:

[THAA]: Total Haloacetic Acids (μg/L); (μg/L or μmoles/L)

[CAA]; [BAA]; [DCAA]; [TCAA]; [BCAA]; [DBAA]: Individual HAA Species (μg/L)

t: Reaction Time (hr); $2 \leq t \leq 168$

$[Cl_2]$: Applied Chlorine Dose (mg/L), $1.11 < [Cl_2] < 24$

[DOC]: Dissolved Organic Carbon (mg/L); $1.0 < [DOC] < 4.6$

$[Br^-]$: Concentration of Br^- (μg/L); $36 < [Br^-] < 308$

$[Cl_2]$:[DOC]: $1 \leq [Cl_2]:[DOC] \leq 3$ (mg/mg)

*Source Waters: SPW, BRW, SRW, HMR, PBW, ISW, STW and SXW

Data Simulation/Internal Validation

A data simulation for all of the treated waters is shown in Figure 4.10; comparisons of predicted versus measured THAAs were made with the entire data base (n = 288). Although correlations between measured and predicted values were good, the models showed a tendency to overpredict at lower THAA levels and underpredict at higher THAA levels. However, the simulations generally show least error at levels near the proposed standard (60 ug/L). Figure 4.10 also elucidates data subsets derived from alum versus iron coagulation. The underprediction at higher THAA levels appeared to be associated with the SXW source which is the only source with a high DOC remaining after coagulation.

Predicted versus measured values for TCAA, DCAA and BCAA were also plotted (Figure 4.11). Compared to Figure 4.8, better correlations were obtained for the coagulated waters than the raw waters. However, these treated water models showed a tendency to overpredict at lower THAA levels and to underpredict at higher THAA levels. Thus, the models tend to overpredict for conditions least conducive to THAA formation and underpredict for conditions most conducive to THAA formation.

Predicted Models Based on Reactivity Coefficient, ϕ

We also took a different (alternative) approach to modeling HAA formation in treated waters, based on changes (reductions) in precursor reactivity (HAA/DOC) after coagulation. This approach involves use of a reactivity coefficient, ϕ, which is used to adjust the DOC term in the raw-water models, based on the premise:

$$\phi = (HAA/DOC)_{trt}/(HAA/DOC)_{raw} \qquad \text{where } \phi = 0 - 1.0 \qquad (4.2)$$

The DOC term in the raw water models is adjusted to reflect a different (lower) reactivity such that $DOC = \phi(DOC_{trt})$. Based on an anticipated reduction in reactivity, the parameter ϕ would be expected to vary from 0 to 1.0 for coagulant-treated waters. Table 4.5 summarizes ϕ values for THAA formation at different reaction times. Model simulations based on this approach are shown in Figures 4.12 and 4.13 for reaction times of 24 and 96 hours, respectively. As can be seen, there is good prediction by ϕ-adjusted raw water models for the treated waters. Figure 4.14 shows one example for this type of simulation with the BRW source water. Thus, as an alternative to the treated-water models, we can directly predict treated water THAA formation by coupling the ϕ parameter with raw water models. A limitation to this approach is the need to

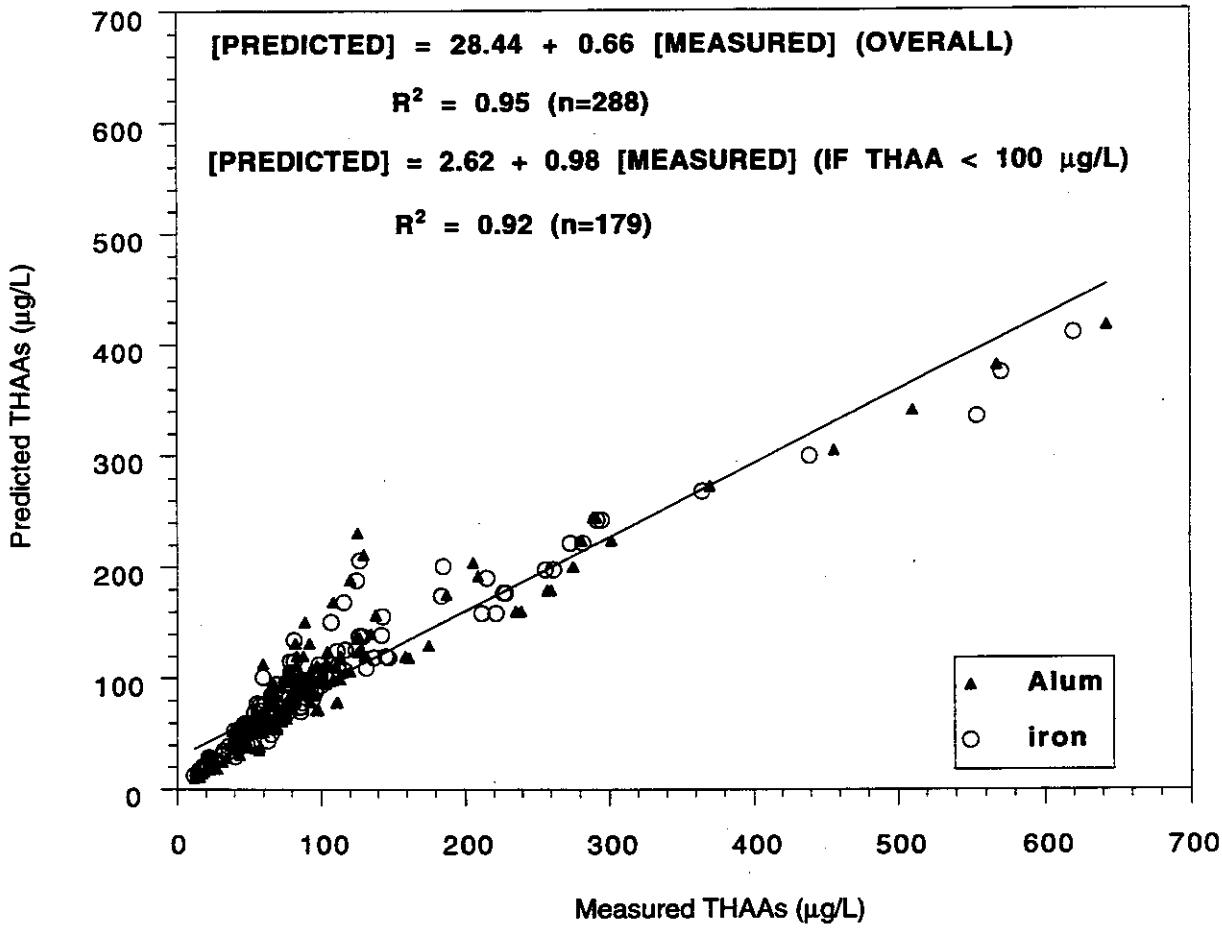

Figure 4.10. Predicted versus Measured Values of THAA for Coagulated/Treated Waters Using Combined Alum plus Iron Treated-Water Models

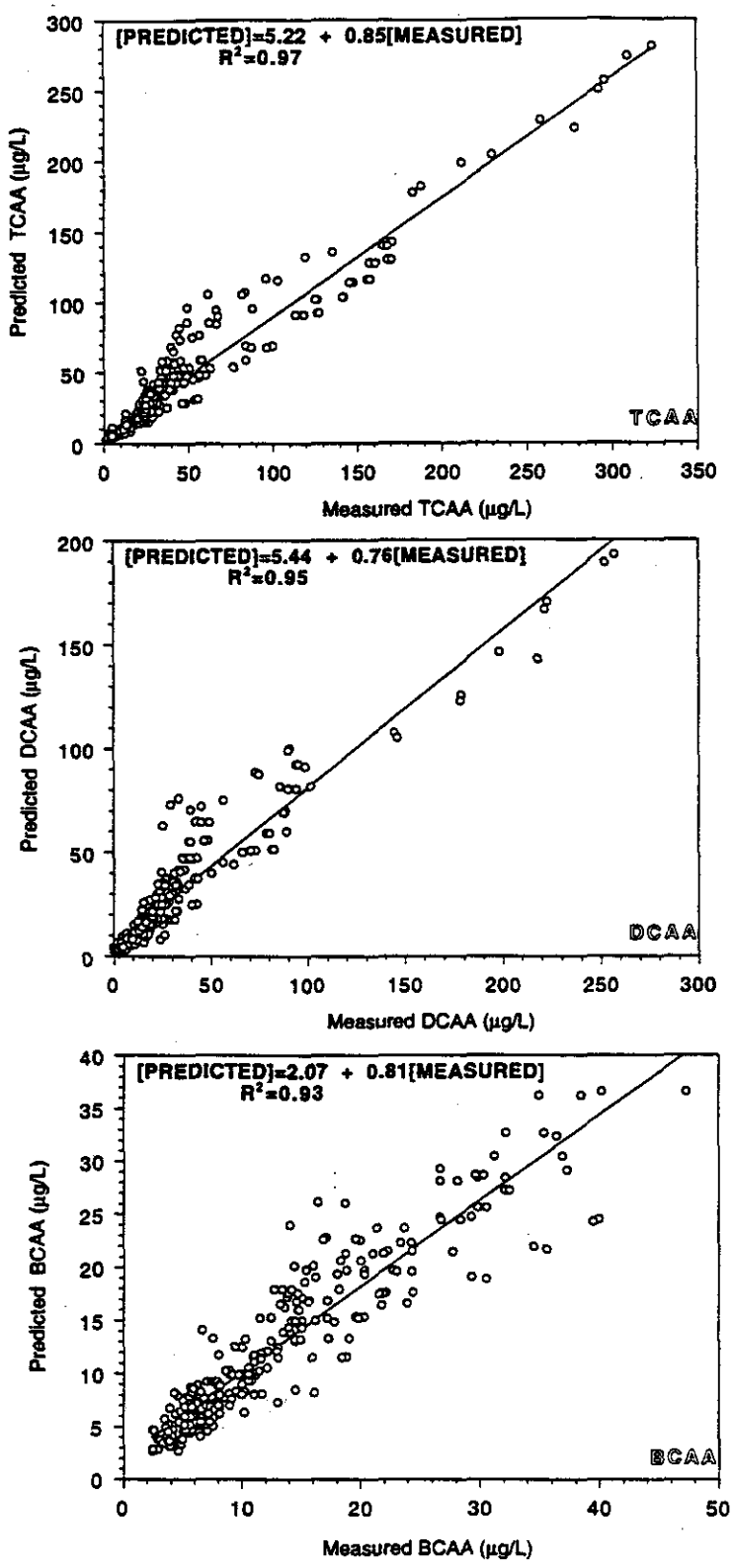

Figure 4.11. Predicted versus Measured Values of TCAA, DCAA and BCAA for Coagulated/Treated Waters

TABLE 4.5 SUMMARY OF REACTIVITY COEFFICIENT, φ VALUES FOR THAAS

Water	Category	DOC (mg/L)	Br⁻(ug/L)	φ(2hr)	φ(24hr)	φ(96hr)
SPW	Raw	4.19	312	1.00	1.00	1.00
	Alum	2.56	306	0.91	0.88	0.75
	Iron	2.58	308	0.91	0.81	0.79
BRW	Raw	3.54	250	1.00	1.00	1.00
	Alum	2.72	245	1.15	0.85	0.84
	Iron	2.63	245	1.10	0.90	0.77
SRW	Raw	4.18	50	1.00	1.00	1.00
	Alum	2.56	48	0.47	0.46	0.41
	Iron	2.55	46	0.46	0.44	0.41
HMR	Raw	5.73	40	1.00	1.00	1.00
	Alum	4.29	37	0.60	0.67	0.61
	Iron	4.23	38	0.47	0.63	0.72
PBW	Raw	10.6	97	1.00	1.00	1.00
	Alum	4.60	97	0.73	0.73	0.72
	Iron	4.20	97	0.74	0.75	0.74
ISW	Raw	2.78	84	1.00	1.00	1.00
	Alum	1.00	83	0.53	0.49	0.58
	Iron	1.03	83	0.35	0.35	0.59
STW	Raw	4.36	71	1.00	1.00	1.00
	Alum	2.91	68	0.97	0.84	0.95
	Iron	2.76	68	0.70	0.66	0.59
SXW	Raw	10.55	68	1.00	1.00	1.00
	Alum	7.77	67	0.86	1.01	0.94
	Iron	7.63	67	0.86	0.91	0.91

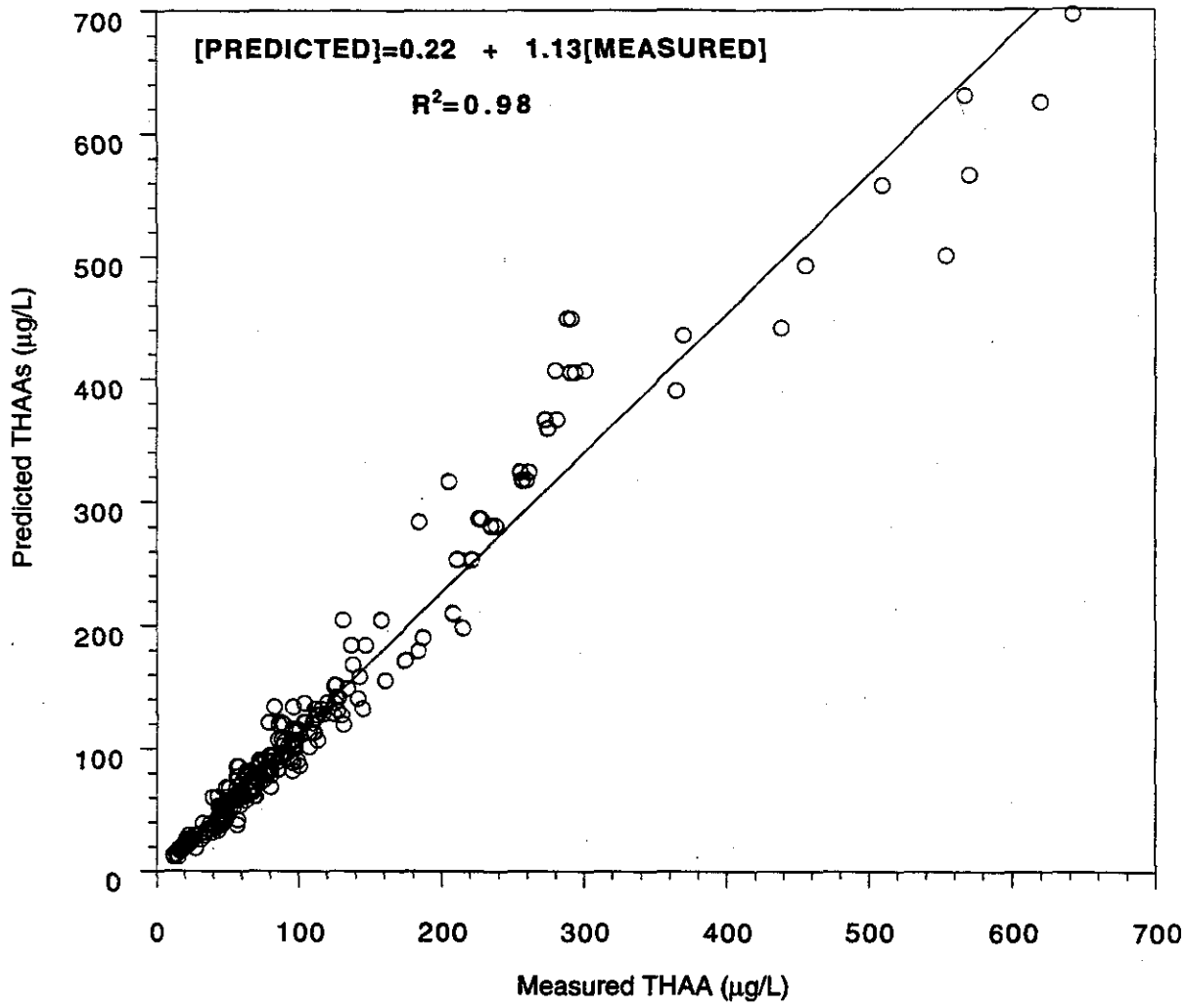

Figure 4.12. Predicted versus Measured Values of THAA for Coagulated/Treated Waters Using Raw/Untreated Water-Models Combined with Ø Concept; 24-Hour Prediction

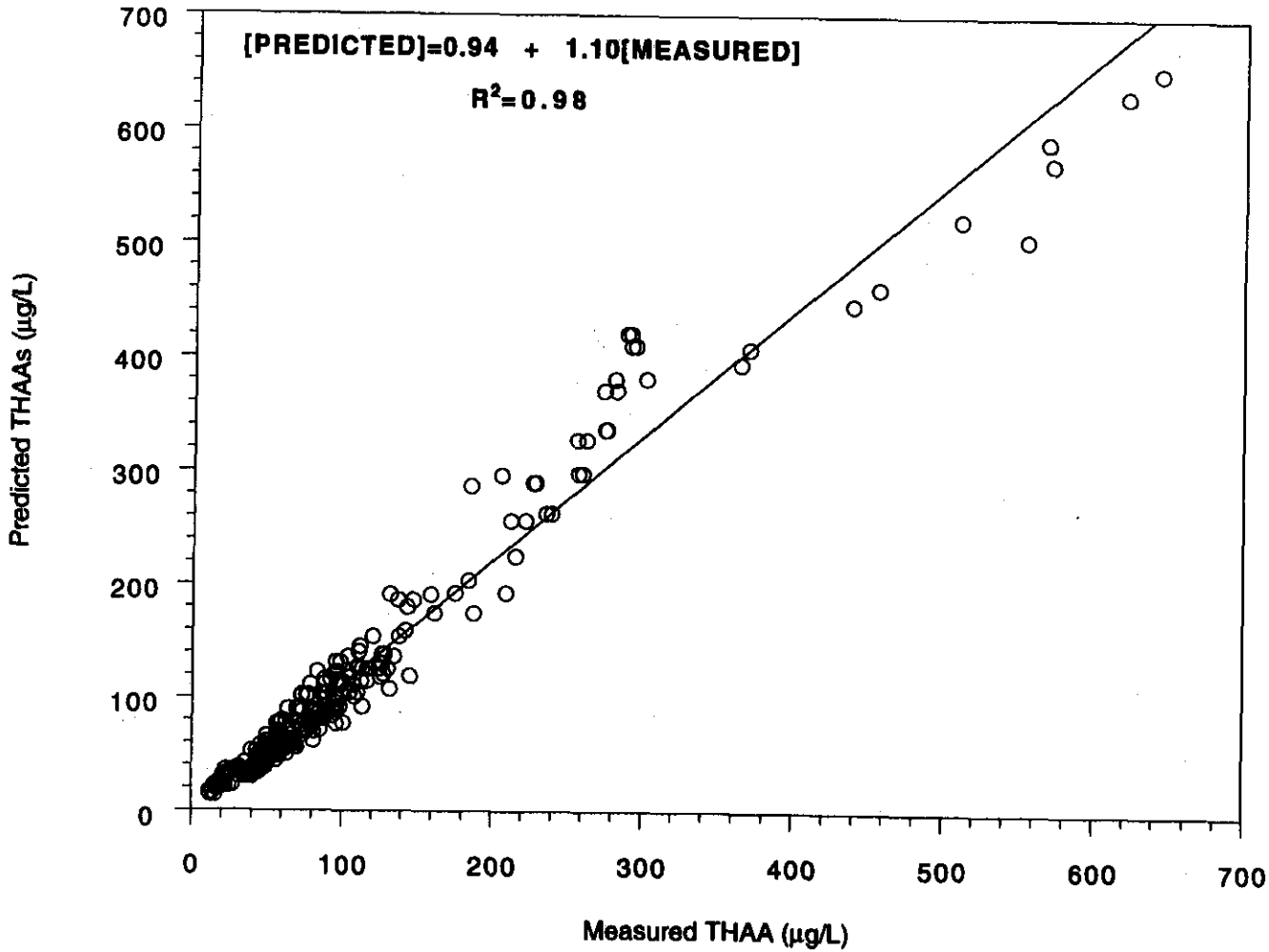

Fig. 4.13 Predicted versus Measured Values of THAA for Coagulated/Treated Waters Using Raw/Untreated Water-Models Combined with Ø Concept; 96 Hour Predictions.

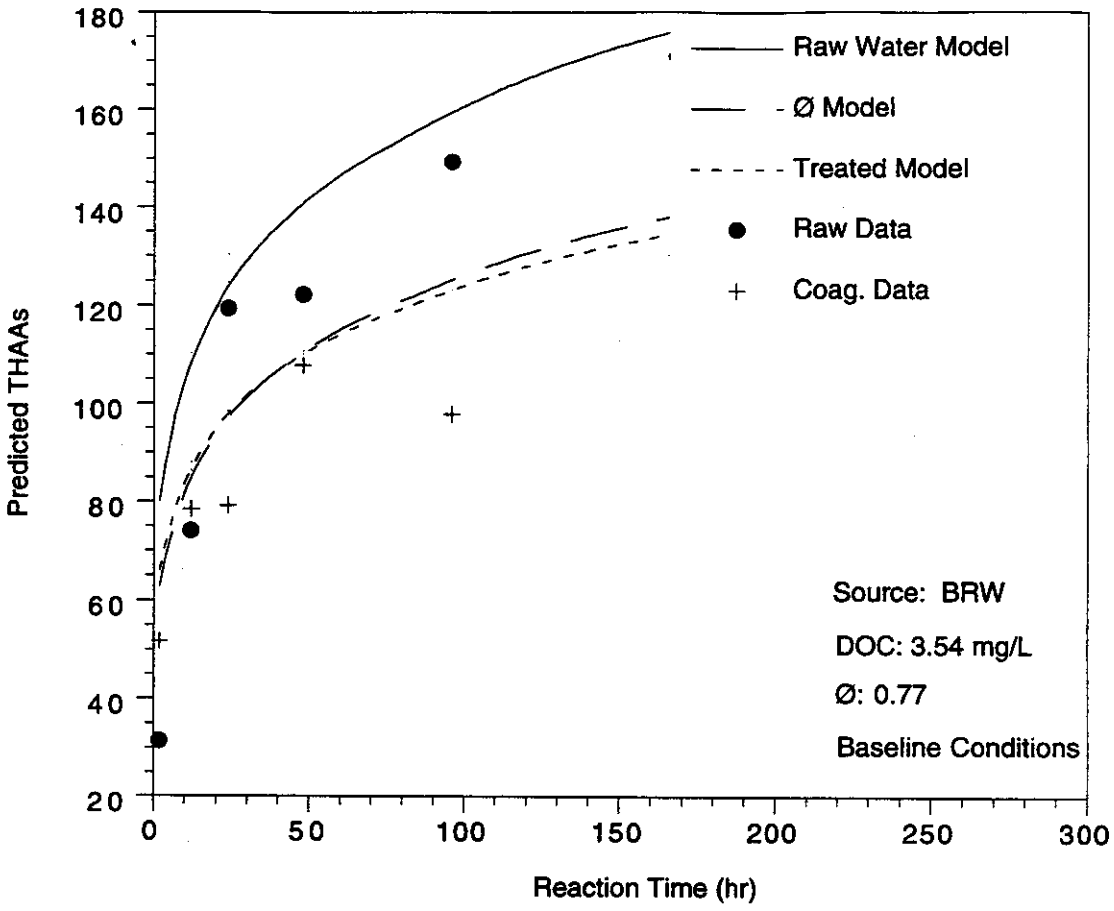

Figure 4.14. Comparison of Predictions from Treated-Water Models versus Raw/Untreated Water Models Combined with Ø Concepts

experimentally determine ϕ for a given set of conditions. Nevertheless, this approach provides a framework for modeling precursor reactivity and associated reductions imparted by coagulation.

External Model Validation

An external validation of the alum-plus-iron coagulated water model; employing literature data, is shown in Figure 4.15 (data shown are from coagulated waters; some boundary condition violations for Br^-). The model predictions appear to be reasonably accurate for a range of source waters subjected to coagulation.

Model Simulations for Coagulation of HAA Precursors

The U.S. EPA will require utilities to consider enhanced coagulation of precursors as a DBP control strategy. A range of TOC removals, ranging from 15 to 50 % will be required, depending on initial TOC and alkalinity conditions. Using the alum-plus-iron coagulated-water models, a simulation of reducing TOC from 4 to 2 mg/L is shown in Figure 4.16. The models presented herein can be used to assess such control strategies.

HAA SPECIATION MODELS; Br^-/DOC AS MASTER VARIABLE

In theory, one would expect chlorinated HAA species to decrease as a function of increasing bromide; brominated HAA species to increase with increasing bromide; and mixed chlorinated/brominated species to first increase then decrease with bromide. Thus, for the HAA species, we examined alternative functionalities to represent bromide effects on HAA species. In particular, we focused on use of a polynomial term to capture bromide effects by simply relating fractional concentrations of individual species (HAA Species/THAA) to the Br^-/DOC ratio. Through prior examination of scatterplots, we found that the ratio of Br^-/DOC, representing the ratio of inorganic to organic precursor, most accurately captures bromide effects on HAA speciation. Figures 4.17 and 4.18 show the fraction of the six HAA species versus Br^-/DOC for all the raw and treated waters; shown are actual data (points) along with model simulations (curves). As Br^-/DOC increases, TCAA and DCAA decrease exponentially, DBAA increases exponentially after a lag, and the intermediate species BCAA increases then decreases in a polynomial pattern. Resultant fractional concentration models are shown in Tables 4.6 and 4.7. Except for TCAA, polynomial functions provided the best data fit; however, in using these functionalities, one must not violate the boundary conditions (ranges of data) used in their formulation. In other words, the overall polynomial pattern

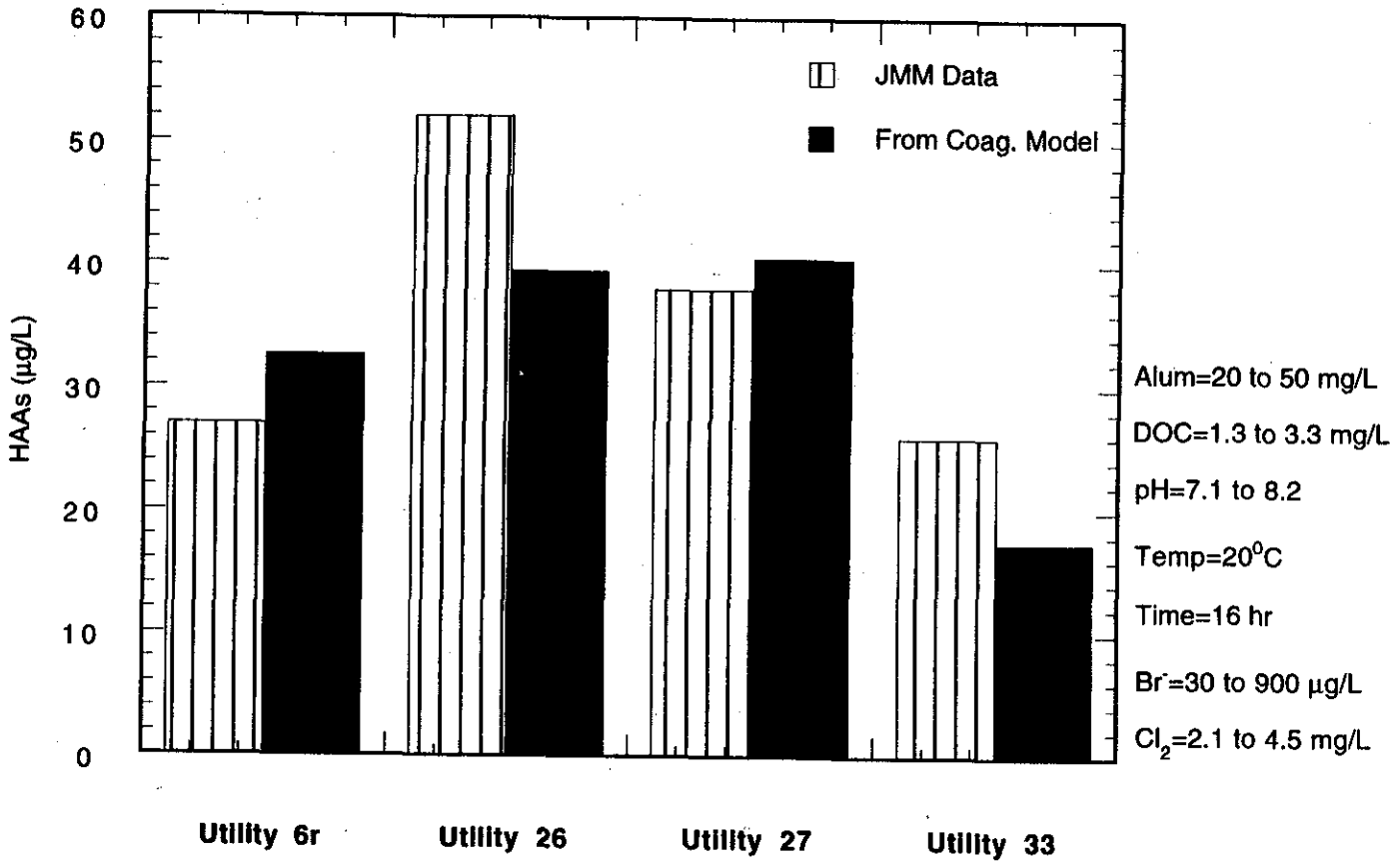

Figure 4.15 External Validation for Coagulated Water Model Using JMM Data

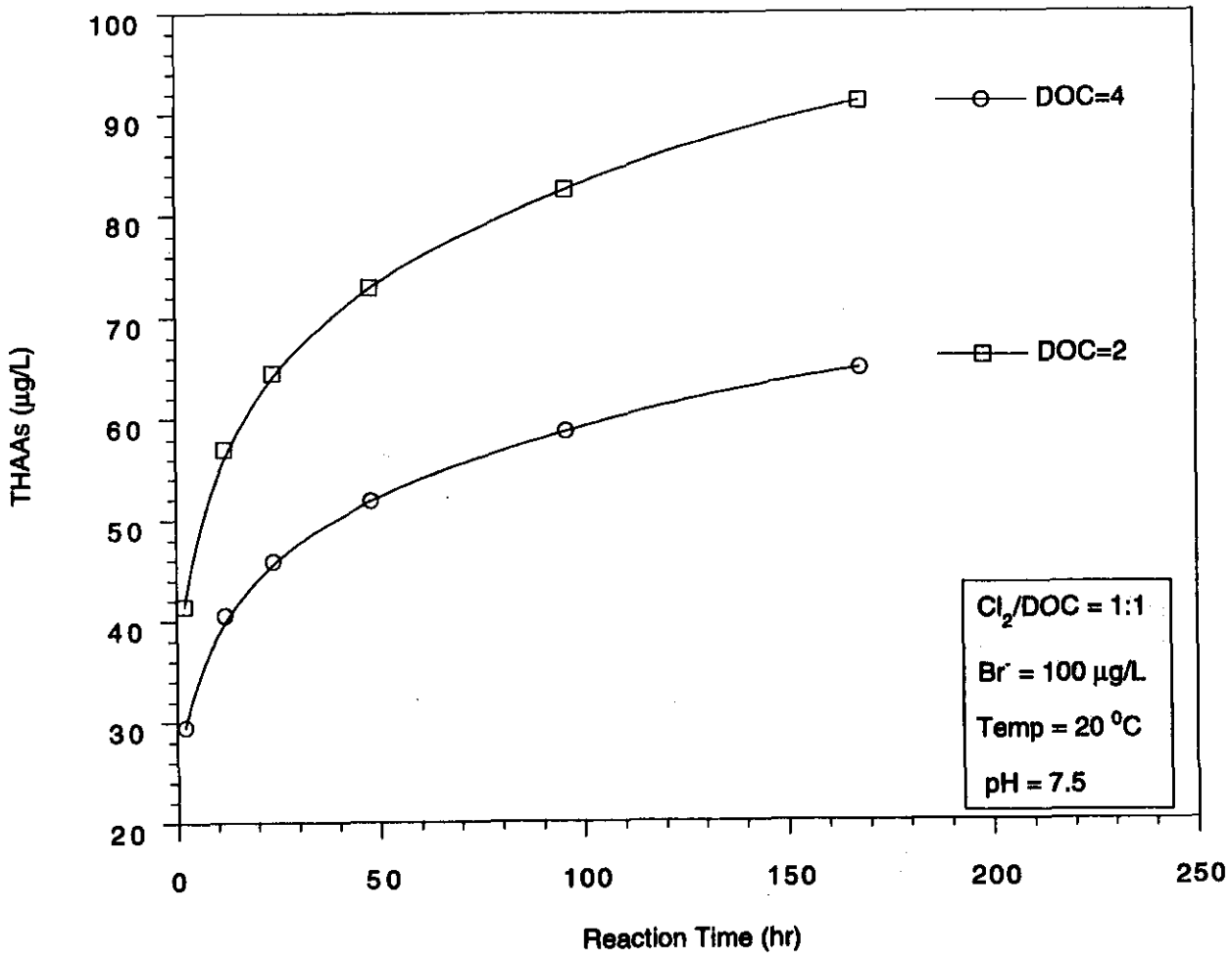

Fig. 4.16 Simulated Effects of Coagulation on THAA Formation

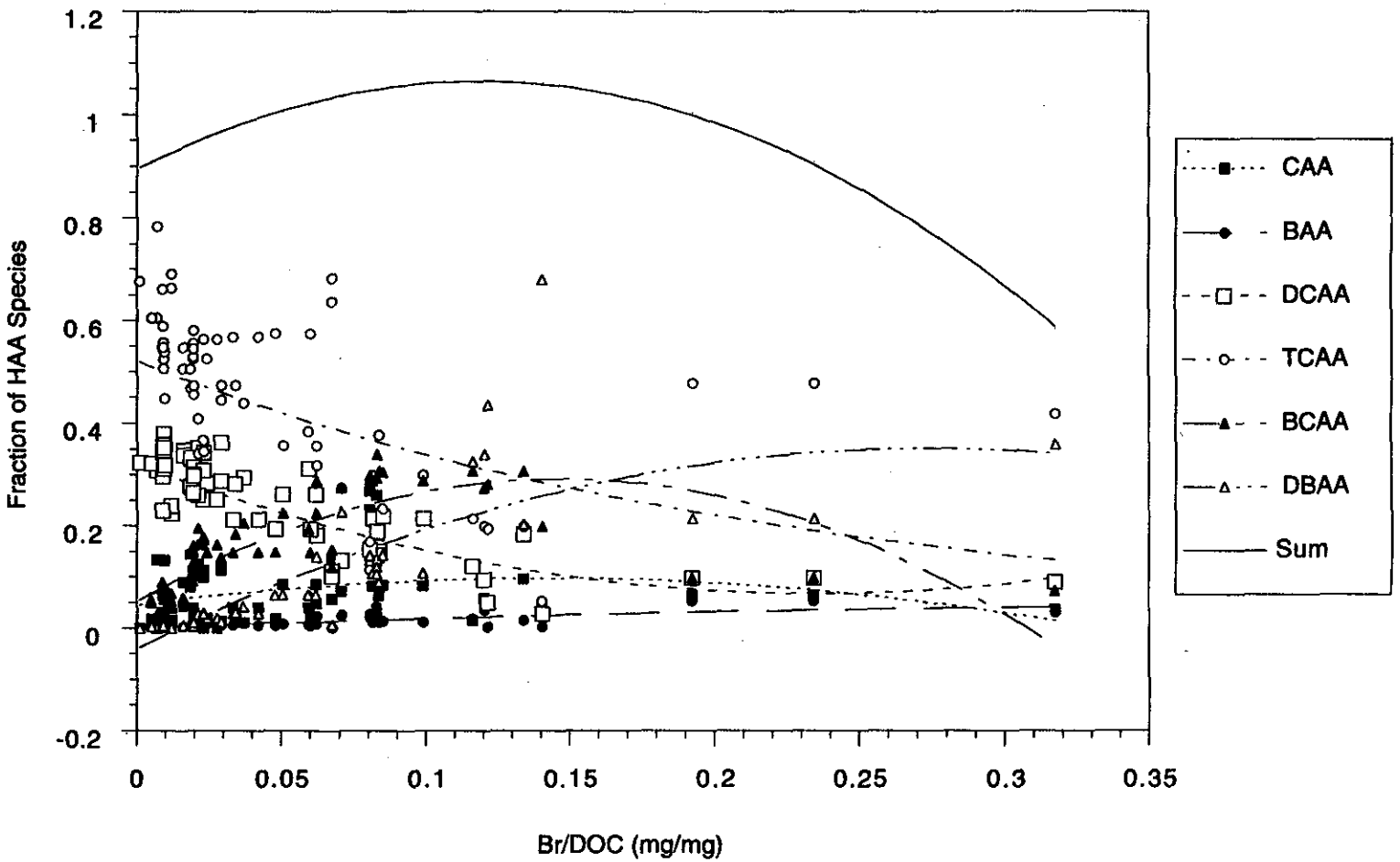

Fig 4.17 Fractional Concentration Speciation Models; 24-hour Predictions (Points Represent Data; Curves Represent Model Simulations)

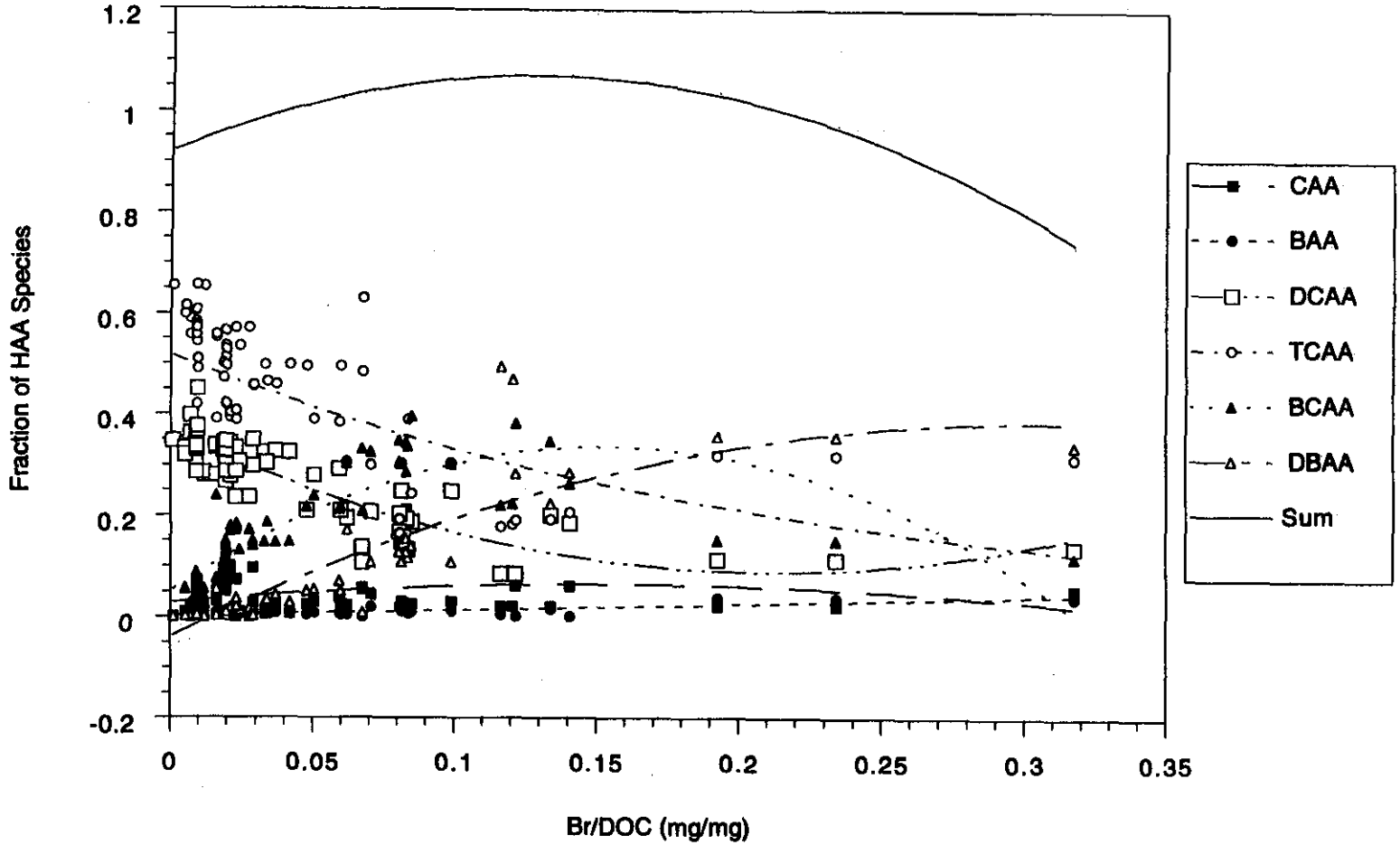

Fig. 4.18 Fractional-Concentration Speciation Models: 96-hour Prediction (Points Represent Data; Curves Represent Model Simulations)

TABLE 4.6 SUMMARY OF FRACTIONAL-CONCENTRATION HAA SPECIATION MODELS*

24-hour

SECOND ORDER POLYNOMIAL FITS
SPECIES FRACTIONAL CONCENTRATION = $a + bX + cX^2$ WHERE X = Br^-/DOC (mg/mg)

Species	a	b	c	r^2
CAA	0.045	0.75	-2.68	0.29
DCAA	0.32	-2.16	4.56	0.72
BCAA	0.052	3.28	-11.2	0.84
BAA	0.0006	0.2	-0.25	0.73
DBAA	-0.041	2.86	-5.24	0.80

EXPONENTIAL FITS
SPECIES FRACTIONAL CONCENTRATION = $a\ e^{bX}$ WHERE X = Br^-/DOC (mg/mg)

Species	a	b	r^2
TCAA	0.52	-4.30	0.60

* All Waters, Number of Cases (n) = 71; Reaction Time = 24 hr

TABLE 4.7 SUMMARY OF FRACTIONAL-CONCENTRATION HAA SPECIATION MODELS*

96-hour

SECOND ORDER POLYNOMIAL FITS
SPECIES FRACTIONAL CONCENTRATION = $a + bX + cX^2$ WHERE X = Br⁻/DOC (mg/mg)

Species	a	b	c	r^2
CAA	0.028	0.477	-1.581	0.25
DCAA	0.364	-2.604	6.150	0.86
BCAA	0.050	3.738	-12.220	0.85
BAA	0.003	0.093	0.109	0.76
DBAA	-0.041	2.800	-4.604	0.88

EXPONENTIAL FITS
SPECIES FRACTIONAL CONCENTRATION = $a\,e^{bX}$ WHERE X = Br⁻/DOC (mg/mg)

Species	a	b	r^2
TCAA	0.518	-4.496	0.74

* All Waters, Number of Cases (n) = 71; Reaction Time = 96 hr

suggests an increase then decrease as a function of the independent variable; a dependent variable which is known to only increase or decrease can be modeled by an appropriate region/range of the polynomial function.

Because coagulation does not remove bromide, Br^-/DOC ratios are higher in the treated waters. Consequently, data shown at higher Br^-/DOC ratios in Figure 4.17 and 4.18 corresponds to treated water data. The fractional concentration models portrayed in Tables 4.6 and 4.7 were calibrated using both raw/untreated and treated water data; thus, they pertain to, and are applicable to both. No external validation of these models was performed.

SECTION 5

TRIHALOMETHANE MODELS

Trihalomethanes (THMs) are important by-products formed during the chlorination of drinking water. The maximum contaminant level (MCL) for THMs in drinking water was first regulated at 100 ug/L in 1979. A new MCL of 80 ug/L is being proposed for THMs. The mechanisms and kinetics of THM formation have been long and extensively studied. THM precursors in natural waters have been identified as predominantly humic substances (Rook,1974; Oliver, 1979). Humic substances typically comprise 50 % of the dissolved organic carbon (DOC) in natural water. Humic substances include two fractions; fulvic acids (80-90%) and humic acids (10-20%). The THM formation potential for humic substances has been investigated by Lynn (1982) who showed that fulvic acids, particularly the molecular weight fraction between 5,000 - 10,000 daltons, contributed most of the THM formation upon chlorination. Trends of greater THM formation potential with high phenolic content and larger molecular size of humic substances were observed by Oliver, *et al* . (1983); they also showed that THM formation correlated with color. Miller and Uden in 1983 studied the effects of reaction time, pH, and chlorine-to-carbon ratio (Cl_2/DOC) on chloroform and other chlorination products.

A predictive model for chloroform formation from humic acid was developed by Engerholm and Amy (1983). Amy et al. (1987b) developed a non-linear regression model to predict THM formation in raw source waters; the five independent variables involved in model development included pH, temperature, bromide ion concentration (Br^-), applied chlorine concentration and nonvolatile total organic carbon (NVTOC). Only one reaction time of 96 hours was considered. The general non-linear model based on a relationship between 96-hour trihalomethanes formation potential (THMFP) and individual variables, was formulated from the following general equation:

$$THMFP = b_o + (Br^-)^{b1} + b_2 \text{ Log } (Cl_2) + b_3 \text{ (pH)} + 10^{[b4 \text{ (Temp)}]} + b_5\text{(NVTOC)} \qquad (5.1)$$

Amy, *et al.* (1987a) formulated THM predictive models for raw waters, which have formed the basis for EPA and AWWA sponsored efforts to develop overall DBP formation models. Amy's models were based on nine geographically distributed natural waters, and included seven independent variables: pH, TOC, temperature, Br^- concentration, UV_{254}, chlorine dose, and reaction time. Models based on a log-log transformation of variables were found to be more accurate

than non-linear models. Amy's models described the chlorination of raw/untreated water, whereas the models of Chadik and Amy (1987) attempted to address treatment effects on THM formation kinetics.

This chapter presents statistically-based empirical models for predicting the kinetics of total trihalomethanes (TTHM) formation, as well as individual trihalomethane species in both raw/untreated waters and chemically-treated (coagulated) waters. Resultant power-function TTHM and THM species predictive models for raw/untreated sources were based on data derived from eleven source waters; BGW, BRW, HMR, ISW, MGW, SLW, SPW, SRW, SXW, VRW and PBW. Eight of these source waters, excluding BGW, MGW, and SLW, were used in developing models for coagulated waters.

INDIVIDUAL PARAMETER EFFECTS ON TTHM AND THM SPECIES

The model building process requires an understanding of the effects of individual parameters (independent variables) on TTHM formation as well THM species. The effects of pH, temperature, chlorine dose (Cl_2/DOC), bromide concentration, reaction time, and DOC are shown in Figure 5.1. Except for DOC effects, Figure 5.1 contrasts two representative sources, VRW and HMR; DOC effects are shown for 10 sources encompassing a broad range. The positive effects of each of these parameters is apparent, although some parameters have a linear effect while others exert a nonlinear effect. DOC provided better correlations than UV absorbance as a precursor parameter; due to their colinearity, only DOC was included in the models.

Figure 5.2 shows the effects of individual parameters on each of the four THM species. These effects are straightforward with the exception of bromide; chloroform is inversely related (an exponential decrease), bromodichloromethane and dibromochloromethane increase then level off (and would be expected to further decrease polynomially at higher Br- levels), and bromoform increases in an S-shape manner following a logistic function behavior.

TOTAL TRIHALOMETHANES; RAW/UNTREATED WATERS

The weight-based and molar-based models for predicting total THM (TTHM) formation in raw/untreated waters are shown in Table 5.1. These models are based on 11 source waters and a total of 786 cases (n = 786). They include six independent variables; dissolved organic carbon (DOC), chlorine dose (Cl_2), ambient/spiked bromide levels (Br^-), temperature (Temp), pH, and reaction time (t). Assessment of each source water involved a total of 82 measurements, based on an orthogonal matrix of one DOC (ambient), five chlorine doses

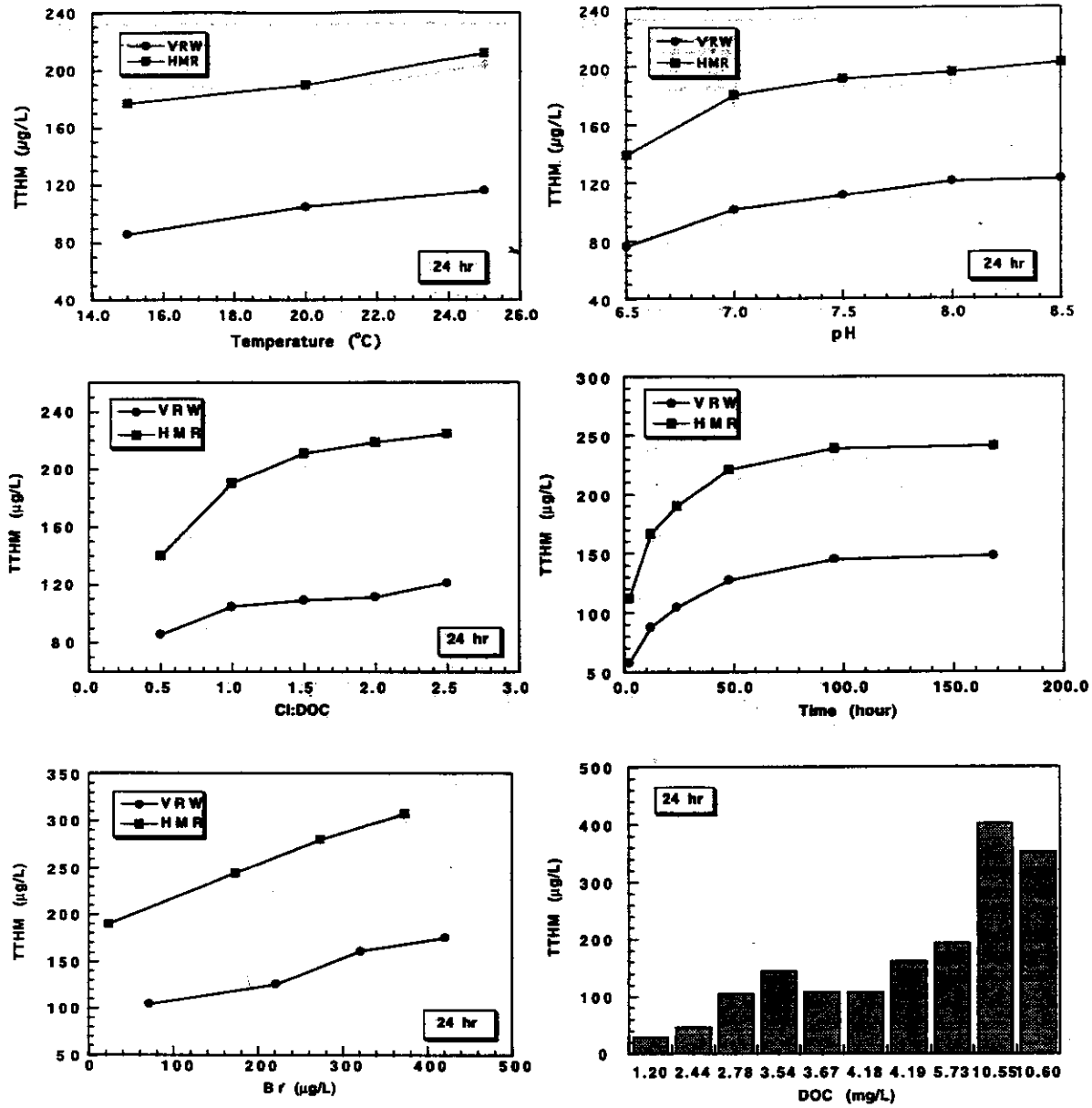

Figure 5.1 Individual Parameter Effects on TTHM Formation in HMR & VRW Sources: Effect of Chlorine, pH, Temperature, Bromide, and Reaction Time (all other parameters held at baseline conditions).

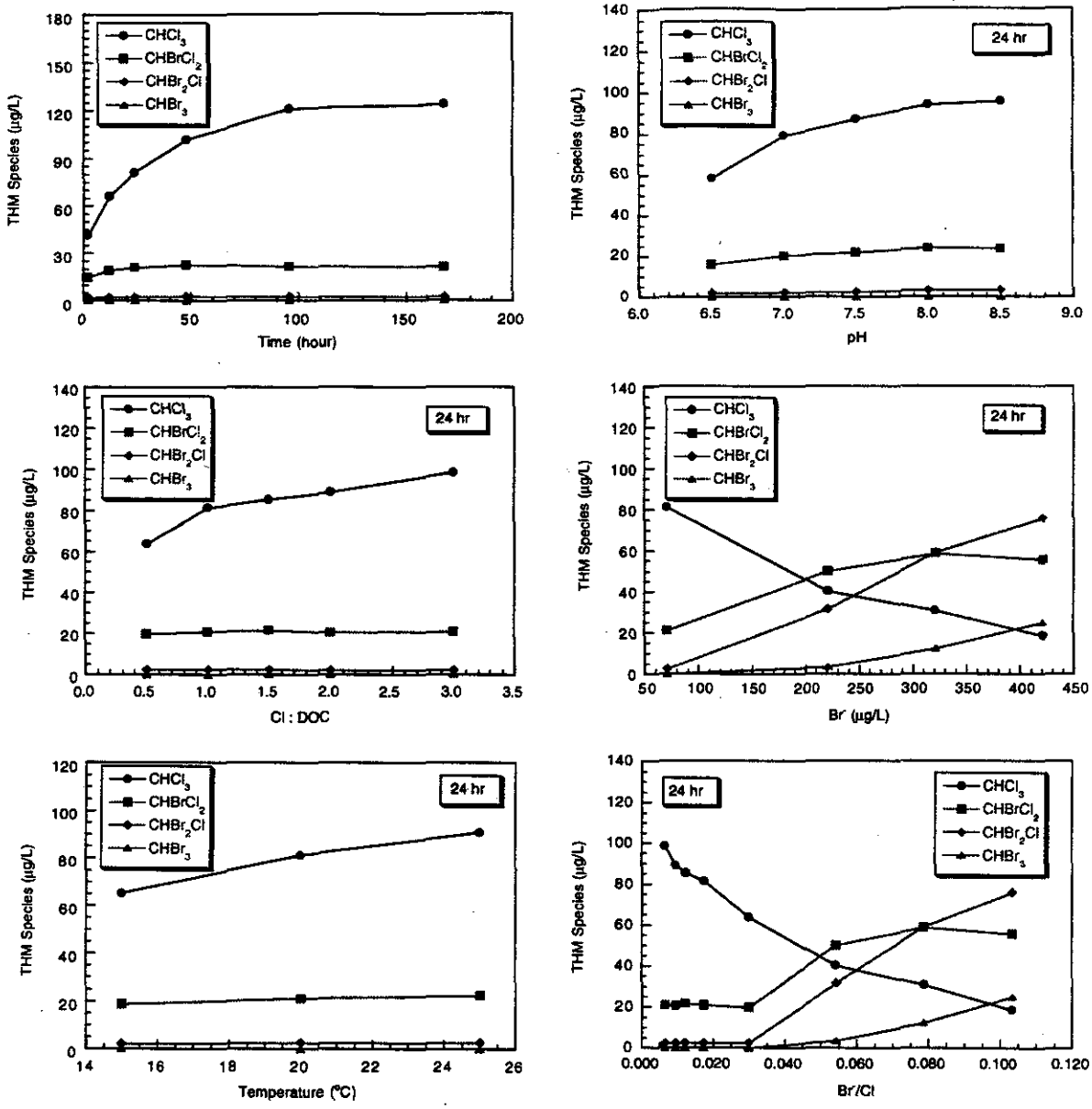

Figure 5.2 Individual Parameter Effects on THM Species Formation in VRW: Effects of Chlorine, pH, Temperature, Bromide, and Reaction Time (all other parameters held at baseline conditions).

Table 5.1 Predictive Raw-Water Models for Trihalomethanes (THM): *Total THMs (TTHM) and THM Species

Weight-Based (μg/L) Models:

$[TTHM] = 10^{-1.385} [DOC]^{1.098} [Cl_2]^{0.152} [Br^-]^{0.068} Temp^{0.609} pH^{1.601} t^{0.263}$
$R^2 = 0.90$ N = 786 F = 1198 $\alpha \leq 0.0001$

$[CHCl_3] = 10^{-1.205} [DOC]^{1.617} [Cl_2]^{-0.094} [Br^-]^{-0.175} Temp^{0.607} pH^{1.403} t^{0.306}$
$R^2 = 0.87$ N = 786 F = 847 $\alpha \leq 0.0001$

$[CHBrCl_2] = 10^{-2.874} [DOC]^{0.901} [Cl_2]^{0.017} [Br^-]^{0.733} Temp^{0.498} pH^{1.511} t^{0.199}$
$R^2 = 0.90$ N = 786 F = 1164 $\alpha \leq 0.0001$

$[CHBr_2Cl] = 10^{-5.649} [DOC]^{-0.226} [Cl_2]^{0.108} [Br^-]^{1.81} Temp^{0.512} pH^{2.212} t^{0.146}$
$R^2 = 0.89$ N = 786 F = 1087 $\alpha \leq 0.0001$

$[CHBr_3] = 10^{-7.83} [DOC]^{-0.983} [Cl_2]^{0.804} [Br^-]^{1.765} Temp^{0.754} pH^{2.139} t^{0.566}$
$R^2 = 0.61$ N = 786 F = 199 $\alpha \leq 0.0001$

Molar-Based (μmoles/L) Models:

$[THMs] = 10^{-1.873} [DOC]^{1.222} [Cl_2]^{0.104} [Br^-]^{0.016} Temp^{0.604} pH^{1.538} t^{0.270}$
$R^2 = 0.91$ N = 786 F = 1198 $\alpha \leq 0.0001$

[TTHM] = Total Trihalomethanes (μg/L) or (μMole/L).
$[CHCl_3]$, $[CHBrCl_2]$, $[CHBr_2Cl]$, $[CHBr_3]$ = Individual Concentrations of THM Species (μg/L).
[DOC] = Dissolved Organic Carbon (mg/L) or (mMole/L)
$1.2 \leq [DOC\ (mg/L)] \leq 10.6$, $0.1 \leq [DOC\ (mMole/L)] \leq 0.883$
$[Cl_2]$ = Applied Chlorine (mg/L) or (mMole/L)
$1.51 \leq [Cl_2\ (mg/L)] \leq 33.55$, $0.0213 \leq [Cl_2\ (mMole/L)] \leq 0.472$
$[Br^-]$ = Concentration of Bromide (μg/L) or (μMole/L)
$7 \leq [Br^-\ (\mu g/L)] \leq 600$, $0.0876 \leq [Br^-\ (\mu Mole/L) \leq 7.509$
Temp = Incubation Temperature(°C)
$15 \leq Temp \leq 25$
pH: $6.5 \leq pH \leq 8.5$
t = Incubation Reaction Time (hour)
$2 \leq t \leq 168$

***Source Waters:** BGW, BRW, HMR, ISW, MGW, SLW, SPW, SRW, SXW, VRW, PBW.

(Cl_2/DOC = 0.5, 1, 1.5, 2 and 3 mg/mg), four bromide levels (ambient, ambient + 100 , ambient + 200, ambient + 300 ug/L), three pH levels (6.5, 7.5, and 8.5), three temperatures (15, 20, 25 °C) and six reaction times (2, 12, 24, 48, 96 and 168 hours). Based on the exponents associated with the models, each of the independent variables exerts a positive influence on total THM formation. Both linear and non-linear models were developed preliminarily, with power function models (log/log transforms) deemed as providing the best fit of data. The TTHM models all exhibited a good coefficient of determination, R^2 = 0.90.

Figure 5.3 shows data simulation in which predicted (modeled) results are compared against measured (experimental) values; this internal validation demonstrates the good simulation capabilities of the TTHM model. It is noteworthy that the molar-based model for TTHM does not provide significantly better predictive capabilities than the weight-based model.

THM SPECIES; RAW/UNTREATED WATERS

The development of THM speciation models can provide an indirect means of estimating total THM formation (summation of individual species), can help describe the relative importance of each THM component behavior under various conditions, and can elucidate the influence of bromide ion on THM species distribution. Individual THM species models were first developed by Chowdhury, *et al.* (1991). Their models allow a quantitative assessment of bromide effects on overall THM formation as well as THM speciation; however, they are only valid for raw/untreated waters. Predictive models for THM species formation for both raw/untreated and treated water have been developed in this study. These models will be discussed in this (raw/untreated) and the next (treated) section.

Table 5.1 also shows weight-based models for predicting individual THM species formation. The R^2 values for the three models which predict chloroform ($CHCl_3$), bromodichloromethane ($CHBr_2Cl$), and dibromochloromethane ($CHBr_2Cl$) formation range from 0.87 to 0.90, while for bromoform ($CHBr_3$), the R^2 was only 0.61. Bromide plays a very important role in THM species formation and distribution. Bromide has a negative effect on chloroform formation and a positive influence on the brominated species, at least over the range of the indicated boundary conditions. Formation of brominated versus chlorinated THM species is affected by the competition between bromine and chlorine. The boundary conditions for the TTHM and THM species models are listed in Table 5.1. Besides use of the TTHM predictive model, there is an alternative approach for predicting TTHM through summation of individual (predicted) THM

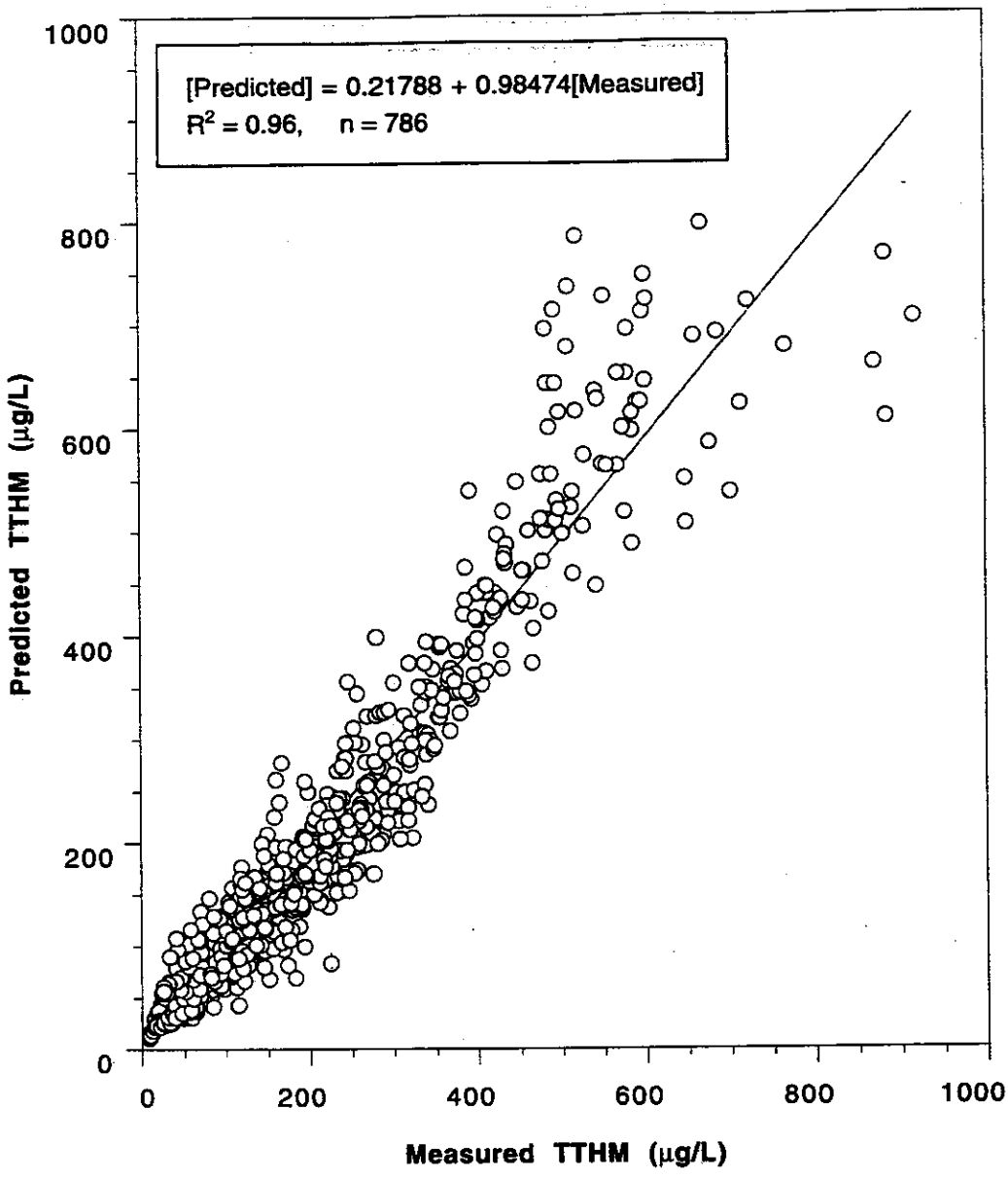

Figure 5.3 Predicted versus Measured Values for Raw/Untreated Water TTHM; Weight-Based (µg/L) Model

species from the THM species models. Figure 5.4 shows the relationship between the summation of predicted THM individual species (from individual species models) versus TTHM from the overall model; it is apparent that both approaches have merit, although the TTHM model is superior in predictive capability based on its R^2 (0.90) compared to the R^2 (0.61 - 0.90) values for each of the four species models. As shown in Figure 5.4, the summation approach tends to overpredict.

COAGULATED WATERS

One of the objectives of this research was to define coagulation effects on the formation and kinetics of TTHM and THM species. Coagulation was emphasized in this effort because of the recent regulatory emphasis placed on precursor removal. Proposed regulations will require that utilities evaluate enhanced coagulation if their TOC level before post-disinfection is ≥ 2 mg/L. Jar tests were employed to evaluate precursor removal by both alum and iron (ferric chloride) coagulation; the precursor removals observed were described in Chapter 3. Coagulant doses were selected through screening experiments as those providing a target DOC reduction of between 25% to 50%. Chlorination of coagulated waters was carried out at a pH of 7.5, a temperature of 20 °C, and ambient bromide level. Cl_2/DOC ratios of 1 and 3 mg/mg were employed over reaction times of 2 to 168 hours. In these models, temperature and pH were not varied.

A major effect of chemical coagulation is that it increases the ratio of Br^-/DOC. While removal of the organic precursor (DOC) is achieved, the inorganic precursor (Br^-) passes conservatively through the coagulation process. The net effect of this increase in Br^-/DOC ratio is a shift toward the formation of brominated THMs.

Table 5.2 shows predictive coagulated-water models for TTHM and THM species formation based on alum as a coagulant for eight water sources (n = 143). Corresponding boundary conditions are also indicated in Table 5.2. In the predictive model for TTHM, the exponents show the positive effect of DOC, chlorine dose, bromide level and reaction time. Bromide shows a negative effect on $CHCl_3$ formation. In the THM species models, chlorine dose appears to negatively affect $CHBrCl_2$ and $CHBr_3$; this is likely just a statistical anomaly arising from the simultaneous interaction of both chlorine and bromine (from chlorine oxidation of bromide) in forming brominated THM species.

Table 5.3 shows coagulated-water models for TTHM and THM species formation with iron as a coagulant. A comparison of model exponents shown in

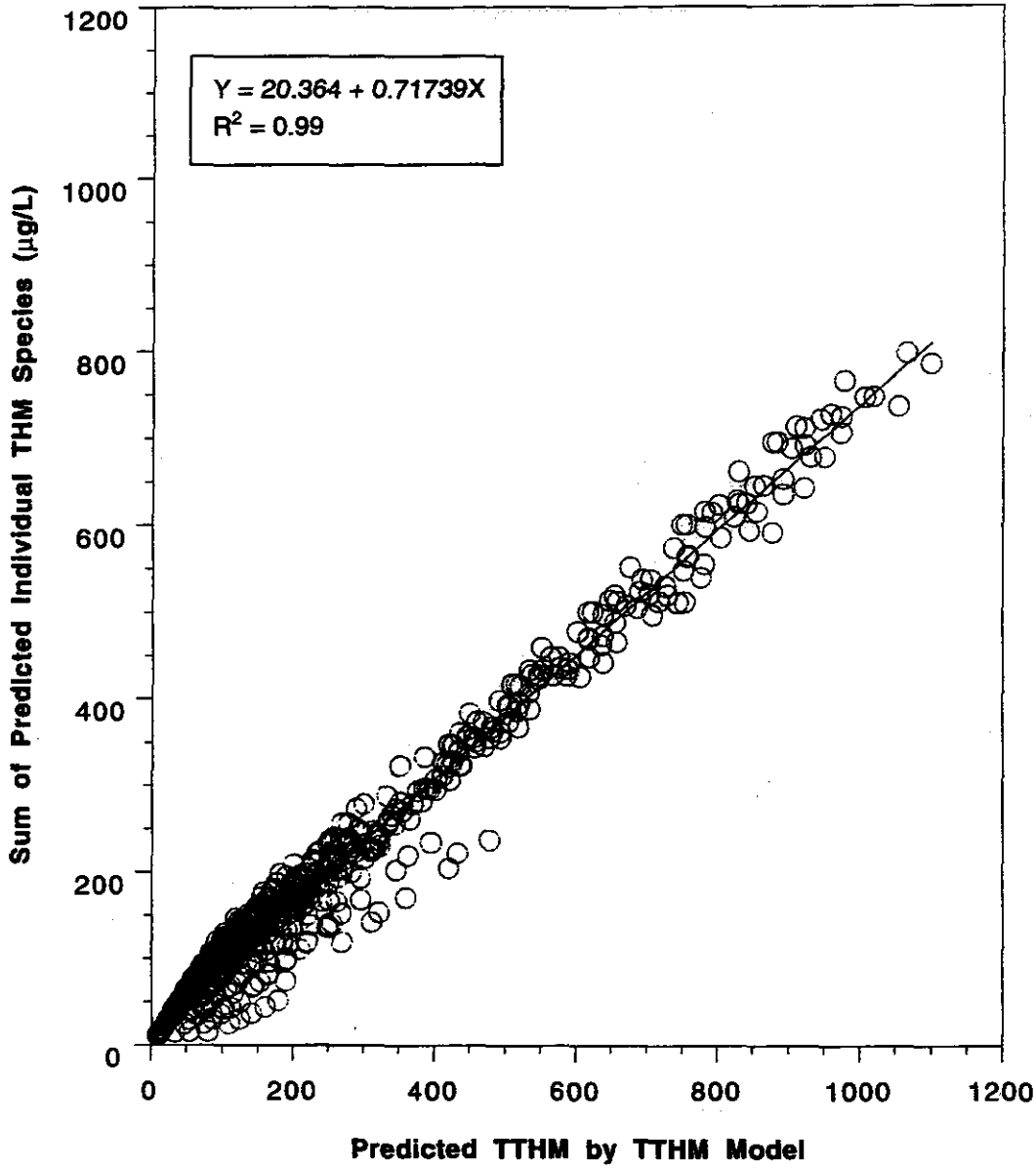

Figure 5.4 **Summation of Predicted THM Species vs Predicted Raw-Water TTHM; Weight-Based Models (µg/L)**

Table 5.2 Predictive Coagulated-Water Models for TTHM and THM Species: Alum Models*

Alum Coagulated Water Models:

$$[TTHM] = 10^{0.651}\,[DOC]^{0.752}\,[Cl_2]^{0.246}\,[Br^-]^{0.185}\,t^{0.258}$$
$R^2 = 0.87$ $N = 143$ $F = 224$ $\alpha \leq 0.0001$

$$[CHCl_3] = 10^{1.331}[DOC]^{1.11}\,[Cl_2]^{0.324}[Br^-]^{-0.532}\,t^{0.341}$$
$R^2 = 0.90$ $N = 143$ $F = 323$ $\alpha \leq 0.0001$

$$[CHBrCl_2] = 10^{-0.203}[DOC]^{0.504}\,[Cl_2]^{0.126}[Br^-]^{0.474}\,t^{0.187}$$
$R^2 = 0.84$ $N = 143$ $F = 181$ $\alpha \leq 0.0001$

$$[CHBr_2Cl] = 10^{-5.398}[DOC]^{0.943}\,[Cl_2]^{-0.228}[Br^-]^{2.678}\,t^{0.175}$$
$R^2 = 0.31$ $N = 143$ $F = 15$ $\alpha \leq 0.0001$

$$[CHBr_3] = 10^{-9.6}[DOC]^{0.203}\,[Cl_2]^{-0.639}[Br^-]^{4.487}\,t^{0.319}$$
$R^2 = 0.73$ $N = 143$ $F = 92$ $\alpha \leq 0.0001$

[TTHM] = Total Trihalomethanes (µg/L)

$[CHCl_3]$, $[CHBrCl_2]$, $[CHBr_2Cl]$, $[CHBr_3]$ = Individual Concentrations of four THM Species (µg/L)

[DOC] = Dissolved Organic Carbon in Coagulated Water (mg/L)
$1.00 \leq [DOC\ (mg/L)] \leq 7.77$

$[Cl_2]$ = Applied Chlorine (mg/L)
$1.11 \leq [Cl_2\ (mg/L)] \leq 24.75$

$[Br^-]$ = Concentration of Bromide (µg/L)
$36 \leq [Br^-\ (\mu g/L)] \leq 308$

pH = 7.5

Temp = 20 °C

t = Incubation Reaction Time (hour)
$2 \leq t \leq 168$

***Source Waters:** BRW, HMR, ISW, SPW, SRW, SXW, VRW, PBW

Table 5.3 Predictive Coagulated-Water Models for TTHM and THM Species: Iron Models*

Iron Coagulated Water Models:

$[TTHM] = 10^{0.387} [DOC]^{0.839} [Cl_2]^{0.287} [Br^-]^{0.259} t^{0.270}$
$R^2 = 0.88$ N = 143 F = 248 $\alpha \leq 0.0001$

$[CHCl_3] = 10^{1.092} [DOC]^{1.179} [Cl_2]^{0.378} [Br^-]^{-0.454} t^{0.326}$
$R^2 = 0.92$ N = 143 F = 372 $\alpha \leq 0.0001$

$[CHBrCl_2] = 10^{-0.416} [DOC]^{0.599} [Cl_2]^{0.125} [Br^-]^{0.533} t^{0.205}$
$R^2 = 0.84$ N = 143 F = 177 $\alpha \leq 0.0001$

$[CHBr_2Cl] = 10^{-5.127} [DOC]^{0.194} [Cl_2]^{0.433} [Br^-]^{2.427} t^{0.294}$
$R^2 = 0.34$ N = 143 F = 18 $\alpha \leq 0.0001$

$[CHBr_3] = 10^{-9.427} [DOC]^{-0.329} [Cl_2]^{-0.035} [Br^-]^{4.335} t^{0.307}$
$R^2 = 0.72$ N = 143 F = 91 $\alpha \leq 0.0001$

[TTHM] = Total Trihalomethanes (µg/L)

$[CHCl_3]$, $[CHBrCl_2]$, $[CHBr_2Cl]$, $[CHBr_3]$ = Individual Concentrations of four THM Species (µg/L)

[DOC] = Dissolved Organic Carbon in Coagulated Water (mg/L)
$1.00 \leq [DOC\ (mg/L)] \leq 7.77$

$[Cl_2]$ = Applied Chlorine (mg/L)
$1.11 \leq [Cl_2\ (mg/L)] \leq 24.75$

$[Br^-]$ = Concentration of Bromide (µg/L)
$36 \leq [Br^-\ (\mu g/L)] \leq 308$

pH = 7.5

Temp = 20 °C

t = Incubation Reaction Time (hour)
$2 \leq t \leq 168$

***Source Waters:** BRW, HMR, ISW, SPW, SRW, SXW, VRW, PBW

Tables 5.3 and 5.2 indicate that the net effects of the two different coagulants on TTHM and THM species formation are similar. A comparison of alum and iron shows that they both have similar capabilities of DOC reduction and THM precursor removal.

Table 5.4 presents coagulated-water models which are based on the combined data base derived from both alum and iron coagulation (n = 286). Data simulation is shown in Figure 5.5 where predicted TTHM is based on the combined alum plus iron treated-water model. Over the higher concentration range, TTHM is under predicted; overpredictions are seen over lower concentration ranges. In contrast to Figure 5.5, which shows data simulation with the entire eight-water data base, Figure 5.6 portrays data simulation for data with each source water separately identified. It can be seen that the model simulates TTHM data well for seven of eight waters, with the exception of SXW.

Coagulation not only removes bulk DOC but also may preferentially remove more reactive THM precursors. Precursor reactivity can be described through use of a reactivity coefficient, ϕ:

$$\phi = (THM/DOC)_{trt}/(THM/DOC)_{raw} \qquad \text{where } \phi = 0 \text{ to } 1.0 \qquad (5.2)$$

Consideration of precursor reactivity can provide an alternative modeling approach for coagulated waters. In this approach, THM levels in treated waters can be estimated by using raw water models in which a $(\phi)DOC_{trt}$ term is substituted for the general DOC_{raw} term; the DOC_{trt} reflects the reduced precursor level while the ϕ term adjusts for the reduced reactivity of the precursor remaining compared to the raw water precursor reactivity. The precursor reactivities of the eight sources evaluated at 2, 24, and 96 hour reaction times are summarized in Table 5.5. Except for SRW and ISW, the ϕ values ranged from 0.55 to 0.86 for alum-treated and from 0.54 to 0.87 for iron-treated waters. Figure 5.7 shows predicted versus measured values for alum and iron coagulated/treated waters using the raw/untreated water-model coupled with the ϕ (24-hour) concept. A comparison of predictions from the treated-water model versus the raw/untreated-water model coupled with ϕ (24-hour) and without ϕ is shown in Figure 5.8, shown as an extension of Figure 5.7. The predictions provided by the treated-water model are most accurate. The predictions by the raw/untreated-water model without ϕ correspond to overpredictions; predictions by the raw/untreated-water model coupled with ϕ represent underpredictions. Thus, the treated water models have most merit in predictive capabilities, while the ϕ based models represent an alternative

Table 5.4 Predictive Coagulated-Water Models for TTHM and THM Species: Combined Alum plus Iron Models*

Weight-Based (μg/L) Models:

$[TTHM]=10^{0.518}\,[DOC]^{0.801}\,[Cl_2]^{0.261}\,[Br^-]^{0.223}\,t^{0.264}$
$R^2 = 0.87$ N = 287 F = 458 $\alpha \le 0.0001$

$[CHCl_3]=10^{1.211}\,[DOC]^{1.149}\,[Cl_2]^{0.345}\,[Br^-]^{-0.492}\,t^{0.333}$
$R^2 = 0.91$ N = 287 F = 680 $\alpha \le 0.0001$

$[CHBrCl_2]=10^{-0.311}\,[DOC]^{0.556}\,[Cl_2]^{0.121}\,[Br^-]^{0.505}\,t^{0.196}$
$R^2 = 0.83$ N = 287 F = 351 $\alpha \le 0.0001$

$[CHBr_2Cl]=10^{-5.248}\,[DOC]^{0.55}\,[Cl_2]^{0.105}\,[Br^-]^{2.549}\,t^{0.234}$
$R^2 = 0.32$ N = 287 F = 34 $\alpha \le 0.0001$

$[CHBr_3]=10^{-9.5}\,[DOC]^{-0.075}\,[Cl_2]^{-0.34}\,[Br^-]^{4.409}\,t^{0.313}$
$R^2 = 0.72$ N = 287 F = 185 $\alpha \le 0.0001$

Molar-Based (μmoles/L) Models:

$[TTHM]=10^{0.188}\,[DOC]^{0.887}\,[Cl_2]^{0.276}\,[Br^-]^{0.084}\,t^{0.276}$
$R^2 = 0.89$ N = 287 F = 561 $\alpha \le 0.0001$

[TTHM] = Total Trihalomethanes (μg/L) or (μmoles/L)

$[CHCl_3]$, $[CHBrCl_2]$, $[CHBr_2Cl]$, $[CHBr_3]$ = Individual THM Species (μg/L)

DOC] = Dissolved Organic Carbon in Coagulated Water (mg/L) or (mMole/L)
$1.00 \le [DOC\ (mg/L)] \le 7.77$, $0.0833 \le [DOC\ (mMole/L)] \le 0.648$

$[Cl_2]$ = Applied Chlorine (mg/L) or (mMole/L)
$1.11 \le [Cl_2\ (mg/L)] \le 24.75$, $0.0156 \le [Cl_2\ (mMole/L)] \le 0.349$

$[Br^-]$ = Concentration of Bromide (μg/L) or (μMole/L)
$36 \le [Br^-\ (\mu g/L)] \le 308$, $0.451 \le [Br^-\ (\mu Mole/L)] \le 3.899$

pH = 7.5

Temp = 20 °C

t = Incubation Reaction Time (hour)
$2 \le t \le 168$

***Source Waters:** BRW, HMR, ISW, SPW, SRW, SXW, VRW, PBW

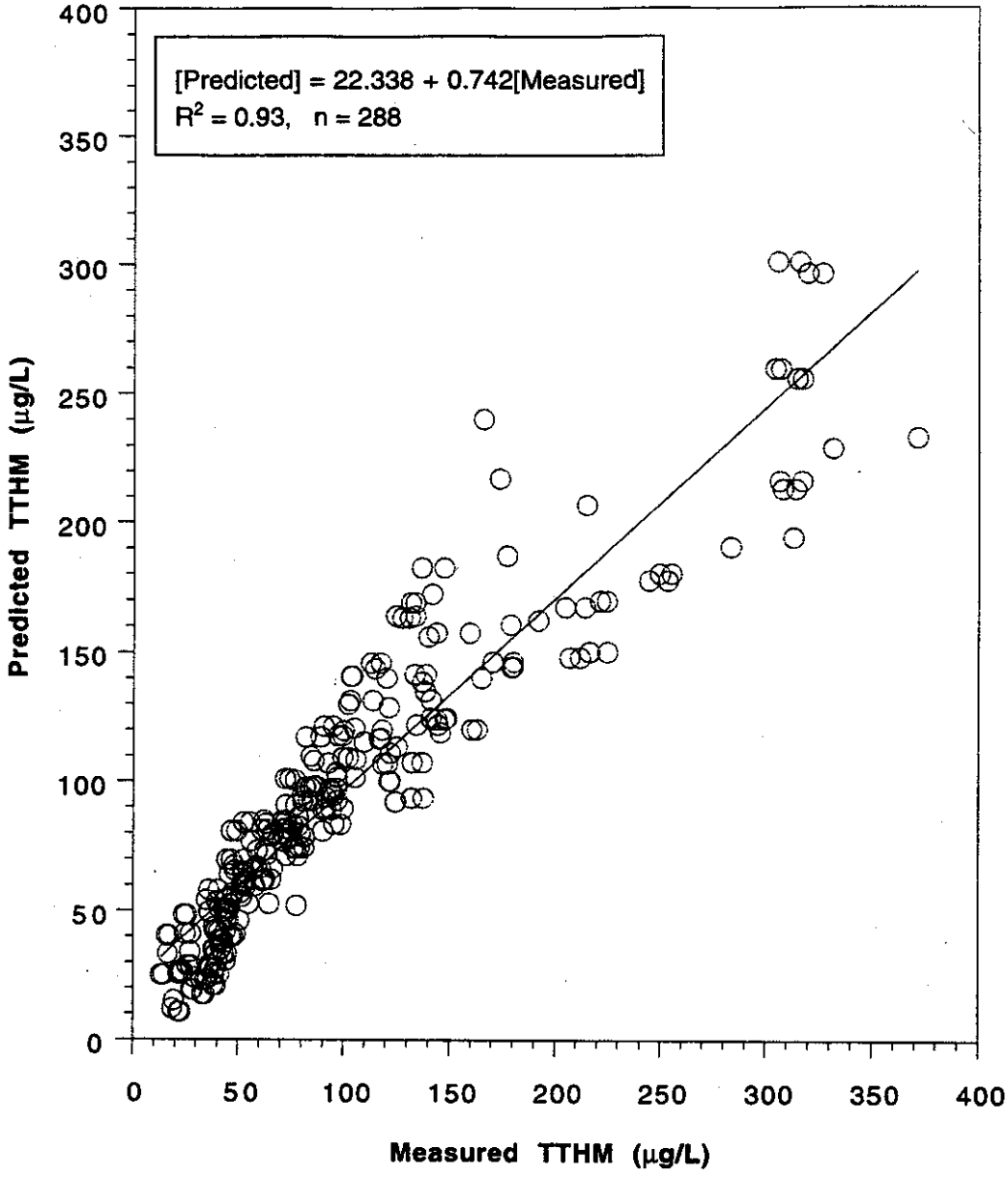

Figure 5.5 **Predicted versus Measured Values of TTHM for Coagulated/Treated Waters Using Combined Alum plus Iron Treated-Water Models**

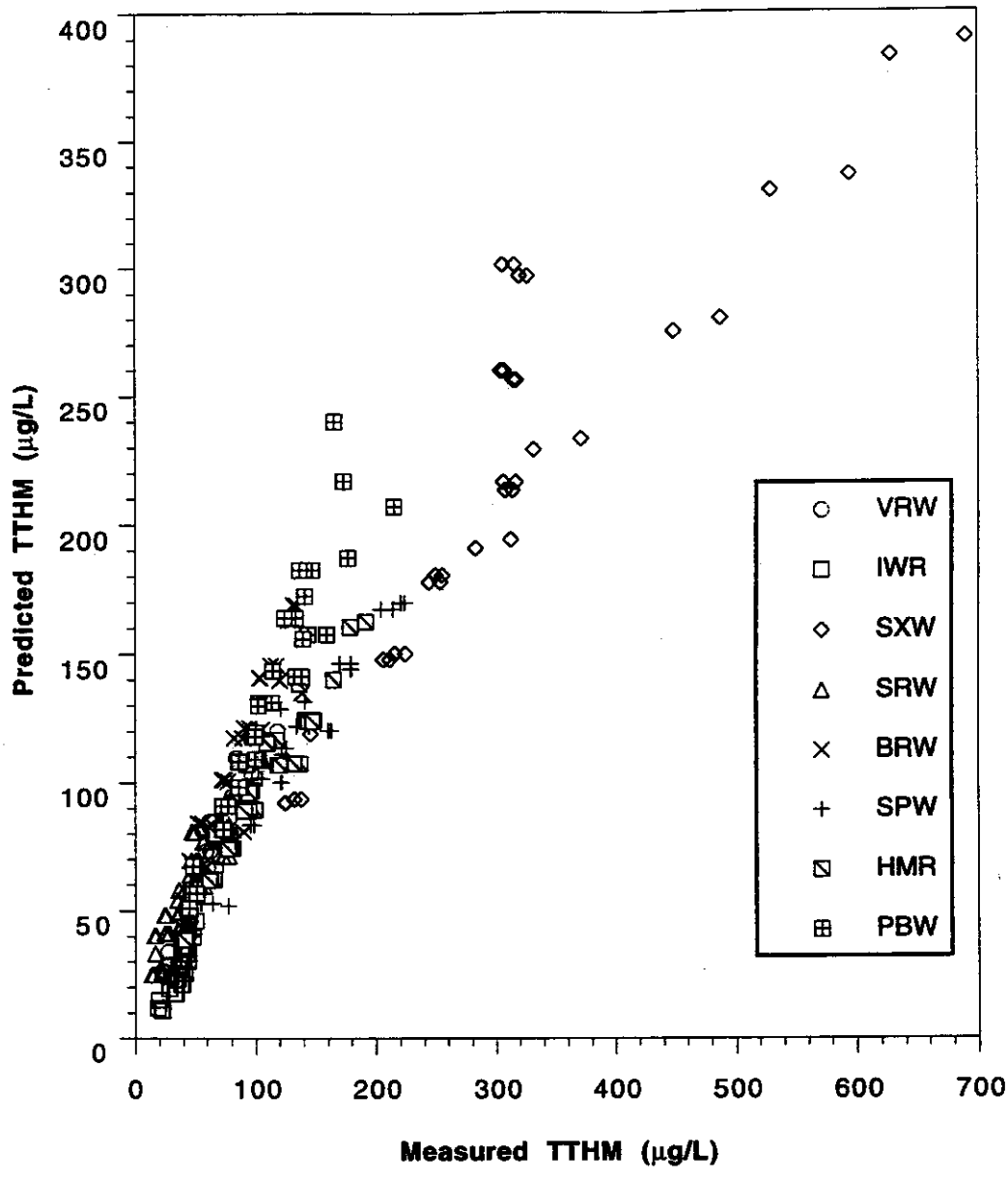

Figure 5.6 **Predicted versus Measured Values of TTHM for Coagulated/Treated Waters Using Combined Alum plus Iron Treated-Water Models; Individual Sources**

Table 5.5 Summary of Reactivity Coefficient, Ø, Values for TTHM

Water		DOC (mg/L)	Br^- (µg/L)	Ø (2 hr)	Ø (24 hr)	Ø (96 hr)
SPW	Raw	4.19	312	1.00	1.00	1.00
	Alum	2.56	306	0.89	0.77	1.00
	Iron	2.58	308	0.93	0.67	1.03
BRW	Raw	3.54	250	1.00	1.00	1.00
	Alum	2.72	245	0.83	0.81	0.57
	Iron	2.63	245	0.92	0.80	0.61
SRW	Raw	4.18	50	1.00	1.00	1.00
	Alum	2.56	48	0.82	0.28	0.72
	Iron	2.55	46	0.54	0.38	0.67
HMR	Raw	5.73	40	1.00	1.00	1.00
	Alum	4.29	37	0.50	0.56	0.76
	Iron	4.23	38	0.50	0.54	0.68
PBW	Raw	10.6	97	1.00	1.00	1.00
	Alum	4.6	97	0.57	0.67	0.62
	Iron	4.2	97	0.59	0.62	0.62
ISW	Raw	2.78	84	1.00	1.00	1.00
	Alum	1.00	83	1.01	1.03	1.00
	Iron	1.03	83	0.85	0.90	1.01
VRW	Raw	3.67	71	1.00	1.00	1.00
	Alum	2.56	68	0.67	0.69	0.74
	Iron	2.35	68	0.62	0.63	0.67
SXW	Raw	10.55	68	1.00	1.00	1.00
	Alum	7.77	67	0.88	0.86	0.85
	Iron	7.63	67	0.84	0.87	0.90

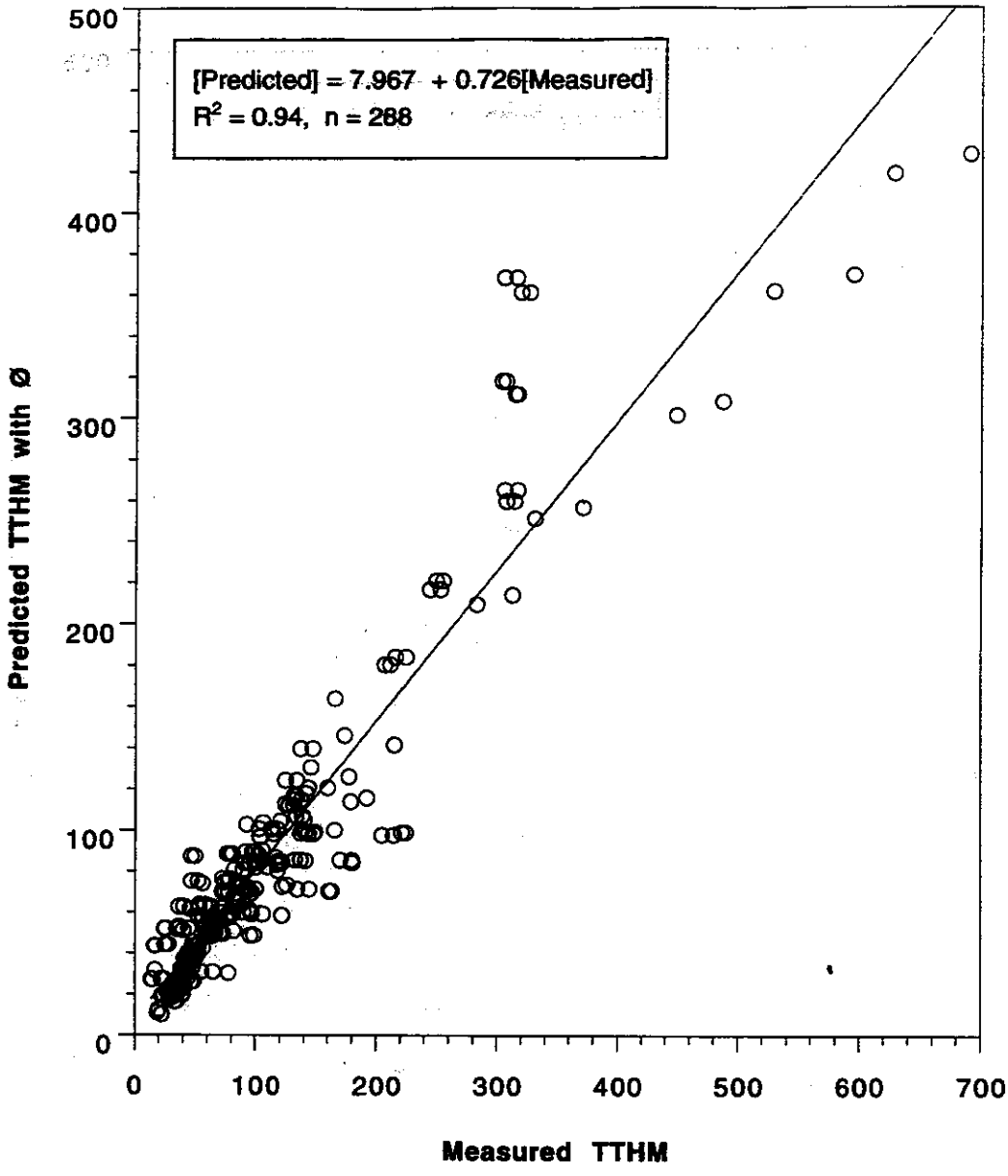

Figure 5.7 **Predicted versus Measured Values of TTHM for Alum and Iron Coagulated/Treated Waters Using Raw/Untreated Water-Modelswith Ø (24-hour) Concept.**

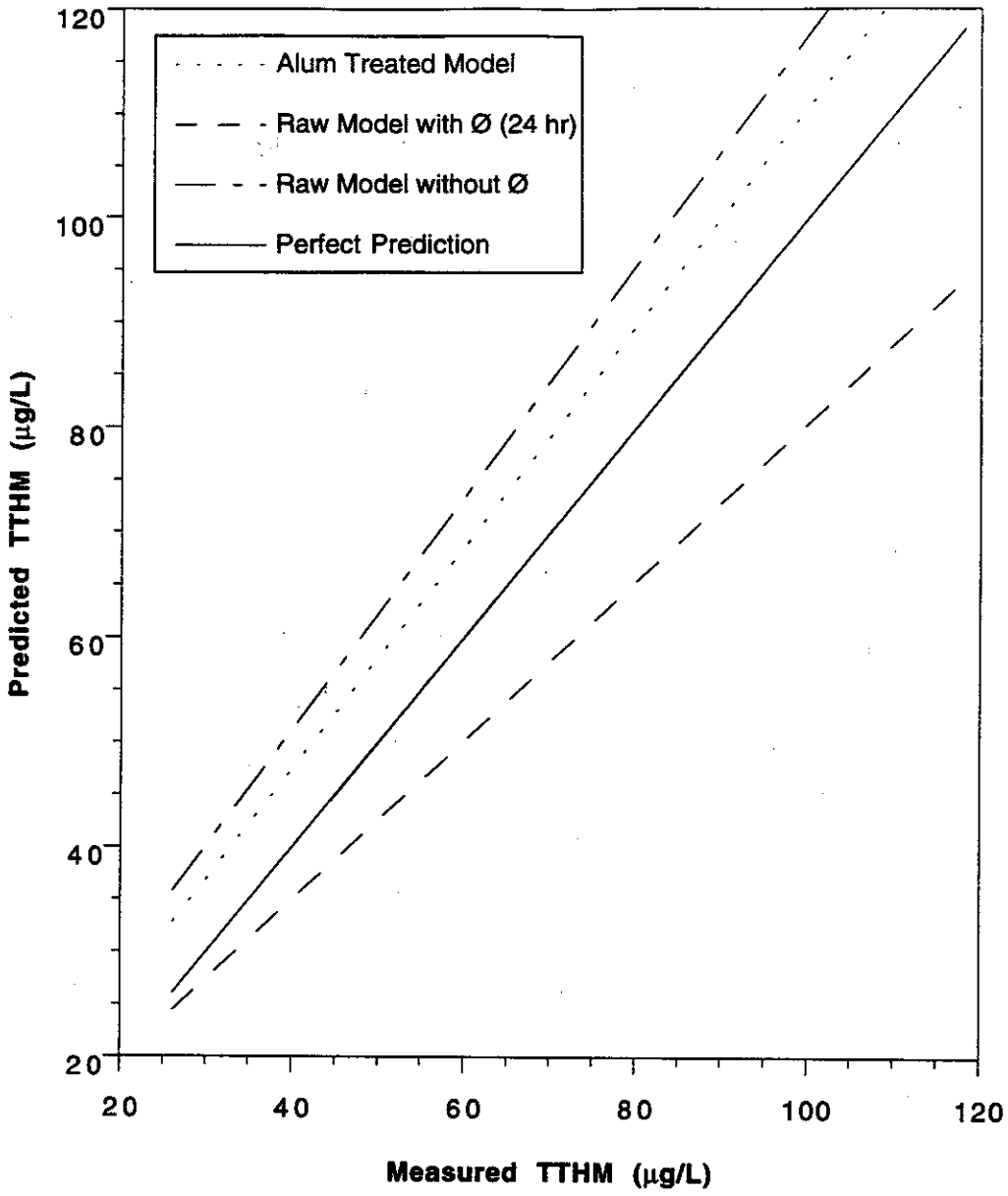

Figure 5.8 Comparison of Predictions from Treated-Water Models versus Raw/Untreated Water Models with Ø.

framework based on precursor activity.

EFFECTS OF BROMIDE ON THM SPECIES FORMATION

Bromide ion (Br^-) is often found in drinking water sources through various pathways including geochemical weathering, connate seawater, and seawater intrusion. The concentrations of Br^- in natural surface and ground waters, except seawater, exhibit a wide range from less than 0.01 mg/L to more than 1 mg/L, with an average of about 0.1 mg/L. During chlorination, Br^- is oxidized by chlorine to form hypobromous acid (HOBr) and/or hypobromite ion (OBr^-) (Gordon, 1987):

$$HOCl + Br^- \rightarrow HOBr + Cl^- \qquad (5.3)$$

Hypobromous acid can react with natural organic matter (NOM) to produce brominated DBPs such as bromoform. Collectively, the relative amounts of HOCl and HOBr determine the THM species distribution.

Gould et al. (1983) studied the effects of Br^- on total trihalomethane and individual THM species formation kinetics. They formulated the order of THM species formation kinetics: $CHCl_3 < CHBrCl_2 < CHBr_2Cl < CHBr_3$ (Gould, 1983). In other words, the THM species having higher Br^- concentration form faster than those having less Br^- concentration.

Of the four THM species, three are brominated. The amount of bromide ion present influences the overall THM formation as well as speciation. Of course, besides this inorganic THM precursor, DOC represents the organic THM precursor. Through examination of scatter-plot trends, we found that the ratio of Br^-/DOC, the ratio of inorganic to organic precursor, most accurately captures bromide effects on THM speciation. We developed fractional concentration models for each species as a function of the ratio of Br^-/DOC. In these models, fractional THM species concentrations, ranging from 0 to 1.0, were defined by the ratio of THM species/TTHM; thus, the individual species fractional concentrations should sum to 1.0 for TTHM = Σ(THM Species). Fractional concentration models as function of Br^-/DOC at reaction times of 24 hours and 96 hours are shown in Tables 5.6 and 5.7, respectively. These models are based on both raw and treated waters; thus, they can be used to predict THM species for both raw and treated waters. As Br^-/DOC increases, $CHCl_3$ decreases exponentially; the two intermediate species, $CHBrCl_2$, and $CHBr_2Cl$, increase then decrease in a polynomial pattern. In theory, $CHBr_3$ should increase in an inverse (S-shaped) manner as a function of Br^-/DOC. However, we found a better statistical fit by using a polynomial function with the

Table 5.6 Summary of Fractional-Concentration THM Speciation Models; 24-Hours

Exponential Fit
Species = $(a)(exp^{bx})$ where x = Br^-/DOC

Species	a	b	r^2
Chloroform	0.670	- 9.667	0.93

2nd order Polynomial Fits
Species = $a + bx + cx^2$ where x = Br^-/DOC

Species	a	b	c	r^2
Bromodichloromethane	0.218	1.817	- 6.465	0.54
Dibromochloromethane	- 0.0285	4.679	- 10.236	0.95
Bromoform	- 0.0315	1.782	- 2.619	0.93

(n = 71 total; = 43 for raw waters; = 28 for treated waters)

Table 5.7 Summary of Fractional-Concentration THM Speciation Models; 96-Hours

Exponential Fit
Species = $(a)(exp^{bx})$ where x = Br^-/DOC

Species	a	b	r^2
Chloroform	0.727	- 9.178	0.95

2nd order Polynomial Fits
Species = $a + bx + cx^2$ where x = Br^-/DOC

Species	a	b	c	r^2
Bromodichloromethane	0.170	2.375	- 7.460	0.69
Dibromochloromethane	- 0.0318	4.524	- 10.359	0.95
Bromoform	- 0.0266	1.516	- 1.496	0.93

(n = 71 total; = 43 for raw waters; = 28 for treated waters)

stipulation of boundary conditions to prevent decreasing predictions at very high Br^-/DOC levels. Data simulations are presented in Figures 5.9 and 5.10, showing measured and predicted THM species (fractional concentrations) versus Br^-/DOC (mg/mg) at 24-hour and 96-hour reaction times, respectively.

SIMULATION AND VALIDATION OF TTHM PREDICTIVE MODEL

Internal data simulation/validation has been discussed in the previous sections. External validation can be conducted by employing literature data not used in the calibration of the model. Based on available literature data, an external validation of the TTHM predictive raw-water model was performed by using data from a data base created by James M. Montgomery Engineers (1991). All measured TTHM values from eight utilities in their data base are employed in the validation. These eight utilities have the following raw water characteristics: pH values from 6.8 to 8.5 with an average of 7.59; TOC concentrations from 3.0 to 11 mg/L with an average of 5.51 mg/L; bromide levels from less than 10 to 430 ug/L with an average of 119 ug/L. The THM formation experiments done by JMM were conducted by providing a chlorine dose from 3.0 to 25.3 mg/L (Cl_2/TOC of 1.0 to 2.3 mg/mg) with an average of 10.93 mg/L; reaction temperature was kept constant at 20 °C; reaction time was varied from 0.1 to 98.7 hours. Figure 5.11 shows predicted TTHM versus measured TTHM provided using the JMM data base, here highlighting molar predictions. Eighty cases (n = 80) are involved. Regression of predicted versus measured values shows a generally good fit of data, with an intercept of 0.0218, a slope of 1.174 and a R value of 0.917. The value of the slope (> 1) indicates that the model slightly overpredicts.

An attempt to compare two TTHM predictive models, the one developed in this study and the original model developed by Amy and Chadik (1987 (hereafter the "Amy model") was accomplished using these same TTHM data from the JMM data base. A linear regression of predicted TTHM by the "Amy model" against measured TTHM shows an intercept of -0.181, a slope of 1.31, and a R value of 0.958. The "Amy model", based on its regression slope, appeared to overpredict even more than the model developed in this study. The accuracy of the predictions depends on the conditions underlying model development such as source water selection. The experimental matrix design used in creating the data base is also important. Fewer reaction times selected over shorter time periods may cause inaccurate predictions over shorter time frames. In this study, only three reaction times were selected within 24 hours while in the development of "Amy model" seven reaction times were selected within 24 hours. This could be one of the reasons why the R value for the "Amy model" is greater than the one developed in this study since 70% of JMM's data falls

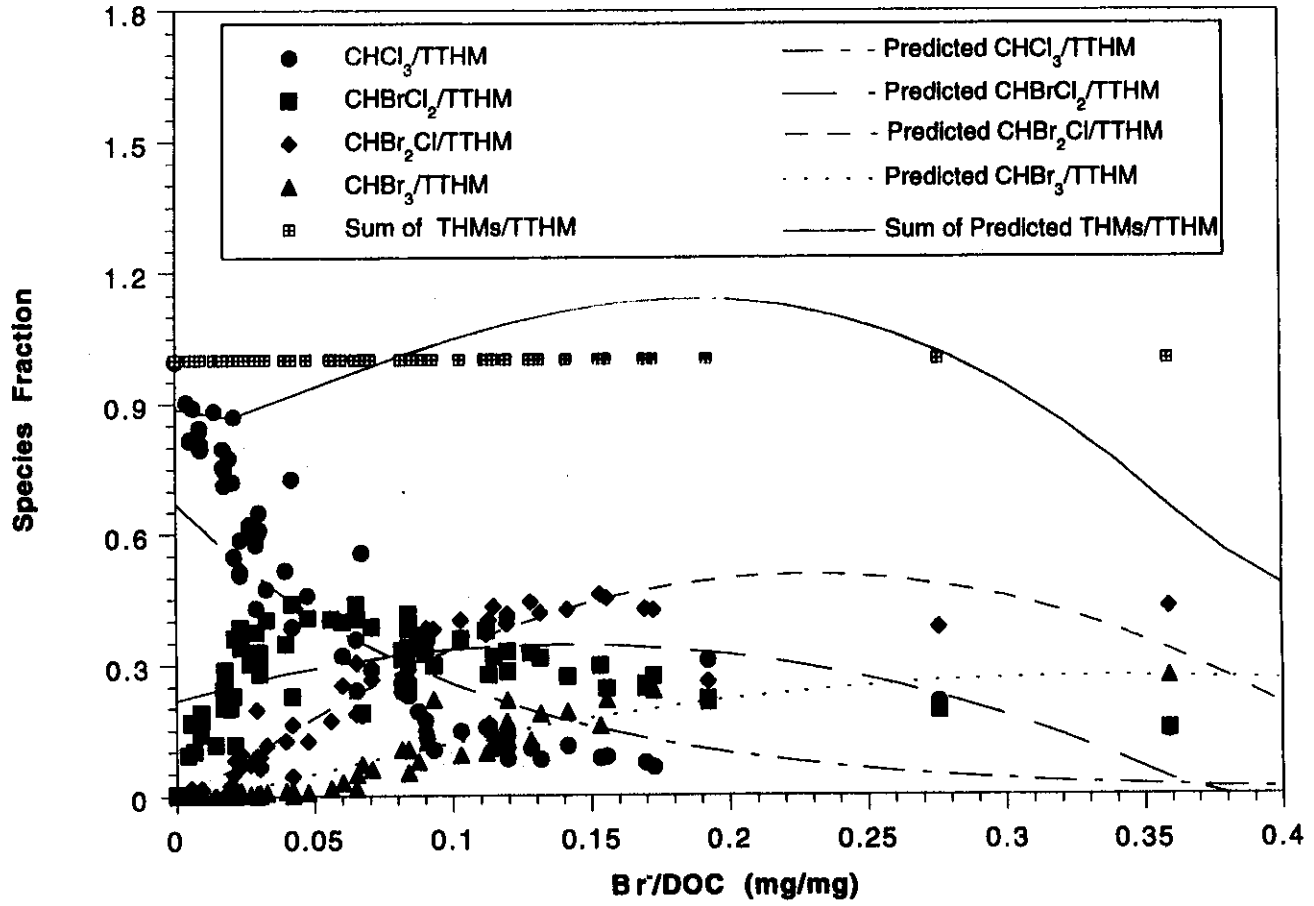

Figure 5.9 Fractional-Concentration Speciation Models; 24-Hour Predictions

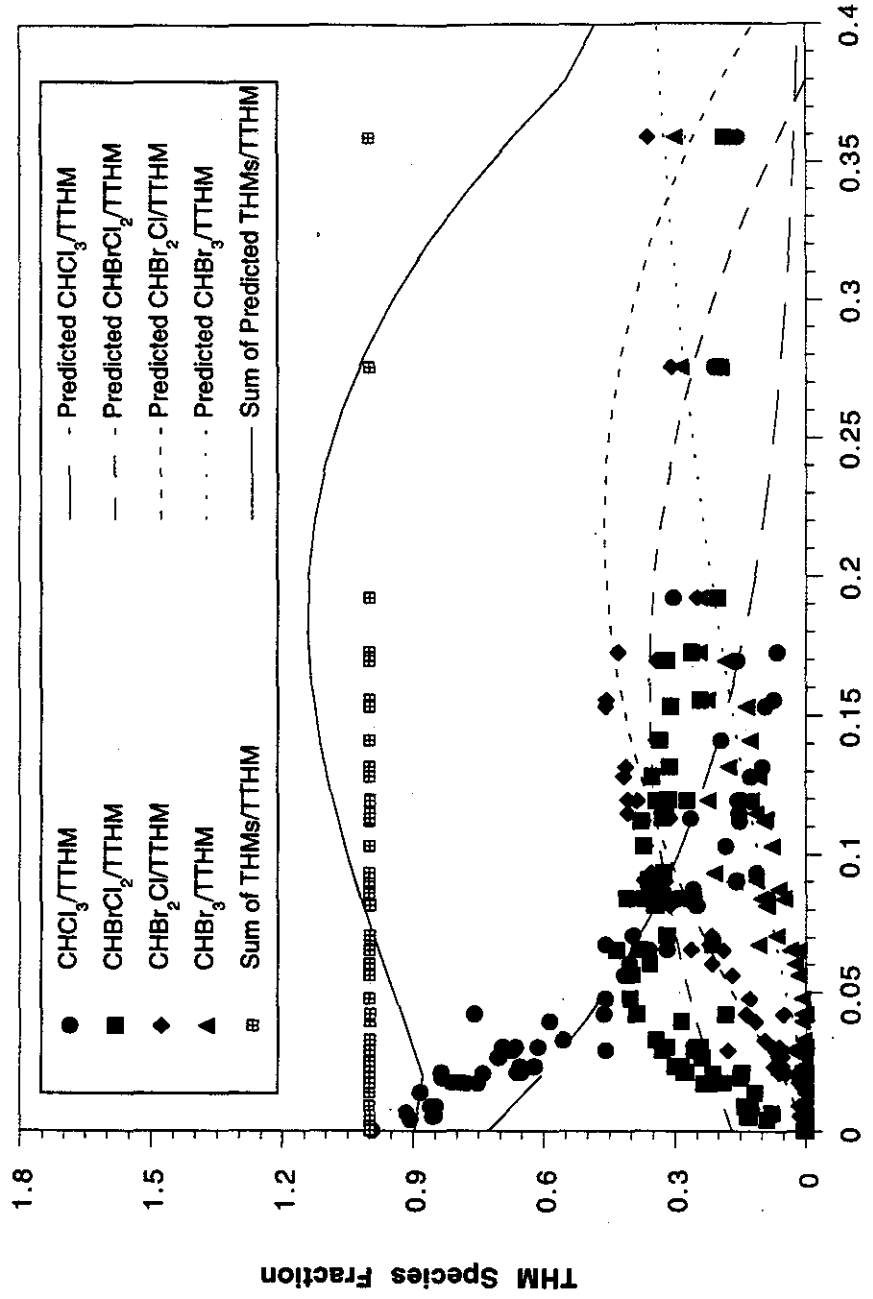

Figure 5.10 Fraction-Concentration Speciation Models; 96-Hour Predictions

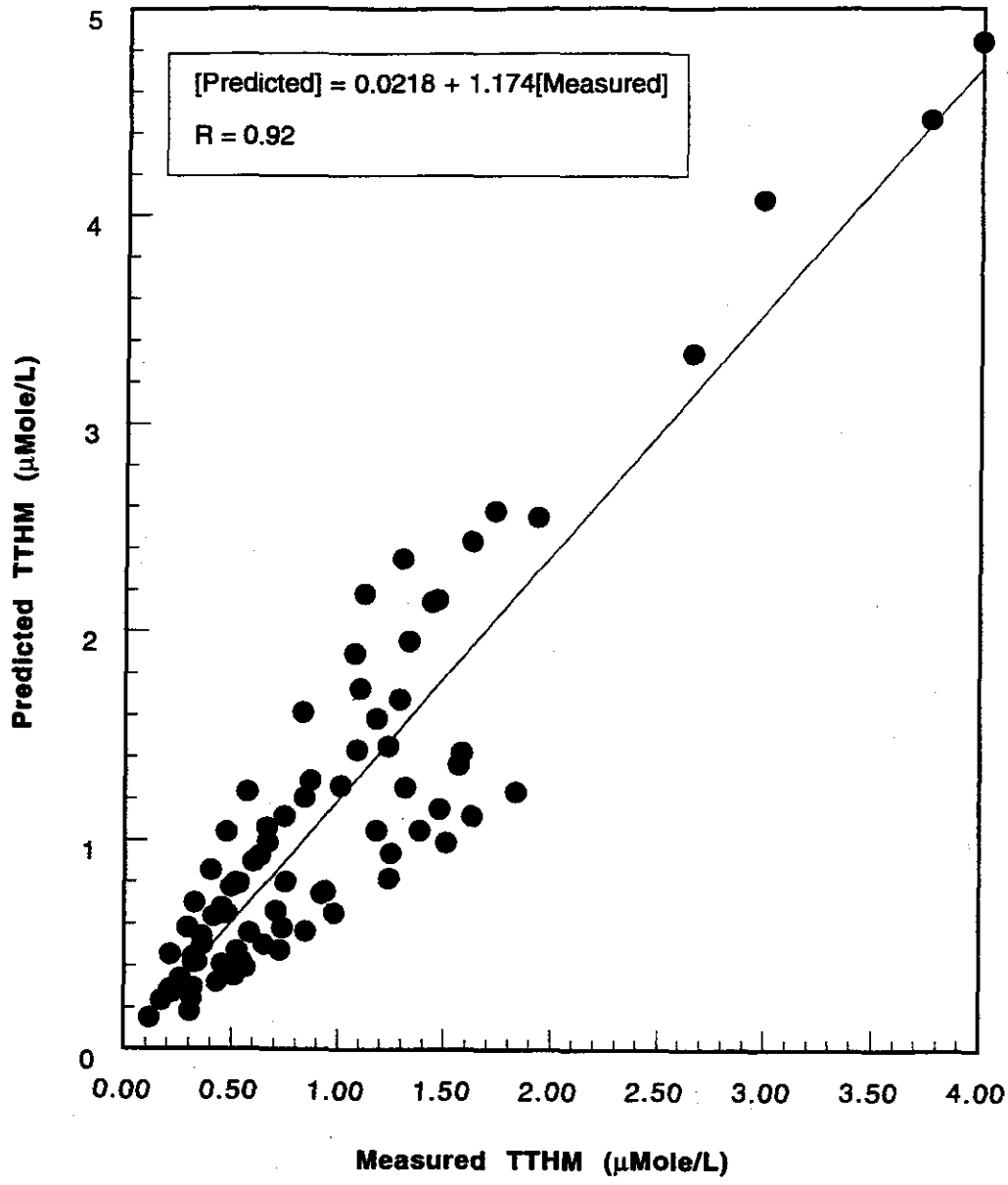

Figure 5.11 **Overall External Validation Using JMM Data with Raw Water TTHM Model (Data from JMM Utilities 3, 5, 6, 7, 12, 21, 26 and 33 at TOC=3.0-11 mg/L, pH=6.8-8.5, Cl_2=3.0-25.3 mg/L, Br^-=10-430 µg/L, Temperature=20°C and Time=0.1-98.7 Hours)**

within a reaction time range of less than 24 hours.

Figure 5.12 shows an external validation of reaction kinetics with the TTHM raw water model using JMM utility 3 data in which the raw water parameters and experimental condition were as follows: TOC = 3.53 mg/L, Cl_2 dose = 7.7 mg/L, Br^- = 10 ug/L, pH = 6.7 and temperature = 20 °C. All predicted values fall within " 20 percent of the measured values.

Figure 5.13 shows a simulation of the effects of coagulation on TTHM formation by the combined alum plus iron treated-water model. This simulation shows that when DOC is reduced from 4 to 2 mg/L, TTHM is reduced by slightly more than 50% when all other independent variables are constant. In this way, the coagulated-water models can be used to assess the effects of coagulation on THM formation.

An external validation of the TTHM treated water model was conducted by using selected data from the JMM data base (JMM 1992). The results of this validation analysis are summarized in Figure 5.14, which shows measured versus predicted TTHM values derived from the alum treated-water model and the combined alum plus iron treated-water model. The six measured values shown are from six different utilities reflecting the following water qualities: pH values from 6.8 to 7.5; TOC (after coagulation) from 2.9 to 3.5 mg/L; bromide levels from 30 to 360 ug/L. The TOC removal ranged from 17% to 50%. The experiments were conduced at a reaction temperature of 20 °C, a reaction time of 16 hours, and chlorine dose from 2.7 to 8.4 mg/L. Figure 5.14 shows excellent predictive capabilities by both the alum treated-water model and the combined alum plus iron treated-water model.

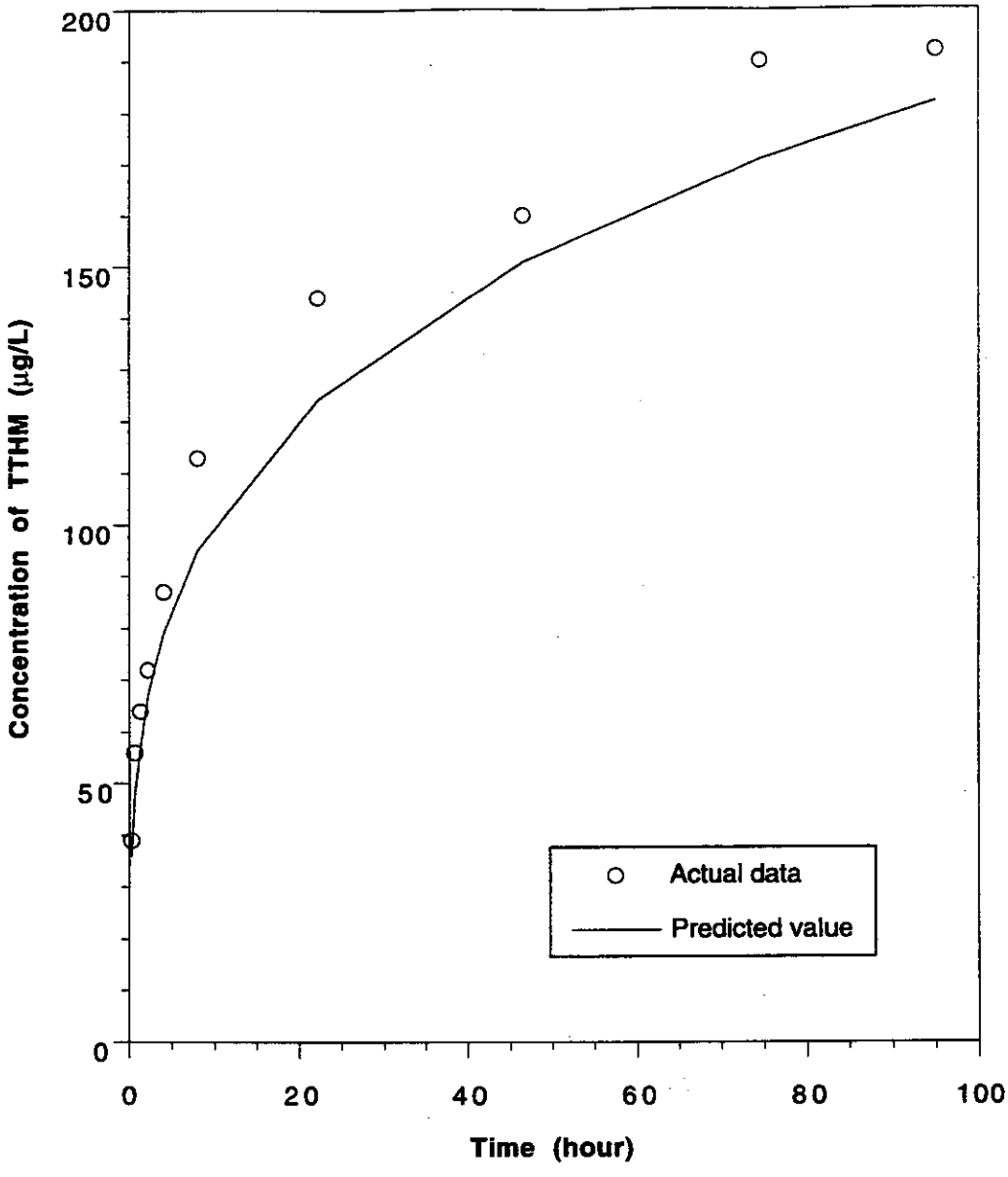

Figure 5.12 **External Validation of Kinetics Using JMM Data with TTHM Raw Water Model (Data from JMM Utility 3 at TOC=3.53 mg/L, Cl_2 Dose=7.7 mg/L, Br^-=10 µg/L, pH=6.7 and T=20 °C)**

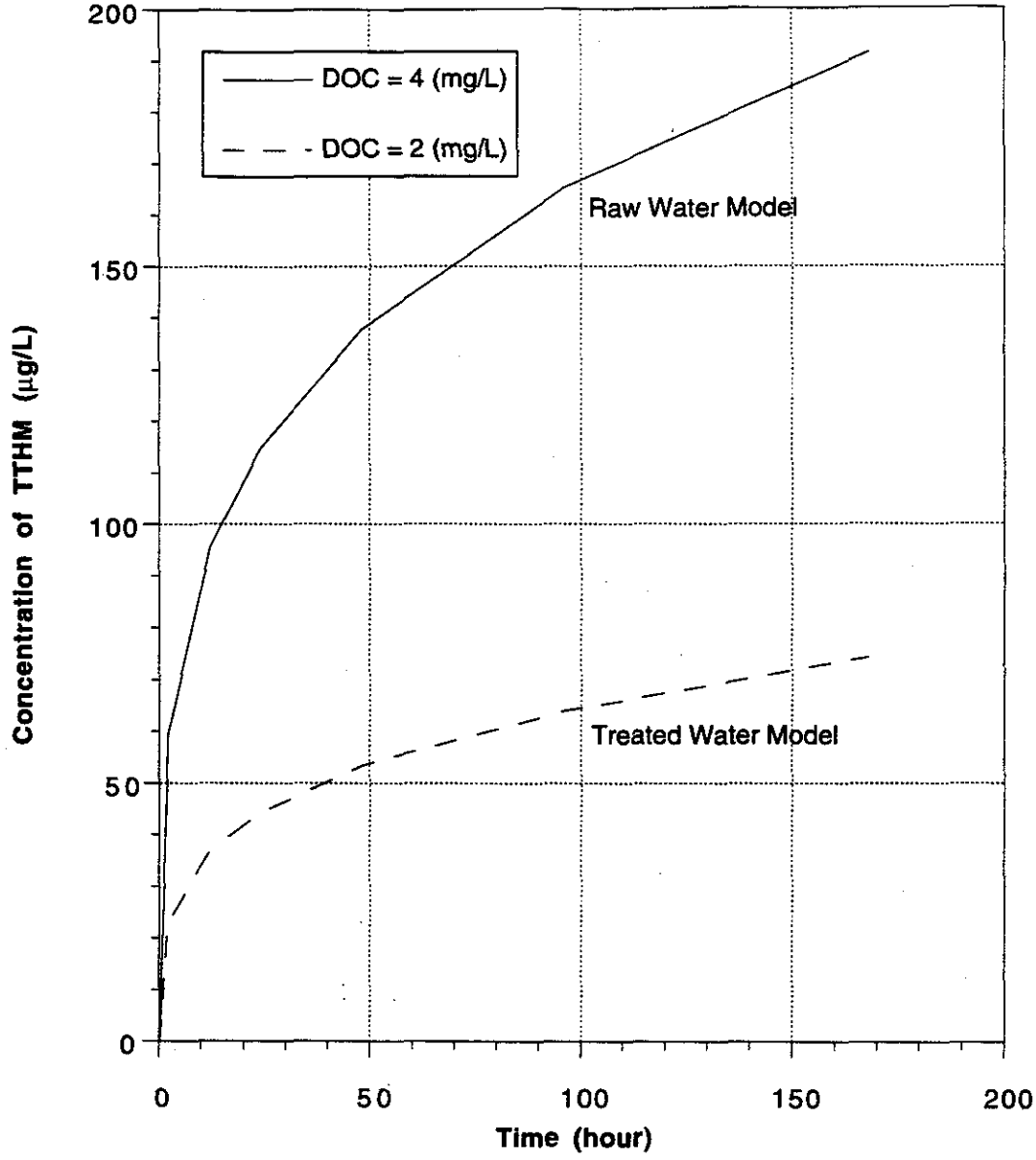

Fig. 5.13 Simulated Effects of Coagulation on THM Formation (Simulated by Raw and Combined Alum plus Iron Treated Water Model at Br^- = 100 µg/L, pH = 7.5, Cl_2/DOC = 1, Temperture = 20 °C)

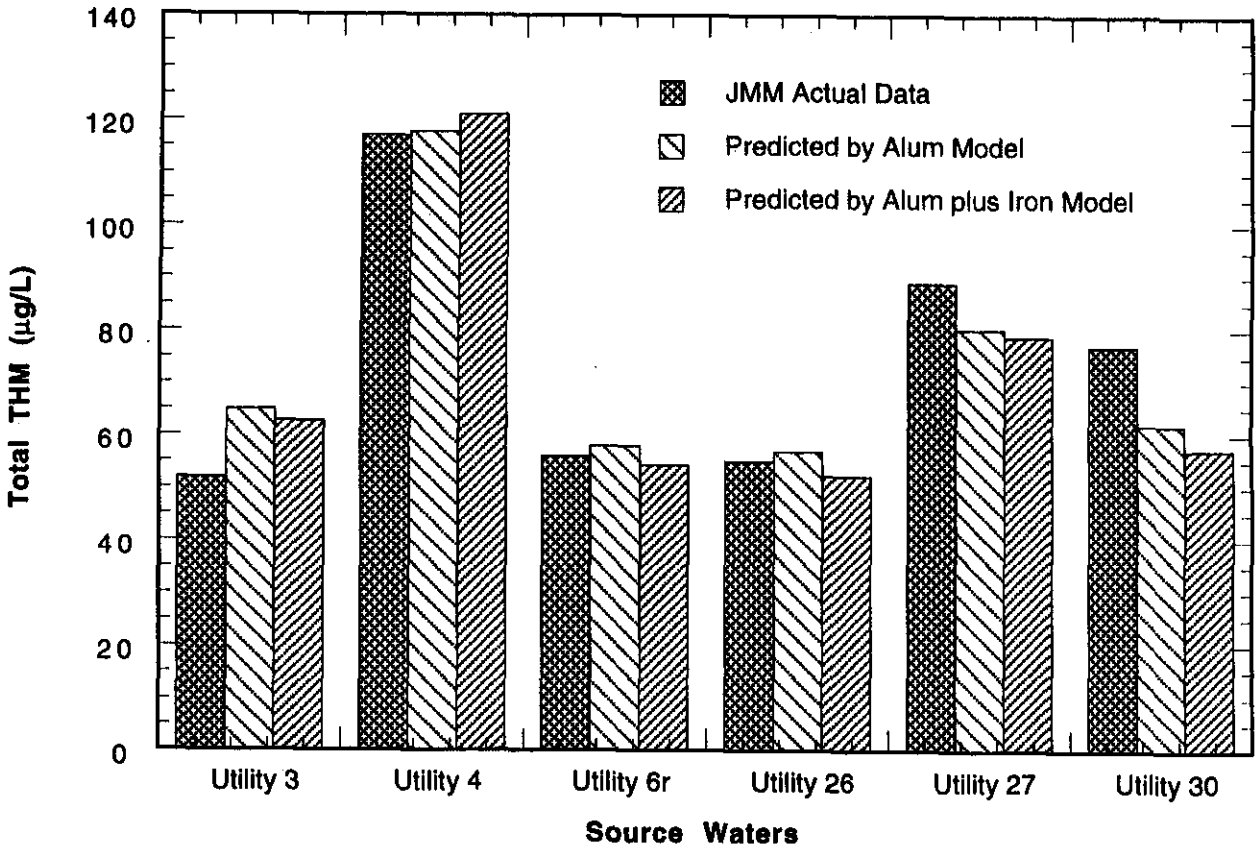

Figure 5.14 **External Validation of Alum Treated-Water Model and Combined Alum plus Iron Treated-Water Model Using JMM Data Base (pH=6.8-7.5, TOC=2.9-3.5 mg/L, Br^-=30-360 µg/L, Cl_2=2.7-8.4 mg/L, T=20 °C and Time=16 Hours)**

SECTION 6

CHLORAL HYDRATE MODELS

Chloral hydrate (CH) is a chlorination by-product of increasing regulatory interest. Its molecular formula is $C_2HCl_3(OH)_2$, and it is an unstable compound which may decompose into chloroform or undergo oxidation to trichloroacetic acid (Reckhow and Singer, 1985). The actual mechanism for chloral hydrate formation is unclear; it has been suggested that, during chlorination, chloral (trichloroacetaldehyde) is first formed which then hydrolyzes into chloral hydrate. Upon high-pH hydrolysis, chloroform is the decomposition product of chloral hydrate (Miller and Uden, 1983).

This chapter presents a model of the kinetics of chloral hydrate (CH) formation. The effects of influential independent variables on CH formation are discussed and modeled. Predictive raw/untreated water and treated water (after coagulation) models have been developed.

RAW/UNTREATED WATERS

Measurements of CH were made for each of eleven source waters, including two groundwaters, BGW and MGW. Since the DOC values of the two groundwater sources were low, 1.20 and 2.44 mg/L, detectable levels of CH were not observed upon chlorination in these sources. Statistical analysis showed that the experimental results derived from these two sources strongly influenced CH predictive model capabilities. Thus, we elected to exclude these data from the data base for the CH predictive model. Thus, the final predictive raw-water models for CH are based on nine source waters: BRW, HMR, ISW, SLW, SPW, SRW, SXW, VRW and PBW (n = 622).

Effects of Independent Variables on CH Formation

The effects of six independent variables (model parameters); DOC, chlorine dose (Cl_2), bromide level (Br^-), pH, temperature (Temp), and reaction time (t); on CH formation have been investigated. Figure 6.1 shows that four of these variables exert positive effects; bromide shows a negative effect, and pH shows mixed effects. For some waters, pH exhibited a clearly positive effect while, for other waters, CH first increased then decreased with increasing pH from 6.5 to 8.5. A control experiment demonstrated that hydrolysis of CH becomes significant at pH levels of higher than 9.0, with effects particularly pronounced at pH levels of higher than 10. Since the CH models stipulate a boundary condition of pH = 8.5, CH hydrolysis does not

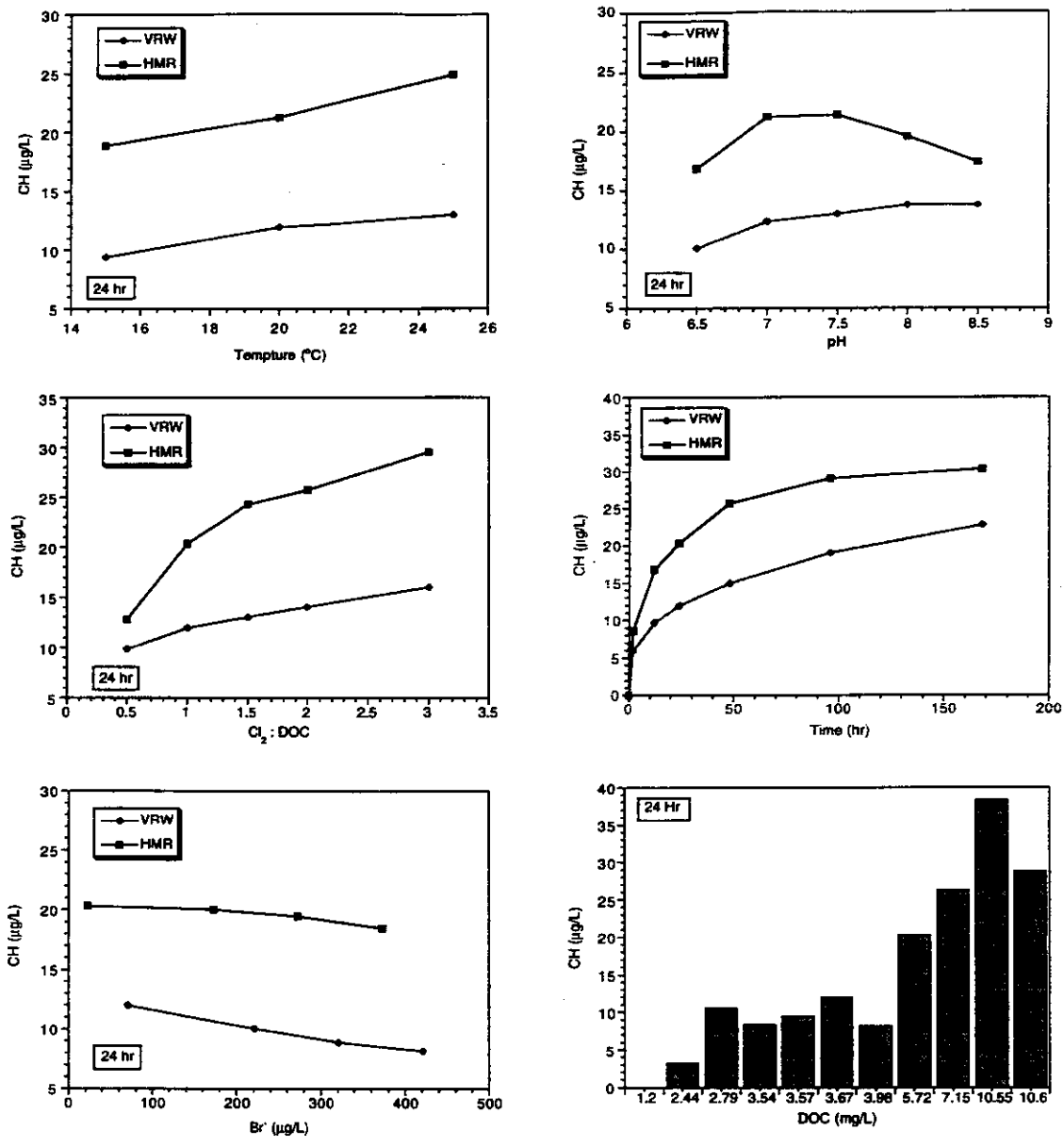

Figure 6.1 Individual Parameter Effects on CH Formation: Effects of Chlorine, pH, Temperature, Bromide, DOC, and Reaction Time (other parameters held at baseline condition).

affect the models developed herein. The effect of Br^- is particularly noteworthy; it is hypothesized that a brominated analog of chloral hydrate is formed in the presence of Br^- at the expense of chloral hydrate itself.

Predictive Raw/Untreated Water Model for Chloral Hydrate

Through statistical analysis by stepwise multiple regression, we developed models in the following format:

$$\text{Logarithmic Models:} \quad \log Y = \log b_0 + b_1 \log X_1 + \ldots \qquad (6.1)$$

or

$$\text{Power-function Models:} \quad Y = 10^{b0}\, X_1^{b1} \ldots \qquad (6.2)$$

where Y = CH
X_i = independent variable(s)
b_i = regression coefficients

The logarithmic or power-function model format provided the best simulation of CH formation. Table 6.1 summarizes the predictive raw-water model for CH. The model exponents indicate the positive influences of DOC, chlorine dose, temperature, pH, and reaction time on CH. A polynomial function for the pH term was evaluated; however, this approach did not improve model simulation capabilities. The bromide exponent shows a negative influence on CH formation. Boundary conditions for all independent variables are shown in Table 6.1. Modeling testing, in the form of scatterplots of predicted versus measured values, is summarized in Figure 6.2. The model shows underprediction over higher concentration ranges.

COAGULATED WATERS

Predictive treated-water models for CH formation were generated based on eight source waters; BRW, HMR, ISW, SPW, SRW,SXW, VRW and PBW. Alum, iron and alum plus iron (combined) models are presented in Table 6.2. In these treated water models, there are only four independent variables: DOC, chlorine dose (Cl_2/DOC = 1 and 3), bromide level (amb. + spikes), and reaction time. In chlorination experiments with coagulated waters, temperature was maintained constant at 20 °C, and pH at 7.5. Generally, alum and iron coagulation showed similar capabilities of CH precursor removal. Figure 6.3 shows data simulations of predicted versus measured values of CH for coagulated/treated waters using the combined alum plus iron treated-water model; the model generally tended to underpredict CH values.

Table 6.1 Predictive Raw-Water Models for Chloral Hydrate (CH)*

$$[CH] = 10^{-1.971}\,[DOC]^{1.009}\,[Cl_2]^{0.138}\,[Br^-]^{-0.044}\,Temp^{0.872}\,pH^{0.885}\,t^{0.343}$$

$R^2 = 0.81$ $\quad N = 622$ $\quad F = 426$ $\quad \alpha \leq 0.0001$

[CH] = Concentration of Chloral Hydrate (µg/L)

[DOC] = Dissolved Organic Carbon (mg/L)
$2.78 \leq [DOC\ (mg/L)] \leq 10.6$

$[Cl_2]$ = Applied Chlorine (mg/L)
$1.89 \leq [Cl_2\ (mg/L)] \leq 33.55$

$[Br^-]$ = Concentration of Bromide (µg/L)
$7 \leq [Br^-\ (\mu g/L)] \leq 600$

Temp = Incubation Temperature(^oC)
$15 \leq Temp \leq 25$

pH: $6.5 \leq pH \leq 8.5$

t = Incubation Reaction Time (hour)
$2 \leq t \leq 168$

***Source Waters:** BRW, HMR, ISW, SLW, SPW, SRW, SXW, VRW, PBW

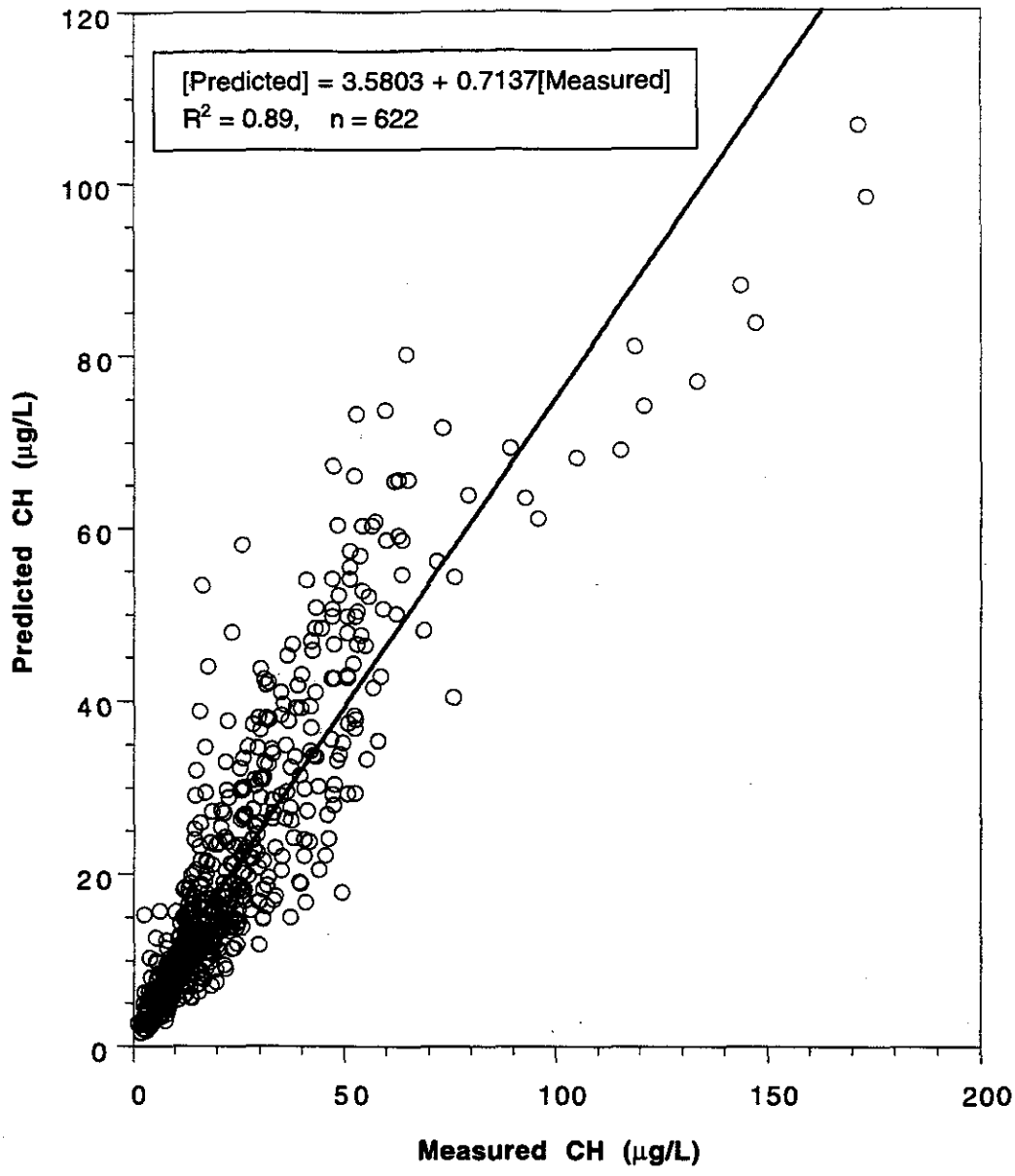

Figure 6.2 **Predicted versus Measured Values for Raw/Untreated Water CH.**

Table 6.2 Predictive Coagulated-Water Models for Chloral Hydrate (CH); Alum, Iron, and Combined Alum plus Iron Models*

Alum Coagulated Water Model:

$$[CH] = 10^{0.816}\,[DOC]^{0.806}\,[Cl_2]^{0.333}[Br^-]^{-0.601}\,t^{0.402}$$

$R^2 = 0.87$ $N = 143$ $F = 225$ $\alpha \leq 0.0001$

Iron Coagulated Water Model:

$$[CH] = 10^{0.694}\,[DOC]^{0.76}\,[Cl_2]^{0.423}[Br^-]^{-0.573}\,t^{0.404}$$

$R^2 = 0.88$ $N = 143$ $F = 247$ $\alpha \leq 0.0001$

Combined Alum plus Iron Model:

$$[CH] = 10^{0.755}\,[DOC]^{0.785}\,[Cl_2]^{0.375}\,[Br^-]^{-0.586}\,t^{0.403}$$

$R^2 = 0.87$ $N = 286$ $F = 474$ $\alpha \leq 0.0001$

[CH] = Concentration of Chloral Hydrate (µg/L)

[DOC] = Dissolved Organic Carbon in Coagulated Water (mg/L)
$1.00 \leq [DOC\ (mg/L)] \leq 7.77$

$[Cl_2]$ = Applied Chlorine (mg/L)
$1.11 \leq [Cl_2\ (mg/L)] \leq 24.75$

$[Br^-]$ = Concentration of Bromide (µg/L)
$37 \leq [Br^-\ (\mu g/L)] \leq 308$

pH = 7.5

Temp = 20 °C

t = Incubation Reaction Time (hour)
$2 \leq t \leq 168$

***Source Waters:** BRW, HMR, ISW, SPW, SRW, SXW, VRW, WPSW

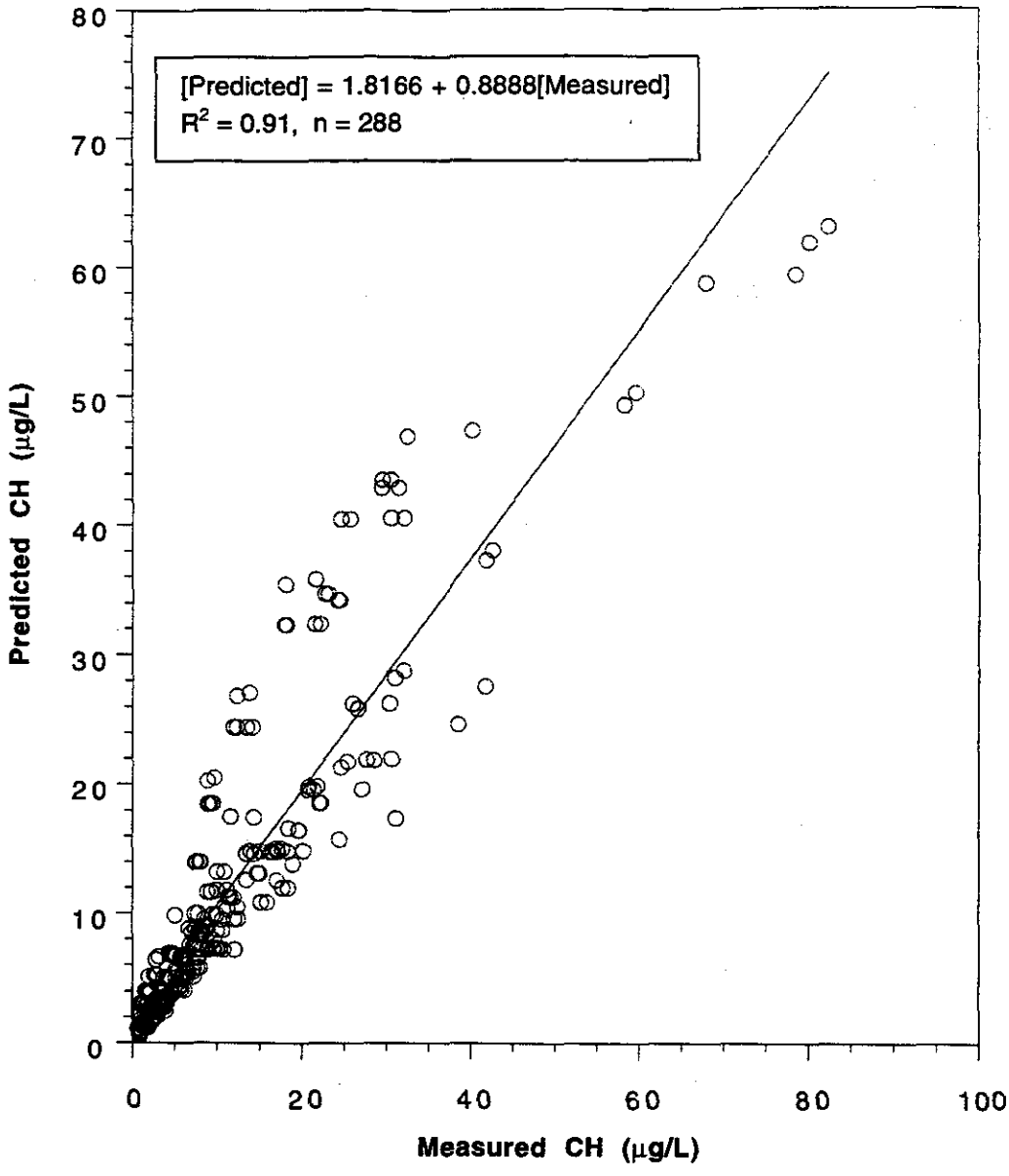

Figure 6.3 **Predicted versus Measured Values of CH for Coagulated/Treated Waters Using Combined Alum plus Iron Treated-Water Models.**

An alternative approach, based on the CH formation reactivity of the DOC, was also assessed, based on a reactivity coefficient, ϕ:

$$\phi = (CH/DOC)_{trt}/(CH/DOC)_{raw} \qquad (6.3)$$

A summary of the reactivity coefficient, ϕ, values for CH is shown in Table 6.3. Values of ϕ at reaction times of 2, 24, and 96 hours are calculated and listed. For the eight waters, one water (SXW) had ϕ values of greater than 1.0; one water (BRW) had ϕ values of less than 0.3, and the other six waters had ϕ values reflecting an average of 0.67. Figure 6.4 shows predicted versus measured values of CH for coagulated/treated waters using the raw/untreated water-model combined with the ϕ (24-hour) concept. Using this approach, the term $\phi(DOC_{trt})$ is substituted into the raw model for the DOC term. The scatterplot (Figure 6.4) demonstrates that this modeling approach results in some degree of underprediction for CH.

The effects of coagulation on DOC reduction and CH precursor removal can be simulated by using the predictive treated-water model for CH formation. Figure 6.5 shows that after DOC is reduced from 4 to 2 mg/L by coagulation (TOC = 2 mg/L represents the proposed regulatory action level), CH values are reduced by more than 50%, based on simulation with the combined alum plus iron treated water model (Br^- = 100 ìg/L, pH = 7.5, Cl_2/DOC = 1 mg/mg, and temperature = 20 °C).

SURROGATE CORRELATIONS BETWEEN CH AND TTHM OR CHLOROFORM

Correlations between CH and TTHM or chloroform are shown in Figure 6.6, representing plots of measured CH versus measured TTHM or chloroform for the entire data base and ranges of parameters such as pH (6.5 - 8.5). These plots suggest that CH exhibits a strong linear correlation with chloroform or TTHM. This implies that THM predictive models can be used to approximate CH formation through these correlations. (Poorer correlations were observed between total HAAs and either CH or TTHM).

Table 6.3 Summary of Reactivity Coefficient, Ø, Values for CH

Water		DOC (mg/L)	Br^- (µg/L)	Ø (2hr)	Ø (24 hr)	Ø (96 hr)
SPW	Raw	4.19	312	1.00	1.00	1.00
	Alum	2.56	306	1.02	0.50	0.71
	Iron	2.58	308	0.73	0.40	0.41
BRW	Raw	3.54	250	1.00	1.00	1.00
	Alum	2.72	245	0.41	0.22	0.28
	Iron	2.63	245	0.64	0.25	0.19
SRW	Raw	4.18	50	1.00	1.00	1.00
	Alum	2.56	48	1.11	0.98	1.24
	Iron	2.55	46	0.93	0.96	1.00
HMR	Raw	5.73	40	1.00	1.00	1.00
	Alum	4.29	37	0.74	0.61	1.02
	Iron	4.23	38	0.71	0.59	0.85
PBW	Raw	10.6	97	1.00	1.00	1.00
	Alum	4.6	97	0.58	0.73	0.75
	Iron	4.2	97	0.55	0.63	0.69
ISW	Raw	2.78	84	1.00	1.00	1.00
	Alum	1.00	83	0.64	0.54	0.73
	Iron	1.03	83	0.58	0.53	0.75
VRW	Raw	3.67	71	1.00	1.00	1.00
	Alum	2.56	68	0.66	0.84	0.93
	Iron	2.35	68	0.62	0.75	0.86
SXW	Raw	10.55	68	1.00	1.00	1.00
	Alum	7.77	67	1.01	1.12	0.93
	Iron	7.63	67	0.87	1.12	1.01

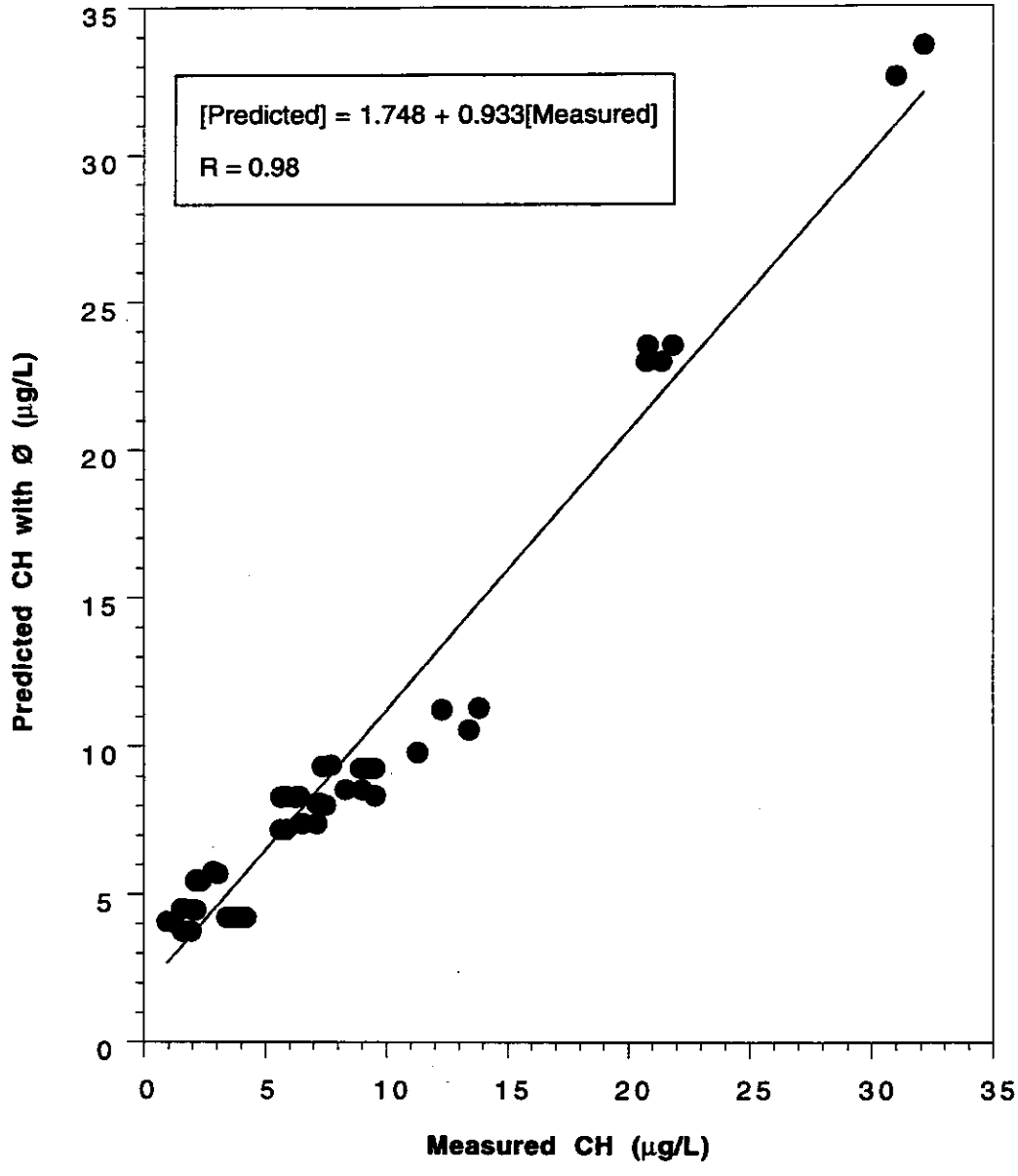

Figure 6.4 **Predicted versus Measured Values of CH for Coagulated/Treated Waters Using Raw/Untreated Water-Models Combined with Ø Concept; 24-Hour Predictions.**

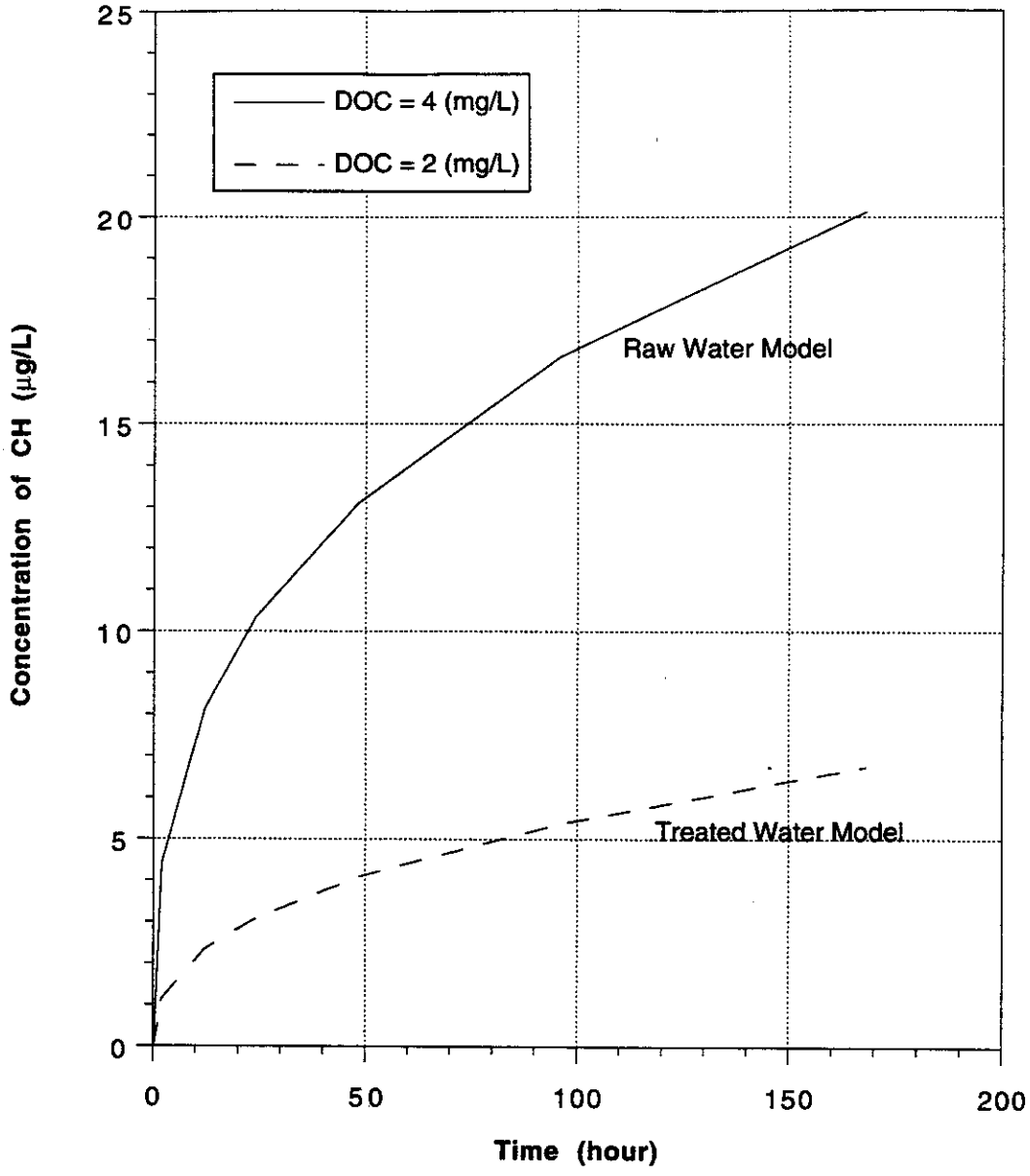

Fig. 6.5 Simulated Effects of Coagulation on CH Formation (Simulated by Raw and Combined Alum plus Iron Treated Water Model at Br^- = 100 µg/L, pH = 7.5, Cl_2/DOC = 1, Temperture = 20 °C)

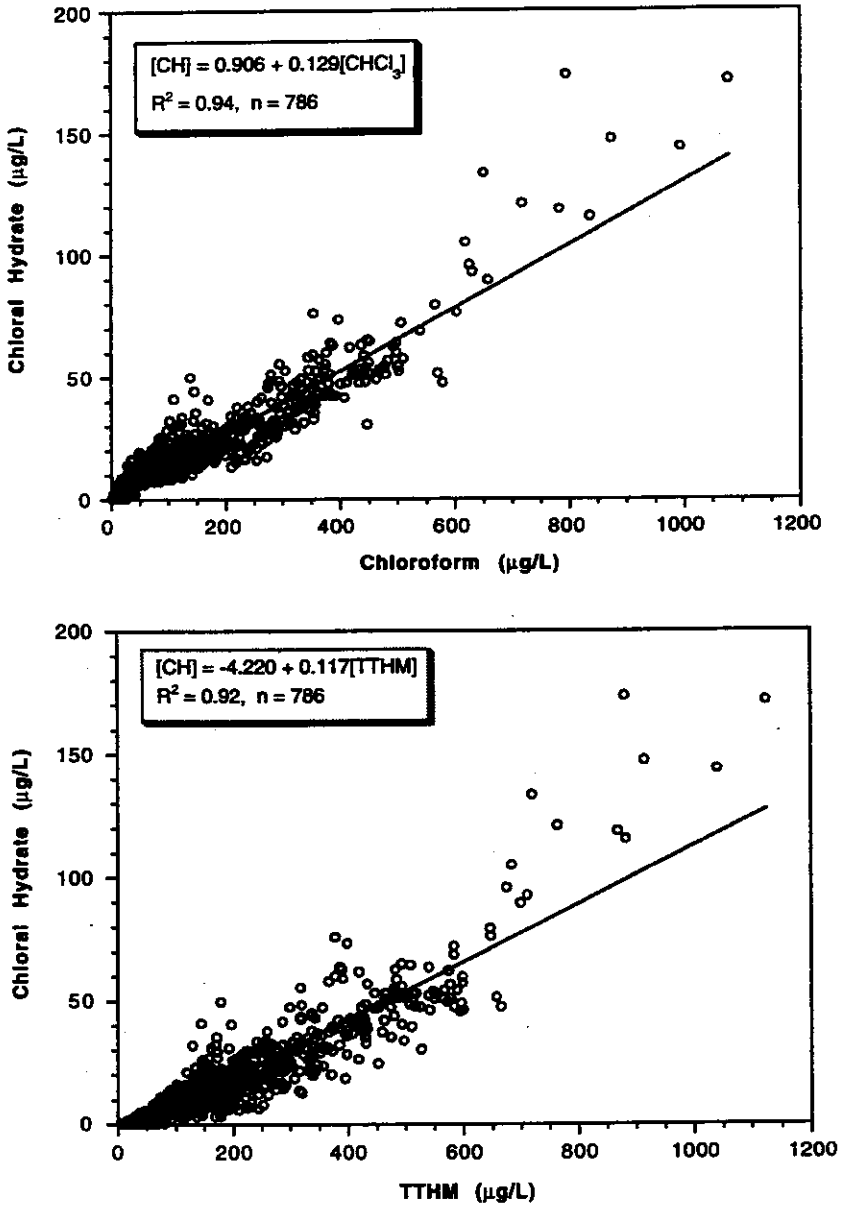

Figure 6.6 Correlations between CH and Chloroform (top) or TTHM (bottom).

SECTION 7

CHLORINE DECAY MODELS

Chlorine is the most widely used chemical for disinfection of drinking waters in the U.S. Evaluation of chlorine disappearance during chlorination not only can help drinking water treatment plants optimize disinfection conditions, but also can help one understand the kinetics and amounts of disinfection by-products formed during chlorination.

This chapter presents and discusses the experimental results of chlorine consumption during DBP formation, and the development of chlorine decay models. Also, this chapter describes DBP formation from the perspective of the concept of chlorine exposure time, represented by C-T, corresponding to integration of the chlorine residual versus time decay curve. This concept represents a different perspective on chlorine demand.

CHLORINE RESIDUAL DECAY MODELS

The chlorine decay model proposed by Qualls and Johnson (1983) represented a semi-theoretical approach to predict free chlorine concentrations as a function of time in natural waters. However, this model was based on a total reaction time of only five minutes. They have indicated that reaction of chlorine with fulvic acid occurs in two stages: a first stage (within one minute) representing a fast reaction following by a second stage (from 1 minute to 5 minutes) representing a slow reaction. The rate of chlorine disappearance was derived as the sum of two first-order reactions (fast and slow reactions) (Qualls and Johnson, 1983):

$$d[Cl_2]/dt = k_1[Cl_2][F1] + k_2[Cl_2][F2] \qquad (7\text{-}1)$$

where $d[Cl_2]/dt$ is the rate of chlorine disappearance, $[Cl_2]$ is the molar free chlorine residual concentration, k_1 and k_2 are the rate constants for fast and slow reaction, respectively, and [F1] and [F2] are the molar concentrations of reactive sites on fulvic acids for fast and slow reactions, respectively.

In this study, the bench-scale experiments were performed to evaluate chlorine decay, based on five different Cl_2/DOC ratios (Cl_2/DOC = 3, 2, 1.5, 1, 0.5 mg/mg) and six reaction times (2, 12, 24, 48, 96, 168 hours) at a temperature of 20 °C, a pH of 7.5, ambient bromide levels, and ambient DOC values. A total of 11 source waters were evaluated in these experiments.

Through an examination of all chlorine decay curves, the resultant kinetics generally suggested pseudo first order disappearance due to the presence of DOC. However, chlorine decay was significantly more rapid within the first twelve hours, with much slower disappearance noted thereafter. The "intersection" of rapid and slow decay occurs somewhere between reaction times of 2 and 12 hours. Two additional chlorine decay experiments were designed to more precisely determine the location of this "intersection point". In these additional experiments, the reaction times chosen were 0.5, 1, 2, 5, 9, 12, 24, 96 and 216 hours; other experimental conditions were maintained the same as conditions in the previous experiments. Curve fitting indicated that the intersection point between rapid and slow decay occurred at about five hours of reaction time. Within the first five hours of reaction time, chlorine concentrations dropped from 30% to 80% depending on Cl_2/DOC ratio; 30% to 50% when Cl_2/DOC = 3, 2 or 1.5 mg/mg, and 50% to 80% when Cl_2/DOC = 1 or 0.5 mg/mg. Based on this analysis, the first order chlorine decay model for "fast decay? was defined as:

$$C_1 = C_o \exp(-k_1 t) \qquad 0 \le t \le 5 \text{ hours} \qquad (7\text{-}2)$$

where C_1 is the predicted chlorine residual (mg/L as Cl_2) at time t (hours), C_o is the initial concentration of chlorine when reaction time is zero (i.e., chlorine dose), and k_1 is the first order reaction rate constant with the units of $hour^{-1}$. The reaction rate constant k_1 was found to have a very strong dependency on DOC, ammonia concentration (mg/L as N), chlorine dose, and Cl_2/DOC ratio. An extensive tabulation of k_1 values appears in Table 7.1 for the baseline experiment along with other experiments within the orthogonal matrix for each of the source waters. This tabulation clearly shows the positive effects of DOC and temperature on chlorine short-term chlorine decay; the effects of pH and bromide are mixed. The tabulation of k_1 values shown in Table 7.1 are both source- and experiment-specific. In an attempt to generalize, the following empirical relationship for predicting k_1 was derived:

$$\ln(k_1) = -0.442 + 0.889 \ln(DOC) + 0.345 \ln(7.6*(NH_3\text{-}N)) - 1.082 \ln(C_o) + 0.192 \ln(Cl_2/DOC) \qquad (7\text{-}3)$$

$$R^2 = 0.62$$

After five hours of reaction time, chlorine decay exhibits slower kinetics. The concentration of chlorine residual after t = 5 hours shows first order decay with a lower reaction rate:

Table 7.1 Reaction Rate Constants of Chlorine Decay

Source Waters	1		2		3		4		5	
	Baseline*		@ Temp = 15 C		@ Temp = 25 C		@ pH 6.5		@ pH 8.5	
	k1	k2	k1	k2	k1	k2	k1	k2	k1	k2
SLW	2.681E-02	2.999E-03	1.969E-02	2.340E-03	3.079E-02	3.822E-03	2.143E-02	3.314E-03	2.309E-02	4.965E-03
SPW	3.483E-02	3.998E-03	2.604E-02	2.582E-03	4.668E-02	3.764E-03	3.124E-02	3.672E-03	3.111E-02	3.669E-03
BRW	2.487E-02	3.297E-03	2.607E-02	1.583E-03	2.865E-02	3.008E-03	3.001E-02	2.677E-03	4.344E-02	2.012E-03
VRW	5.450E-02	1.087E-02	5.355E-02	6.018E-03	6.370E-02	1.368E-02	4.346E-02	9.083E-03	4.596E-02	1.132E-02
MGW	7.178E-02	4.855E-03	5.957E-02	3.220E-03	6.397E-02	6.375E-03	4.324E-02	3.072E-03	6.673E-02	3.361E-03
BGW	3.032E-02	2.753E-03	3.275E-02	2.367E-03	3.955E-02	4.355E-03	3.228E-02	2.246E-03	5.052E-02	4.297E-03
ISW	1.413E-01	1.652E-02	1.107E-01	1.769E-02	1.488E-01	1.581E-02	1.137E-01	1.839E-02	1.447E-01	2.040E-02
SXW	8.684E-02	1.492E-02	6.106E-02	1.473E-02	9.899E-02	1.614E-02	8.511E-02	1.560E-02	8.594W-2	1.716E-02
HMR	1.057E-01	1.959E-02	9.023E-02	1.855E-02	1.416E-01	1.991E-02	9.379E-02	2.104E-02	8.743E-02	1.863E-02
SRW	9.277E-02	1.555E-02	1.037E-01	1.155E-02	1.279E-01	1.422E-02	9.771E-02	1.333E-02	9.936E-02	1.468E-02
PBW	7.611E-02	1.637E-02	7.031E-02	1.299E-02	8.952E-02	1.992E-02	6.906E-02	1.479E-02	6.242E-02	1.547E-02

* Baseline condition is at Temperature = 20°C, pH = 7.5, DOC = ambient, Bromide = ambient, Cl2/DOC = 3 on SLW, SPW and BRW, Cl2/DOC = 1 on VRW, MGW, BGW, ISW, SXW, HMR, SRW and PBW.

N/A: Not Available

Table 7.1 Reaction Rate Constants of Chlorine Decay (Continued)

Source Waters	6 @ ΔBr = 150 µg/L		7 @ ΔBr = 250 µg/L		8 @ ΔBr = 350 µg/L		9 @ Cl2/DOC = 0.5		10 @ Cl2/DOC = 1	
	k1	k2	k1	k2	k1	k2	k1	k2	k1	k2
SLW	2.574E-02	4.093E-03	2.408E-02	3.746E-03	N/A	N/A	1.462E-01	5.983E-02	5.728E-02	4.037E-01
SPW	4.309E-02	3.716E-03	4.309E-02	3.567E-03	N/A	N/A	1.819E-01	5.553E-02	9.772E-02	6.990E-02
BRW	4.193E-02	1.896E-03	4.301E-02	1.670E-03	5.007E-02	9.414E-03	5.877E-02	1.736E-02	5.331E-02	8.956E-03
VRW	5.632E-02	1.130E-02	6.134E-02	1.243E-02	6.784E-02	1.387E-02	1.098E-01	1.168E-02	N/A	N/A
MGW	6.061E-02	4.608E-03	5.754E-02	5.369E-03	6.368E-02	5.080E-03	9.645E-02	6.585E-03	N/A	N/A
BGW	3.443E-02	3.249E-03	3.543E-02	3.265E-03	3.943E-02	3.319E-03	4.214E-02	3.737E-03	N/A	N/A
ISW	1.536E-01	1.232E-02	1.861E-01	1.096E-02	2.060E-01	9.587E-03	2.531E-01	3.742E-02	N/A	N/A
SXW	8.805E-02	1.489E-02	9.567E-02	1.469E-02	9.413E-02	1.481E-02	1.774E-01	1.245E-02	N/A	N/A
HMR	1.220E-01	1.838E-02	1.204E-01	1.866E-02	1.253E-01	1.795E-02	2.126E-01	7.619E-03	N/A	N/A
SRW	1.315E-01	1.362E-02	1.319E-01	1.499E-02	1.337E-01	1.744E-02	1.931E-01	2.458E-03	N/A	N/A
PBW	7.733E-02	1.605E-02	7.521E-02	1.527E-02	7.929E-02	1.565E-02	1.283E-01	1.467E-02	N/A	N/A

* Baseline condition is at Temperature = 20°C, pH = 7.5, DOC = ambient, Bromide = ambient, Cl2/DOC = 3 on SLW, SPW and BRW, Cl2/DOC = 1 on VRW, MGW, BGW, ISW, SXW, HMR, SRW and PBW.

N/A: Not Available.

Table 7.1 Reaction Rate Constants of Chlorine Decay (Continued)

Source Waters	11 @ Cl2/DOC = 1.5		12 @ Cl2/DOC = 2		13 @ Cl2/DOC = 3	
	k1	k2	k1	k2	k1	k2
SLW	4.278E-02	8.025E-03	4.234E-02	4.950E-03	N/A	N/A
SPW	9.005E-02	1.230E-02	4.329E-02	7.178E-03	N/A	N/A
BRW	4.312E-02	5.331E-03	3.037E-02	4.014E-03	N/A	N/A
VRW	3.424E-02	6.392E-03	2.967E-02	3.729E-03	2.270E-02	2.786E-03
MGW	6.195E-02	2.658E-03	5.023E-02	2.454E-03	4.550E-02	2.093E-03
BGW	2.878E-02	2.595E-03	2.441E-02	2.194E-03	2.226E-02	1.452E-03
ISW	7.218E-02	1.424E-02	5.392E-02	7.000E-03	3.897E-02	3.565E-03
SXW	5.932E-02	1.183E-02	4.319E-02	8.159E-03	3.704E-02	4.672E-03
HMR	6.304E-02	2.008E-02	6.074E-02	9.121E-03	4.814E-02	4.612E-03
SRW	8.140E-02	1.264E-02	6.384E-02	8.490E-03	5.640E-02	3.974E-03
PBW	5.428E-02	7.237E-03	4.416E-02	5.126E-03	3.919E-02	3.017E-03

* Baseline condition is at Temperature = 20°C, pH = 7.5, DOC = ambient, Bromide = ambient, Cl2/DOC = 3 on SLW, SPW and BRW, Cl2/DOC = 1 on VRW, MGW, BGW, ISW, SXW, HMR, SRW and PBW.

N/A: Not Available.

$$C_2 = C_{o\text{-}5} \exp(-k_2 t) \qquad 5 \le t \le 168 \text{ hours} \qquad (7\text{-}4)$$

where C_2 is the predicted chlorine residual (mg/L) as Cl_2) after t = 5 hours, $C_{o\text{-}5}$ is the chlorine concentration when reaction time is 5 hours, and k_2 is the first order chlorine decay rate constant for t > 5 hours.

$C_{o\text{-}5}$ can be obtained using the boundary condition of $C_1 = C_2$ at t = 5 hours; by adding Equation (7-2) and (7-4) at t = 5 hours, we obtain:

$$C_{o\text{-}5} = C_o \exp[5(k_2 - k_1)] \qquad (7\text{-}5)$$

Thus, Equation (7-4) can be expressed without $C_{o\text{-}5}$ term as:

$$C_2 = C_o \exp[5(k_2 - k_1)] \exp(-k_2 t) \qquad 5 \le t \le 168 \text{ hours} \qquad (7\text{-}6)$$

Table 7.1 also shows an extensive tabulation of k_2 values; long-term chlorine decay is positively correlated with DOC, temperature, and pH. Generalizing beyond the source- and experiment-specific values tabulated in Table 7.1, k_2 can be estimated from the following empirical expression:

$$\ln(k_2) = -4.817 + 1.187 \ln(DOC) + 0.102 \ln(7.6*(NH_3\text{-}N)) - 0.821 \ln(C_o) - 0.271 \ln(Cl_2/DOC) \qquad (7\text{-}7)$$

$$R^2 = 0.72$$

Figure 7.1 shows predicted and observed chlorine decay at five different Cl_2/DOC ratios using data derived from ISW and the predictive models shown in equations (7-2) and (7-4).

Statistical analysis indicated no correlation between bromide and chlorine decay.

A comparison between the Qualls and Johnson model in equation (7-1) and the models developed in this study, equations (7-2) and (7-4), was conducted for predictions of chlorine residual. At Cl_2/DOC ratios of 0.5, 1.0, 2.0, and 3.0, the fits of Qualls and Johnson model were not as good for prediction of free chlorine residual, particularly for long reaction times, because the Qualls & Johnson model was established on the conditions of low Cl_2/DOC ratio and a 5-minute short reaction period. In full scale treatment, a higher Cl_2/DOC ratio and longer reaction time are involved. Therefore, the application of the models developed in this study are considered to be more appropriate than the Qualls and Johnson model.

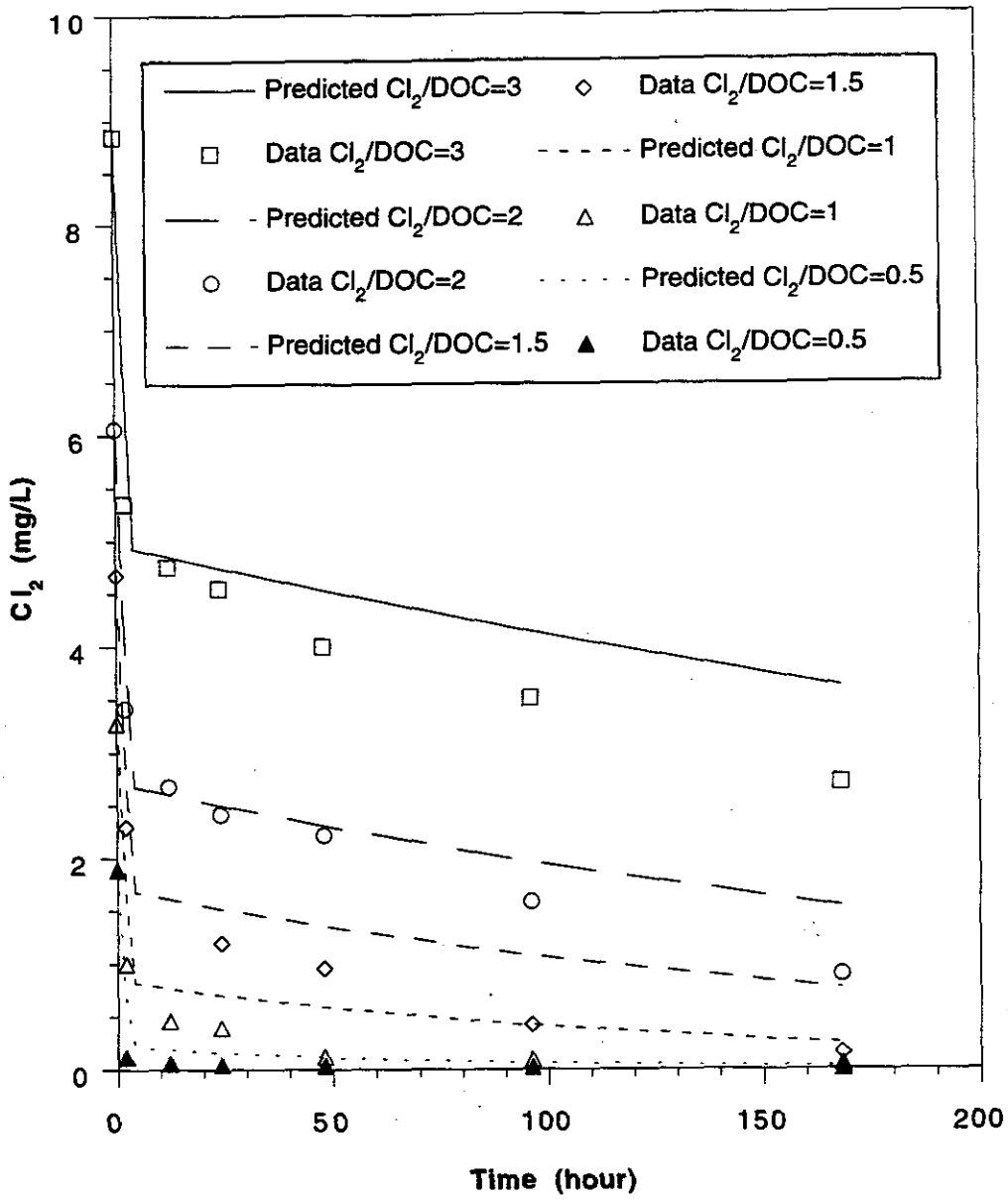

Figure 7.1 **Predicted and Observed Chlorine Decay at Five Chlorine/DOC Ratios, ISW.**

DBP FORMATION VERSUS CHLORINE EXPOSURE (C-T)

The formation of chlorination by-products can potentially be evaluated through use of the chlorine exposure (C-T) concept which is the integration of the chlorine residual versus reaction time curve, with units of mg/L*min. We attempted to discern possible correlations between chlorination DBP formation and C-T, a function of both chlorine dose and decay.

Figure 7.2 portrays total HAA as a function of C-T value for raw/untreated or treated waters at a temperature of 20 °C, a pH of 7.5, ambient DOC, ambient bromide, a Cl_2/DOC = 1 mg/mg, and reaction times of 2, 12, and 24 hours. It is apparent that the pattern of chlorine decay/consumption represented by C-T does not provide an accurate indication of HAA formation. Differences may be partly attributable to variations in ambient Br^- and its role in forming brominated HAAs. It is interesting, however, that there is some clustering of results for coagulated waters, with all sources except SXW behaving comparably.

Figures 7.3 and 7.4 show total THMs and chloral hydrate, respectively, as a function of chlorine exposure for raw/untreated and treated waters under the same conditions as shown for HAAs. Raw-water responses are highly variable for both THMs and CH while treated waters showed some more comparable trends except SXW.

All three figures (Figures 7.2, 7.3, and 7.4) show that each source water exhibits a somewhat unique chlorine demand. Also, the ambient Br^- manifests itself differently in each source water in forming brominated DBPs (see Chapters 4 and 5). It appears that, after coagulation, the NOM remaining in each of the sources exhibits more similar chlorine demands. Establishment of simple correlations between chlorination DBPs and the C-T parameters did not prove viable.

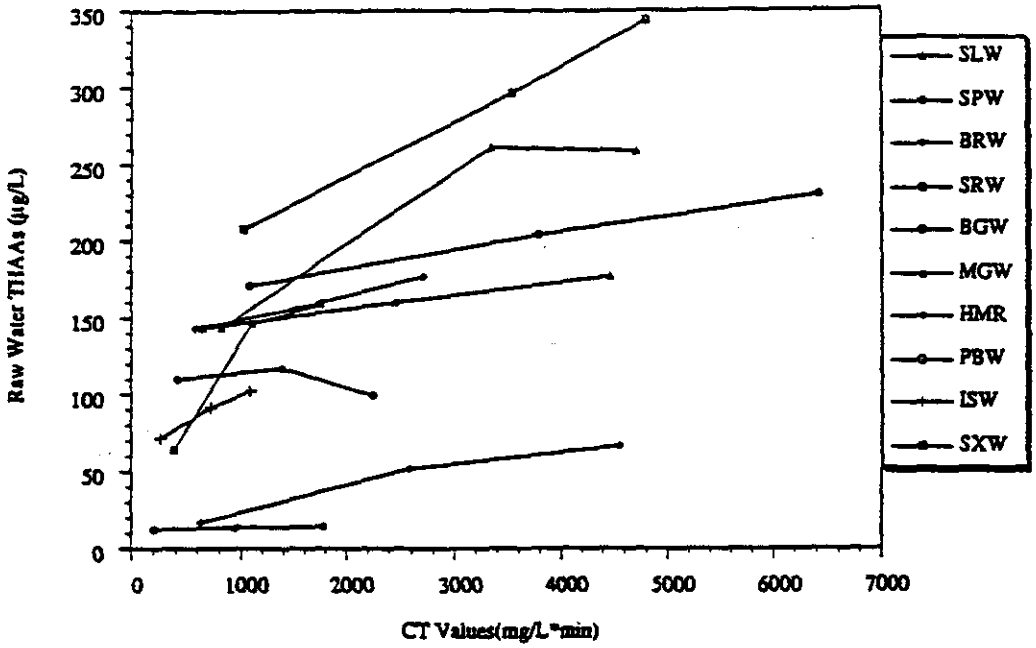

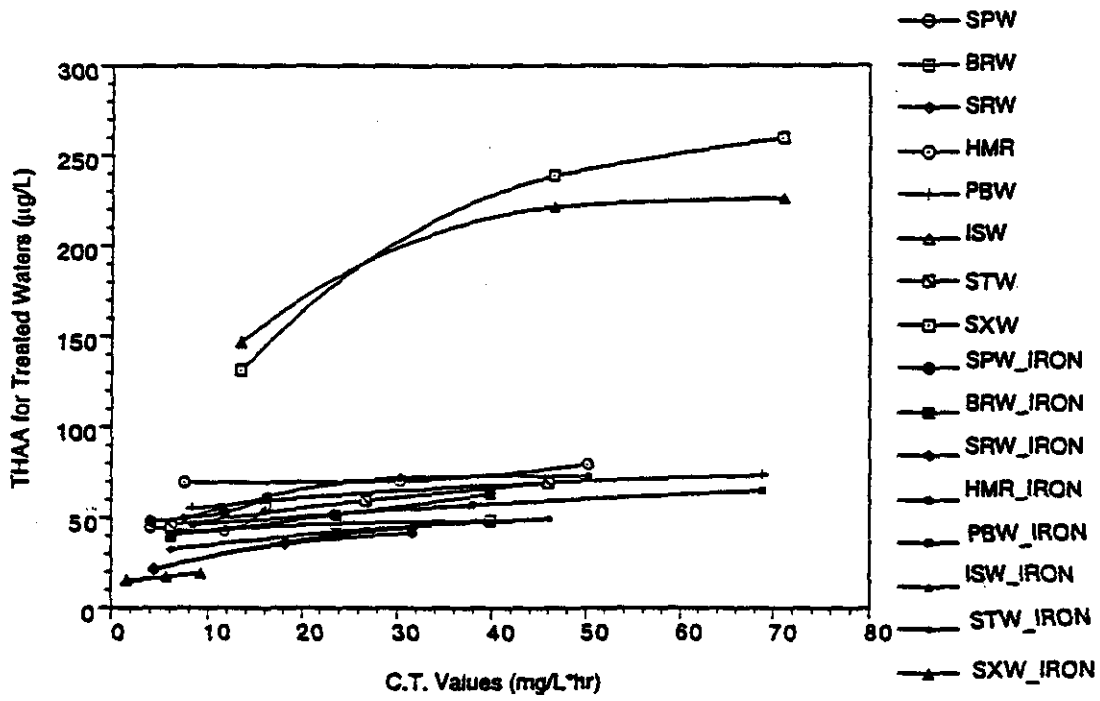

Fig 7.2 THAA as a Function of Chlorine Exposure (C-T) for Raw/Untreated (top) or Treated (bottom) Waters

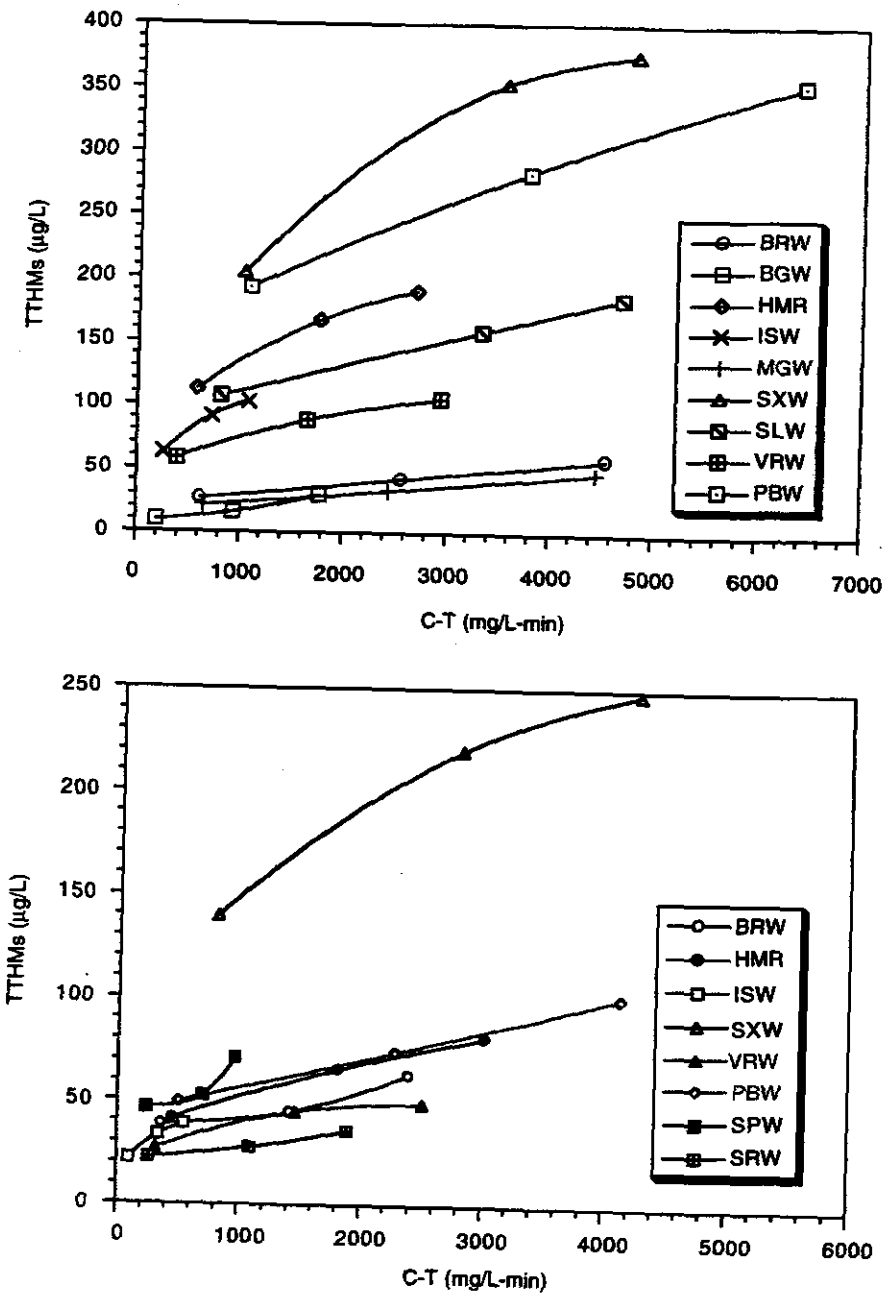

Figure 7.3 TTHM as a Function of Chlorine Exposure (C-T) for Raw/Untreated (top) or Treated (bottom) Waters.

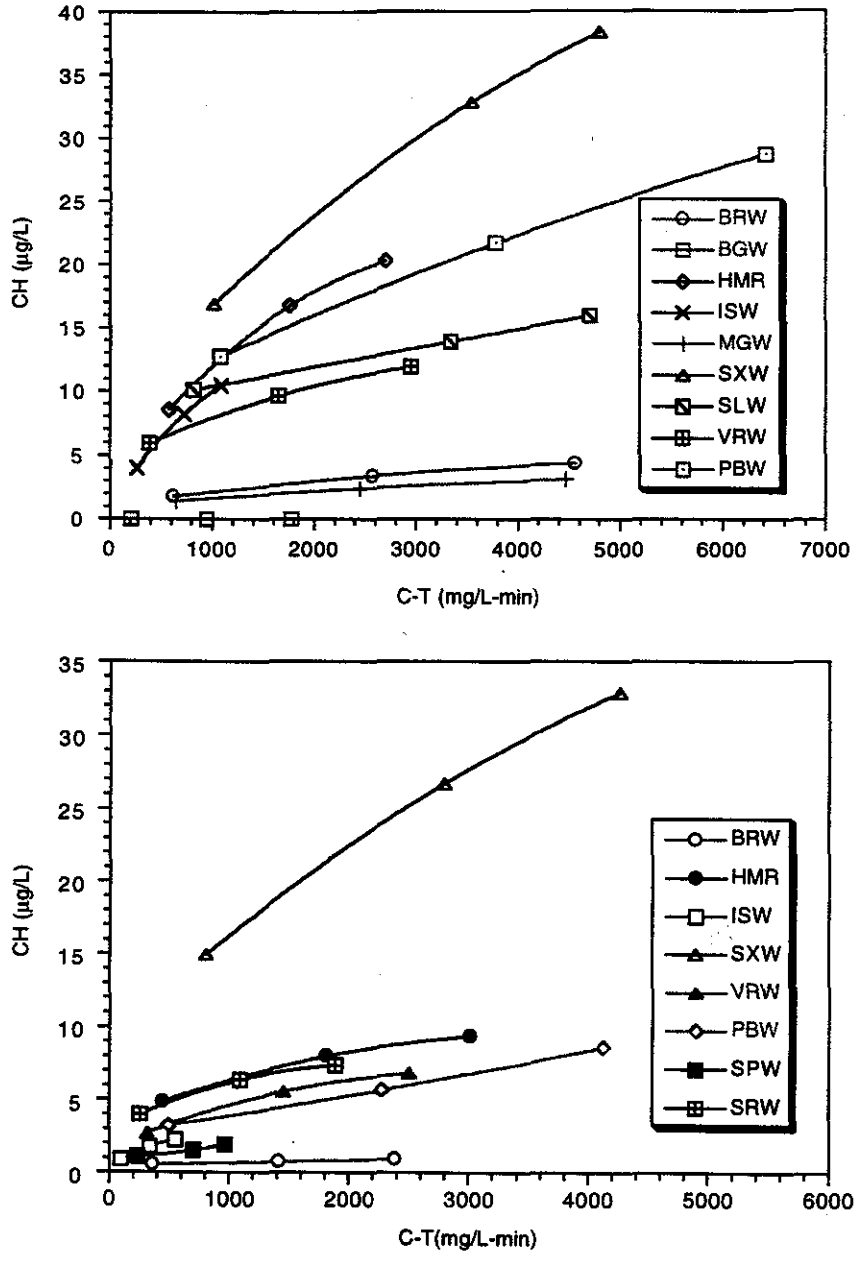

Figure 7.4 CH as Function of Chlorine Exposure (C-T) for Raw/Untreated (top) or Treated (bottom) Waters.

SECTION 8

BROMATE AND OZONE DECAY MODELS

During the oxidation of natural waters containing bromide ion (Br^-) with ozone (O_3), bromate is formed at concentrations ranging from 0-150 ug/L under normal water treatment conditions. Bromide itself occurs ubiquitously, with an average concentration in the U.S. of almost 100 ug/L (Amy et al., 1994). Current studies show that bromate is a carcinogen. The Environmental Protection Agency (EPA) is currently considering a Maximum Contaminant Level (MCL) of 10 ug/L in U.S. drinking waters. Considering that the average bromide ion concentration in U.S. waters is 100 ug/L, it is expected that detectable bromate will form in a majority of waters which are subjected to ozonation. Therefore, an understanding of bromate formation during ozonation and the quantitative effects of water quality parameters (pH, alkalinity, DOC, etc.) is crucial for evaluating various bromate control strategies.

Haag and Hoigne (1983) suggest that bromide can be oxidized, by ozone, according to the following reaction:

$$O_3 + Br^- \rightarrow O_2 + OBr^- \quad k= 160\ M^{-1}s^{-1} \quad (8.1)$$

The above reaction is pH dependent because hypobromite ion (OBr^-) is in equilibrium with hypobromous acid (HOBr) according to the following reaction:

$$HOBr \rightleftharpoons H^+ + OBr^- \quad pK_a= 8.7 \text{ at } 25°C \quad (8.2)$$

Hypobromite ion can further react with ozone to form bromate;

$$2O_3 + OBr^- \rightarrow 2O_2 + BrO_3^- \quad k= 160\ M^{-1}s^{-1} \quad (8.3)$$

The formation of bromate during ozonation can be influenced by water quality parameters (pH, DOC, Br^-, temperature) and various operational/treatment conditions (O_3 dose, dissolved O_3 residual, contact time).

PARAMETERS AFFECTING BROMATE FORMATION

An assessment of water quality characteristics (e.g. Br^-, pH, DOC) can help determine if a bromate problem is likely to occur. An understanding of treatment options can help reduce bromate formation. The effects of each parameter on bromate formation and ozone demand are discussed below.

Effect of pH

The effects of pH on bromate formation and ozone decay have been analyzed for each water source, and it was found that bromate concentration increases upon an increase of pH from 6.5 to 8.5, a trend largely attributable to the high $OBr^-/HOBr$ ratio at higher pH levels. pH has been controlled in our experiments with a 10^{-3} M phosphate buffer; pH was monitored during experiments to assure that pH was constant within ± 0.1 units.

On the other hand, ozone decays faster in high pH waters than low pH waters. This is consistent with what other researchers have found (Weis, 1935; Hoigne and Bader, 1977; Staehelin et al., 1984; Tomiyasu et al., 1985; Grasso, 1987; Gordon, 1987). This behavior is attributed to direct reaction of hydroxide ions with ozone:

$$O_3 + OH^- \rightarrow HO_2 + O_2^- \quad k = 70\ M^{-1}\ s^{-1} \quad (8.4)$$

Figure 8.1a shows the effects of pH on bromate formation for SPW; increasing pH from 6.5 to 8.5 almost doubled the bromate concentration.

Effect of Ozone Dose

For low DOC waters (DOC ≤ 2.0 mg/L), an O_3/DOC = 2 mg/mg was selected as the baseline condition; however for the higher DOC waters (DOC > 2 mg/L), an O_3/DOC = 1 mg/mg was selected in order to provide realistic ozone doses.

Bromate concentration was observed to increase with an increase in O_3/DOC ratio (Figure 8.1b). This is due to the direct reaction of ozone with OBr^- to form BrO_3^-. Bromate does not form after the ozone residual becomes zero (Figure 8.2). This is an important finding because this suggests that bromate primarily forms in treatment plants whereas most of the organic DBPs (e.g., bromoform) form within distribution systems after several hours of reaction time. This is also potentially advantageous because bromate can potentially be removed before treated water leaves the treatment plant.

In the case of high O_3/DOC ratios with low DOC waters, bromate formation steadily increases with time whereas ozone decays very slowly until all bromide is converted into bromate.

Effect of Bromide Concentration

Bromate formation and ozone decay in natural waters have been studied at

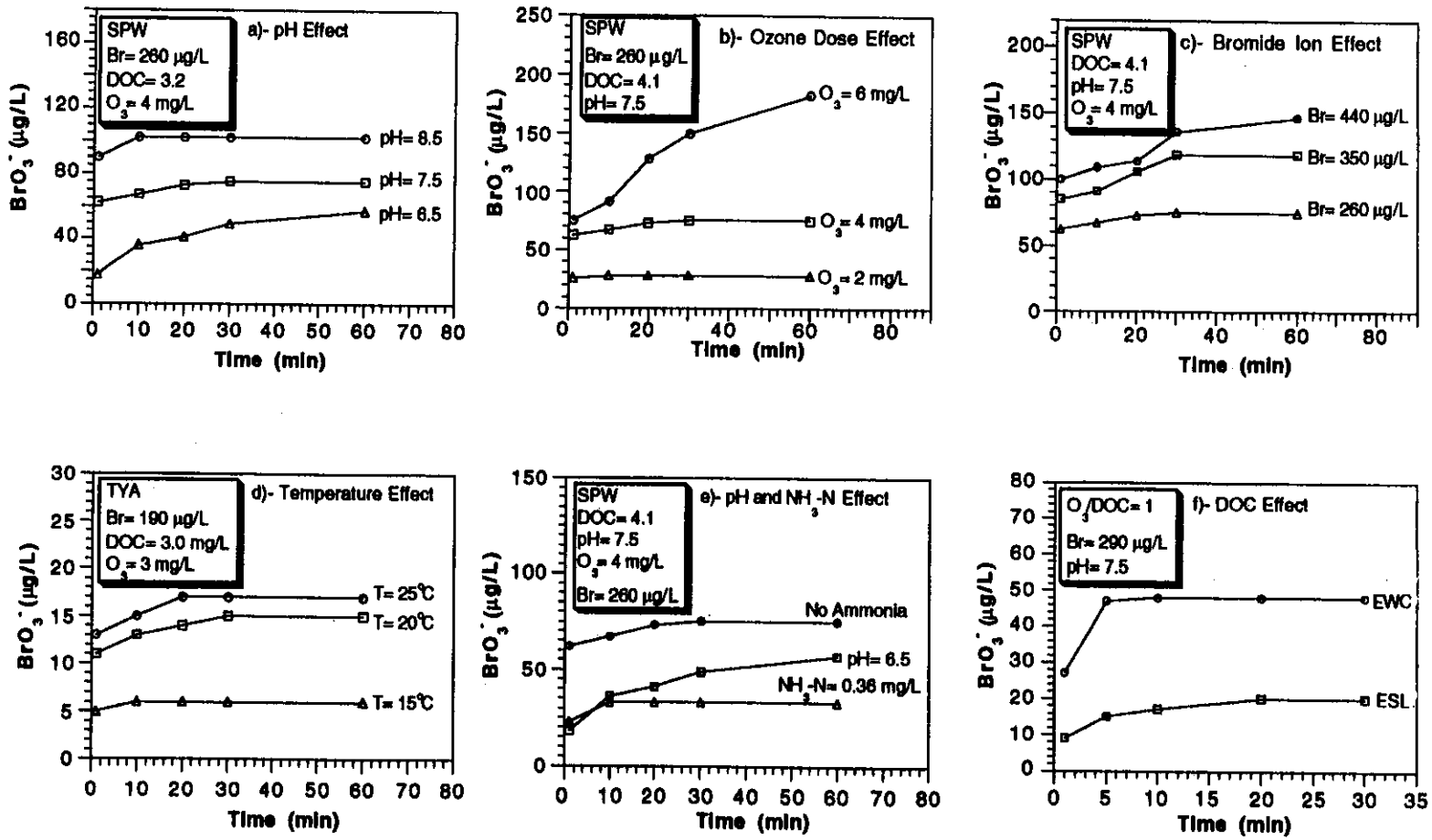

Figure 8.1. Individual Parameter Effects on Bromate Formation; Effects of pH, Ozone Dose, Bromide Ion Concentration Temperature, pH Depression/Ammonia Addition, and DOC

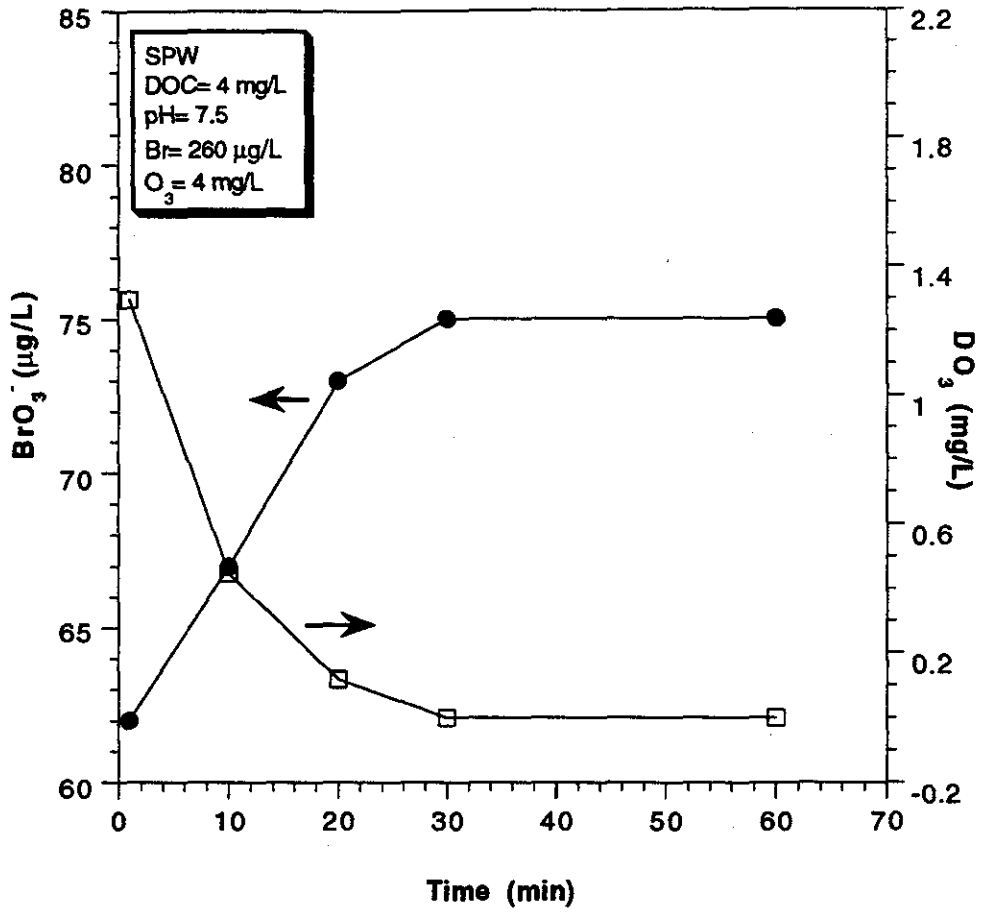

Figure 8.2. Effect of Dissolved Ozone on Bromate Formation

ambient Br^-, and at spiked levels of ambient + 0.1 mg/L (100 ug/L) and ambient + 0.2 mg/L (200 ug/L). In the case of high ambient Br^- levels (Br^- > 80 ug/L), ambient Br^- was chosen as the baseline condition, whereas for the low ambient Br^- levels, ambient + 0.1 mg/L was the baseline condition used in order to produce *measurable* quantities of bromate. A national survey indicates that Br^- levels in raw US drinking water supplies ranges from <0.005 mg/L to almost 0.5 mg/L with a national average of slightly less than 0.1 mg/L (Amy et al., 1994); therefore, the baseline conditions were maintained close to these levels.

Bromate concentration increased with increasing bromide ion concentration (Figure 8.1c), due to direct reaction of ozone with bromide to produce OBr^- which further reacts with ozone to produce bromate.

Siddiqui and Amy (1993) previously showed that BrO_3^- was not formed at bromide concentrations of less than 0.1 mg/L. However, in this study, it is clear that bromate formation is much more problematic than previously thought. Bromate forms (up to 6 ug/L) in waters containing bromide as low as 20 ug/L. This finding is important because bromate is a problem for significantly more water utilities than originally thought. The Siddiqui and Amy (1993) study was restricted by a much higher bromate detection limit than is currently possible. During the time of this study, the detection limit for bromate by IC has been lowered to 2 ug/L. The other difference between their study and this study is that they used a semi-batch mode of ozone application, whereas in this study a true batch mode of ozone application has been emphasized, and it has been found that bromate formation is reactor specific. Differences between two different modes of ozone application will be discussed later. Recent work by Amy et al. (1993) now suggests that there is no actual Br^- threshold level but only the analytical constraint of minimum detection limit (MDL); thus, any level of Br^- can form some BrO_3^- upon ozonation.

Effect of Temperature

From the Arrhenius relationship, the rate constant k of bromate formation can be considered temperature dependent in the following manner:

$$k = (a)e^{-E/RT} \qquad (8.5)$$

where k = rate constant; T = absolute temperature; E = activation energy; R = universal gas constant; and a = constant.

Thus, temperature is a potentially important water quality variable. The

effects of temperature on bromate formation were studied at 15, 20, and 25°C, with 20°C chosen as the baseline condition. The results show that bromate formation increases with increasing temperature (Figure 8.1d). This is generally consistent with what previous researchers have found. Siddiqui and Amy (1993) attribute this to a combination of the temperature-dependent increase in rate constants and a decrease in the pK_a of HOBr-OBr^- with an increase in temperature.

Temperature also has a direct effect on ozone decay; an increase in temperature brings about a decrease in the dissolved ozone concentration (Roth and Sullivan, 1981; Hewes, C. et al. ,1971; Sotelo, J.L. et al., 1989). This occurs due to a drop in the liquid phase driving force and to a higher ozone decomposition rate. Our results agree with the literature, and a higher ozone decomposition was observed with high temperature values.

Effect of Ammonia

The effect of ammonia on the formation of bromate and ozone decay was studied. NH_3/O_3 ratios of 0.2, 0.35, and 0.5 mg/mg were used in the experiments; the NH_3/O_3 = 0.35 mg/mg ratio corresponds to the stoichiometric conversion of Br^- to OBr^- and stoichiometric conversion of OBr^- to monobromamine (i.e., 1 mol of O_3 produces 1 mol of OBr^- which reacts with 1 mol of NH_3 to produce monobromamine, and thus the stoichiometric ratio of NH_3/O_3 can be calculated as; NH_3/O_3 = (1mol)/(1mol) = (17g)/(48g) = 0.35 mg/mg). It has been observed that addition of ammonia decreases bromate formation (Figure 8.1e). This is likely due to direct reaction of OBr^- with ammonia to form monobromamine or reaction of HOBr with ammonia and a corresponding conversion of OBr^- to HOBr. Adding excess ammonia (NH_3/O_3 = 0.5 vs 0.35 mg/mg) did not decrease the bromate formation further. This may possibly be attributable to the reaction competition between OBr^- and O_3 versus OBr^- and NH_3 :

$$OBr^- + 2O_3 \rightarrow BrO_3^- + 2O_2 \qquad k = 100\ M^{-1}\ s^{-1}\ \text{(Haag and Hoigne,1983)} \qquad (8.6)$$

$$OBr^- + NH_3 \rightarrow NH_2Br + OH^- \qquad k = 20\ M^{-1}\ s^{-1}\ \text{(Hoigne and Bader, 1985)} \qquad (8.7)$$

Effect of DOC

DOC exerts a very clear negative influence on bromate formation (Figure 8.1f). This effect is largely in response to its positive influence on ozone decay; i.e., DOC-related ozone demand. However, this effect is very source

specific with DOC from more humic sources generally exerting a greater ozone demand.

Effect of Hydrogen Peroxide

Peroxide effects on the formation of bromate and ozone decay were studied. Our results have shown that addition of peroxide increases bromate formation in some waters and decreases it in other waters. Thus, more work should be performed to understand the mechanisms of the influence of peroxide on bromate formation. Hydrogen peroxide may potentially react with OBr^- to produce bromate:

$$H_2O_2 + OBr^- \rightarrow BrO_2^- + H_2O \quad (8.8)$$
$$BrO_2^- + OBr^- \rightarrow Br^- + BrO_3^- \quad (8.9)$$

Ozone reaction with hydroperoxoide ion (HO_2^-) is very fast ($k = 5.5 \times 10^6\ M^{-1}\ s^{-1}$); thus, the presence of hydrogen peroxide in water significantly affects ozone decay. The ozone decomposition rate increases with increasing pH values. Peroxide effects have been studied only at baseline pH values, and results show that ozone decomposition is faster in the peroxide containing waters.

Peroxide effects are also manifested by its role in promoting hydroxyl radical ($OH\cdot$) formation in the presence of ozone (Hoigne and Bader, 1985), and by its independent role in reducing hypobromite to bromide (Haag and Hoigne, 1983):

$$H_2O_2 + 2O_3 \rightarrow 2OH\cdot + 3O_2 \quad (8.10)$$
$$H_2O_2 + OBr^- \rightarrow Br^- + O_2 + H_2O \quad (8.11)$$

The stochiometric ratio for peroxide production of $OH\cdot$ radicals is H_2O_2/O_3 = 0.35 mg/mg. Above this ratio, there is an excess of peroxide in the system.

Effect of Reaction Time

Reaction time is another parameter which affects bromate formation and ozone decay. Results show that bromate formation is directly related to the dissolved ozone concentration in water, and bromate does not form after dissolved ozone concentration goes to zero. In a majority of the water sources studied, ozone concentration decreased to zero in less than an hour (Figure 8.2), with an ozone half-life ranging from approximately 10 seconds to 30 minutes. Thus, bromate formation does not occur beyond a time frame of about one hour. Ozone reaction with bromide is fast, and most of the bromate formation occurs in the first five minutes after ozone application.

COMPARISON OF REACTOR TYPES

In work performed herein, two different reactor configurations have been employed: (i) semi-batch and (ii) true-batch. In the semi-batch ozonation system, ozone is applied continuously (mg/L-min) to a batch of water (L) for a predetermined application time (min) to achieve a targeted applied dose (mg/L); corresponding measurement of transfer efficiency (typically = 35% to 65%) allows determination of transferred/utilized ozone dose. In the true-batch approach, a stock solution of ozone (≈ 35-40 mg/l) is prepared by exhaustive ozonation of Milli-Q water at 2-3°C and then added to a batch of the source water of interest, and a teflon disk cover is used to prevent any transfer of ozone from the liquid phase to the gas phase.

Since dissolved ozone is directly responsible for bromate formation, the dissolved ozone profile at any time in the reactor is very important. In the semi-batch approach, dissolved ozone concentration increases with time during application (with a possible lag while most ozone demand is being met) and thereafter decreases with time after ozone application has ceased. Bromate also forms in response to the dissolved ozone present in water at any time during the application of ozone. In contrast, in the true batch approach, at time zero (the time of stock introduction), an initial system exists within which the reactants are at their maximum and the products do not exist; after time zero, ozone decays and bromate forms over time. Figure 8.3 shows bromate formation and ozone decay for semi batch and true batch modes of applications. Both reactor configurations have some advantages and disadvantages. The semi-batch mode is physically more similar to pilot-scale or full-scale continuous-flow ozone contactors than true-batch in terms of the continuous introduction of gas. In these systems (semi-batch or continuous-flow), it is necessary to measure transfer efficiency in order to determine utilized ozone dose. On the other hand, transfer efficency is not a concern in the true-batch system, because applied and transferred ozone are identical. In the semi-batch application, one should always be concerned about head space in the reactor and any possible transfer of ozone from the liquid to gas phase. The biggest concern with the true batch approach can be associated with the dilution effect caused by adding a small amount of ozone stock solution to an aliquot of source water; however, dilution effects can be accounted for by redefining the original water characteristics.

MODELING EFFORTS

The experimental methods used in this study along with statistical approaches are explained in Chapter 2. Three type of models that are discussed

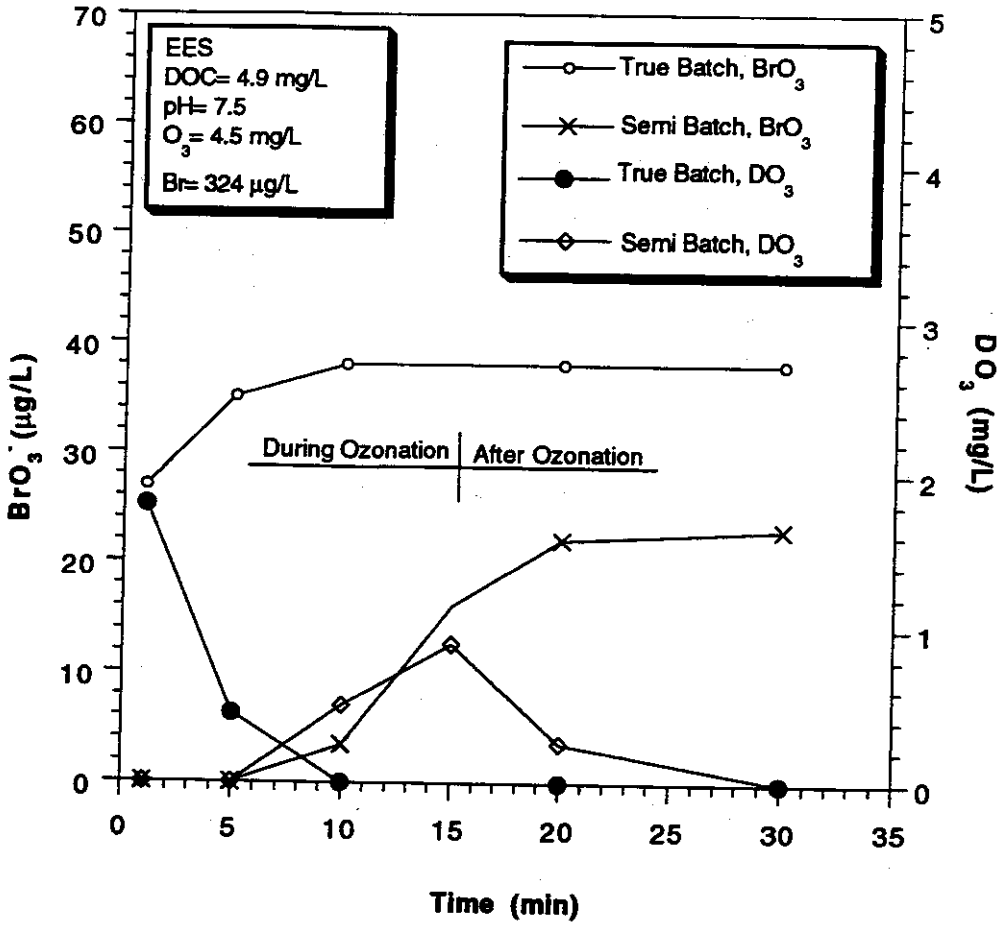

Figure 8.3. Effect of Reactor Type on Bromate Formation

herein were developed (i) semi-batch, (ii) true-batch-EPA, (iii) true-batch-EPA+EBMUD models. Semi-batch models were developed during the beginning stages of the project with data derived from semi-batch ozonation of the first five source waters selected as part of the EPA data base (n=113). True-batch models were developed during later stages with data derived from true-batch ozonation, consisting of two data bases; the EPA data base alone (n= 116) or the combined EPA+EBMUD data base (n= 176). The two true-batch models are similar in format except that the former was calibrated using data from a smaller yet diverse data base derived from six source waters; the latter was calibrated with a larger data base which was influenced by the four California waters comprising the EBMUD sources.

Step-wise multiple regression was used to develop the models according to a power function format; relevant statistical parameters include the number of cases (n) and the multiple coefficient of determination (R^2). Each model was tested through an internal validation, representing a data simulation with data used in model calibration. A perfect data simulation between predicted and measured values would be presented by a regression line with a slope of 1.0, an intercept of zero, and an r^2 of 1.0; this analysis also allows an assessment of model over- or under-prediction.

An important stipulation of the following models is the indicated boundary conditions, defined by the ranges over which each independent parameter was varied. These ranges were defined by the orthogonol matrix employed: O_3/DOC = 0.5, 1.0* 2.0 mg/mg; Br^- = amb., amb. + 0.1*, amb. + 0.2 mg/L; pH = 6.5, 7.5*, 8.5; NH_3/O_3 = 0*, 0.20, 0.35, 0.50 mg/mg; temperature = 15, 20*, 25 C (* = baseline condition; for high ambient Br^- > 80 ug/L, amb. was used as the baseline; for low DOC waters ≤ 2.0 mg/L, O_3/DOC = 2 mg/mg was used as the baseline). The reaction times evaluated ranged from 1 to 60 minutes. For the semi-batch approach, ozone is applied at "absolute" time "zero" until some targeted dose is achieved; thereafter (post-O_3), the DO_3 residual is allowed to decay. The semi-batch models define reaction time (t) as beginning at the end of the application period, a "redefined" time zero.

Ozone Demand Models

Bromide directly reacts with ozone to form bromate, therefore an understanding of ozone decay and its relationship to bromate formation is crucial. Three different ozone decay models (semi-batch, true-batch-EPA, true-batch-EPA+EBMUD) are shown in Table 8.1. The model exponents shown in Table 8.1 demonstrate the ozone demand of DOC and the effect of pH on ozone decomposition. The coefficient associated with alkalinity demonstrates its stabilizing influence on O_3 decomposition. While temperature is not included

TABLE 8.1- PREDICTIVE MODELS FOR OZONE DECAY

a- Semi Batch Model

(Source Waters: BRW, SPW, BGW, MGW, HMR)

$$[DO_3] = 182\ (DOC)^{-2.66}\ (pH)^{-2.66}\ (O_3)^{1.52}\ (Br)^{0.176}\ (t+1)^{-0.53}$$

$R^2 = 0.61$, $F = 34$, $N = 113$, $\alpha < 0.0001$

b- True Batch Model; EPA Data Only

(Source Waters: BGW, PBW, ISW, SPW, TYA, HMR)

$$[DO_3] = 357\ (DOC)^{-1.79}\ (pH)^{-3.66}\ (O_3)^{1.83}\ (Br)^{0.08}\ (t)^{-0.59}\ (Alk)^{0.227}$$

$R^2 = 0.66$, $F = 65$, $N = 116$, $\alpha < 0.0001$

c- True Batch Model; EPA+EBMUD Data

(Source Waters: BGW, PBW, ISW, SPW, TYA, HMR, EIS, ESL, EBC, EES)

$$[DO_3] = 2831\ (DOC)^{-1.942}\ (pH)^{-4.79}\ (O_3)^{1.81}\ (Br)^{0.163}\ (t)^{-0.678}\ (Alk)^{0.236}$$

$R^2 = 0.68$, $F = 83$, $N = 176$, $\alpha < 0.0001$

where

Br^- = Bromide (µg/L) ; $70 \leq [Br^-] \leq 440$

DO_3 = Dissolved Ozone (mg/L) ; $0.05 \leq [DO_3] \leq 4.6$

t = Time (min) ; $1 \leq t \leq 120$

pH; $6.5 \leq pH \leq 8.5$

DOC= Dissolved Organic Carbon (mg/L) ; $1.1 \leq DOC \leq 8.4$

O_3 = Transferred/Utilized Ozone (mg/l) ; $1.1 \leq O_3 \leq 10$

Alk = Alkalinity (mg/l); $13 \leq Alk \leq 316$

as a parameter in the models, it exhibits a significant influence on O_3 decomposition (slower at lower temperature). In the semi-batch model, the reaction time (t) is based on post-ozonation (after O_3 application has ceased) conditions. However, some ozone demand is met during ozonation; hence, the use of the (t + 1) term in the model permits calculation of the ozone residual after ozone application at t = 0. Data simulations, in the form of predicted versus measured comparisons, are shown in Figure 8.4. All of the models show some overpredictions at lower values with underpredictions observed at higher values; predictions are most accurate under conditions leading to medium levels. The ozone residual models have potential relevance in making C-T predictions, a point discussed later in more detail.

Bromate Formation Models

Table 8.2 shows bromate formation models for semi-batch, true-batch-EPA, and true-batch-EPA+EBMUD data bases. Data simulations for all models are shown in Figure 8.5. Again, the reaction time, t, is based on post-ozonation conditions in the semi-batch bromate model. However, bromate can form during ozonation; thus, use of the (t + 1) term in the model permits time-zero (the instant when ozone application has ceased) predictions. The regression lines suggest some propensity towards overpredictions at lower values, and underprediction towards higher values for all the models, with best predictions provided under mid-level conditions. In all of the models, while reaction time is shown to exert a positive effect, bromate does not form after the ozone residual goes to zero. Therefore, the bromate prediction models may potentially be coupled with the corresponding ozone residual models shown in Table 8.1. Once again, temperature effects are not encompassed by the models; greater bromate is observed at higher temperature.

Bromate formation models without ammonia as a parameter are also shown for true-batch-EPA and true-batch-EPA+EBMUD data sets in Table 8.2. Those models provide flexibility to water utilities that do not measure ammonia as a water quality parameter, or that do not contemplate ammonia addition as a control option. Data simulations using these models are shown in Figure 8.6. Again, overprediction at lower values, and underprediction at higher values are observed.

CT Models

In the Surface Water Treatment Rule (SWTR), disinfection is addressed by EPA through the use of CT values (defined as the product of residual ozone concentration in mg/L and effective contact time in minutes). Therefore, having a CT-based model would be useful in helping to understand the

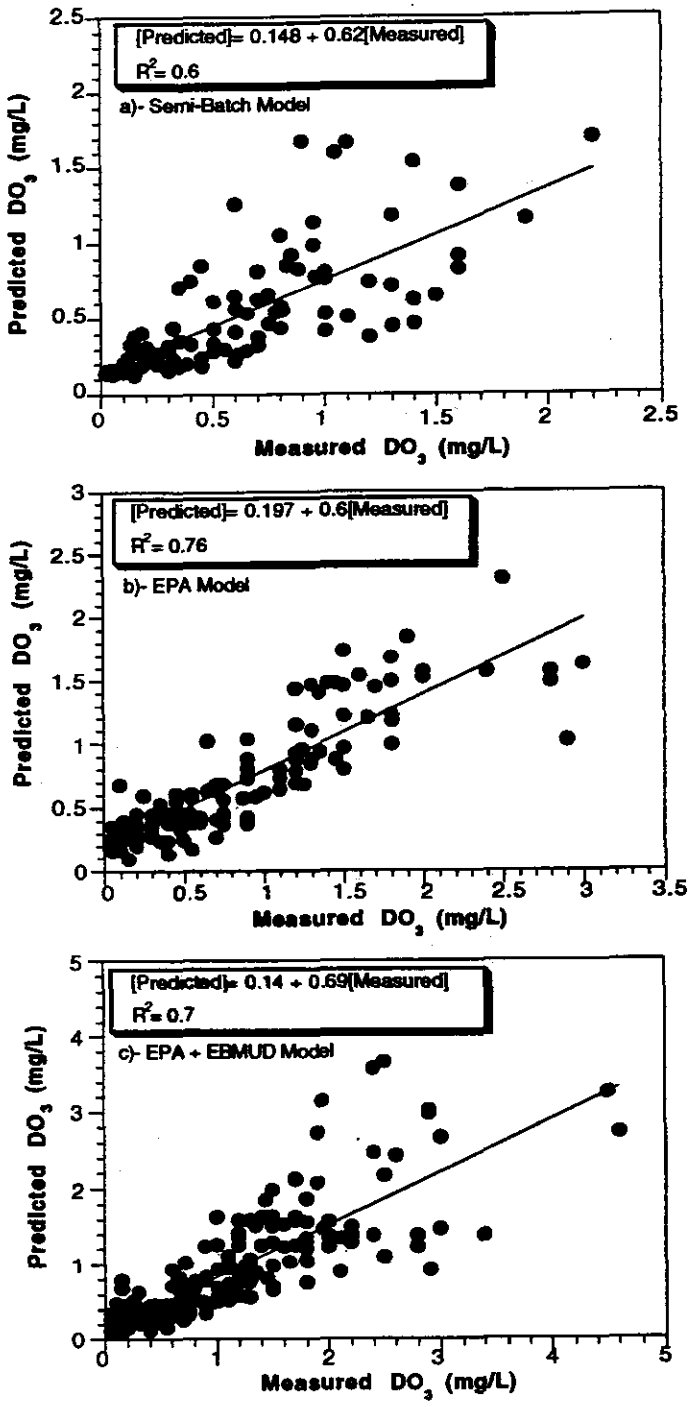

Figure 8.4. Predicted versus Measured Dissolved Ozone Using Semi Batch, True Batch-EPA, and True Batch EPA+EBMUD Models

TABLE 8.2- PREDICTIVE MODELS FOR BROMATE FORMATION

a- Semi Batch Model

(Source Waters: BRW, SPW, BGW, MGW, HMR)

$$[BrO_3] = 5.5x10^{-6} (DOC)^{-1.61} (pH)^{4.54} (O_3)^{1.2} (Br)^{1.06} (t+1)^{0.35}$$

$R^2 = 0.62$, F= 38, N = 113, $\alpha < 0.0001$

b- True Batch Model; EPA Data Only

(Source Waters: BGW, PBW, ISW, SPW, TYA, HMR)

1- without Ammonia

$$[BrO_3] = 2.74x10^{-6} (DOC)^{-1.32} (pH)^{5.4} (O_3)^{1.36} (Br)^{0.86} (t)^{0.31}$$

$R^2 = 0.73$, F= 61, N = 116, $\alpha < 0.0001$

2- with Ammonia

$$[BrO_3] = 1.1x10^{-6} (DOC)^{-1.09} (pH)^{5.71} (O_3)^{1.16} (Br)^{0.834} (t)^{0.29} (NH_3\text{-}N)^{-0.31}$$

$R^2 = 0.78$, F= 83, N = 135, $\alpha < 0.0001$

c- True Batch Model; EPA+EBMUD Data

(Source Waters: BGW, PBW, ISW, SPW, TYA, HMR, EIS, ESL, EWC, EES)

1- without Ammonia

$$[BrO_3] = 4.3x10^{-6} (DOC)^{-1.44} (pH)^{5.24} (O_3)^{1.58} (Br)^{0.79} (t)^{0.292}$$

$R^2 = 0.73$, F= 103, N = 176, $\alpha < 0.0001$

2- with Ammonia

$$[BrO_3] = 2.32x10^{-6} (DOC)^{-1.47} (pH)^{5.35} (O_3)^{1.65} (Br)^{0.81} (t)^{0.28} (NH_3\text{-}N)^{-0.121}$$

$R^2 = 0.75$, F= 106, N = 213, $\alpha < 0.0001$

where

BrO_3^- = Bromate (µg/L) ; $2 \leq [BrO_3^-] \leq 314$

Br^- = Bromide (µg/L) ; $70 \leq [Br^-] \leq 440$

t = Time (min) ; $1 \leq t \leq 120$

pH; $6.5 \leq pH \leq 8.5$

DOC= Dissolved Organic Carbon (mg/L) ; $1.1 \leq DOC \leq 8.4$

O_3 = Transferred/Utilized Ozone (mg/l) ; $1.1 \leq O_3 \leq 10$

NH_3-N = Nitrogen ammonia (mg/l); $0.02 \leq NH_3\text{-}N \leq 3$

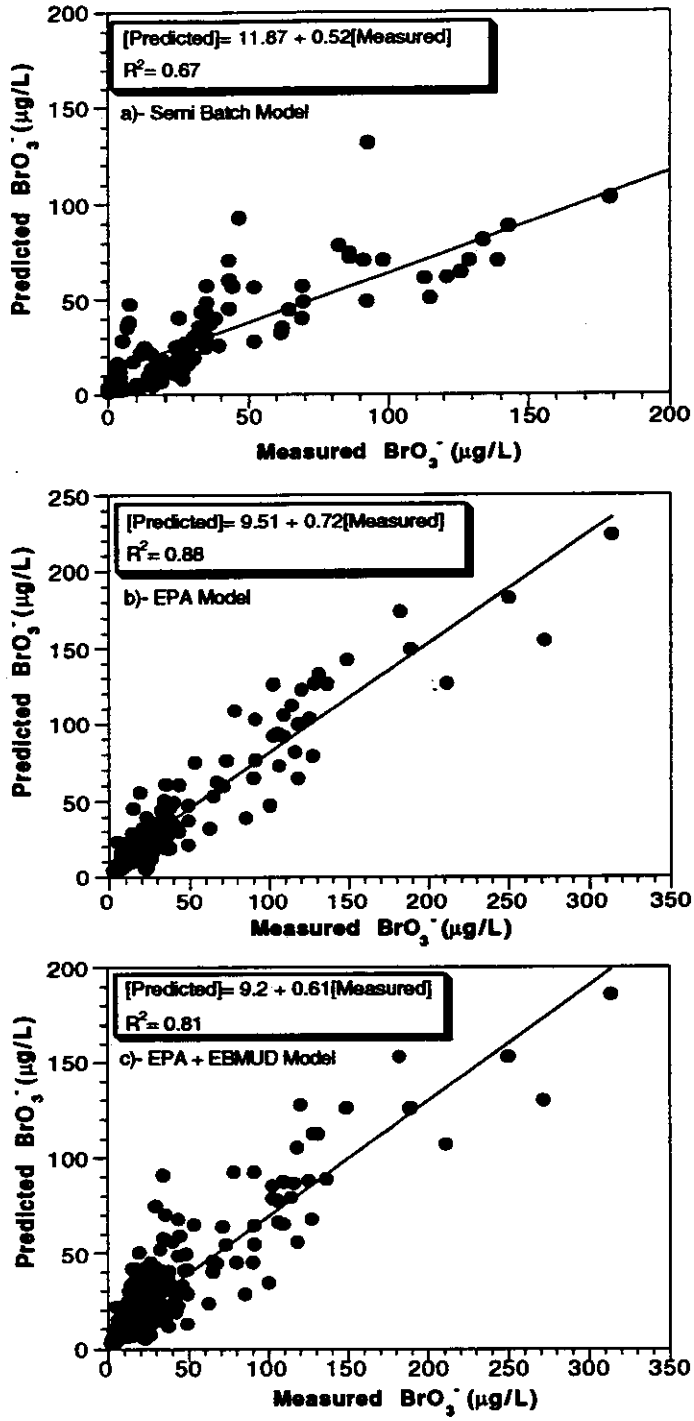

Figure 8.5. Predicted versus Measured Bromate Using Semi Batch, True Batch-EPA, and True Batch EPA+EBMUD Models

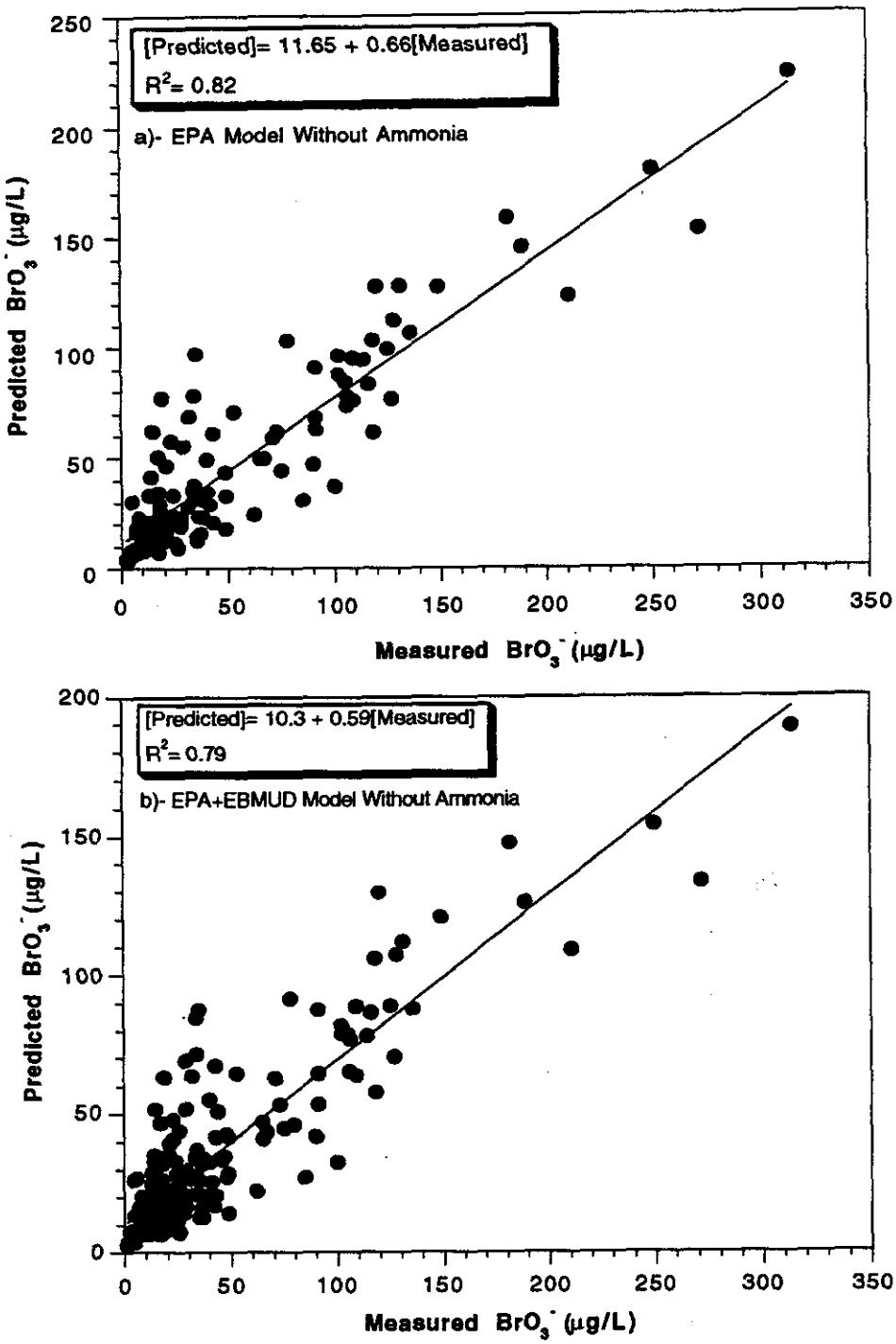

Figure 8.6. Predicted versus Measured Bromate Using True Batch-EPA, and True Batch EPA+EBMUD Models without Ammonia

relationship between DBPs and disinfection levels under certain water quality and operating conditions. The SWTR interpretation of CT involves the DO_3 residual (C) leaving a continuous-flow contactor and the t_{10} residence time (T). In a batch system, this parameter can be approximated by using the exposure time concept developed by Von Gunten and Hoigne (1993) which corresponds to integration of the ozone decay curve (C vs. t).

Table 8.3 shows CT models calibrated with true-batch-EPA and true-batch-EPA+EBMUD data bases. Data simulations with these models are shown in Figure 8.7; in general, there is very good agreement. Model exponents show that increasing pH and DOC will lower CT values, reflecting both the lesser stability of ozone at higher pH values and the ozone demand of DOC. CT values also can be translated to bromate levels by using CT as a variable in bromate prediction models. Table 8.4 shows bromate models with CT as a variable in the model for true-batch-EPA and true-batch-EPA+EBMUD data sets. Data simulations using these models are shown in Figure 8.8. Regression lines suggest overpredictions at lower values and underpredictions at higher values.

Figure 8.9 shows (ultimate) bromate formation as a function of (calculated) CT values for different water sources. The calculated values represent integration of DO_3 vs t curves from t = 0 to several selected points along the decay curve. Besides differences in Br^- levels, the fact that, for the same CT values, each water shows different bromate formation suggests that type of DOC in these waters also is important. This CT concept captures the ozone-demand characteristics of the specific DOC present. Figure 8.10 shows (ultimate) bromate formation as a function of CT for different water sources with equal (adjusted) bromide levels. In comparison to Figure 8.9 (variable bromide), there is less divergence in the bromate formation response of the different waters. Nevertheless, while the divergence is less, it is still significant, indicating the influence of (type and amount) of DOC. Even for those plots corresponding to almost equal DOC levels, there are still differences, indicating the influence of type of DOC.

External Validation of Models

External validation of models is important to check validity of the models. External validation involves use of data *external* to the data base to test the predictive capabilities of models. We elected to use data from several studies summarized in Table 8.5; these include pilot studies (Siddiqui et al., 1993; Krasner et al., 1993) and continuous-flow bench-scale studies (James M. Montgomery Engineers, 1992), conducted over a range of water quality and treatment conditions. Temperature conditions were not considered in these simulations; reaction time was set equal to the hydraulic residence time

TABLE 8.3- PREDICTIVE MODELS FOR CT

a- True Batch Model; EPA Data Only

(Source Waters: BGW, PBW, ISW, SPW, TYA, HMR)

$$[CT] = 9.2\ (DOC)^{-0.809}\ (pH)^{-1.053}\ (O_3)^{1.304}\ (t)^{0.691}$$

$R^2 = 0.96$, F= 602, N = 116, $\alpha < 0.0001$

b- True Batch Model; EPA+EBMUD Data

(Source Waters: BGW, PBW, ISW, SPW, TYA, HMR, EIS, ESL, EWC, EES)

$$[CT] = 14.5\ (DOC)^{-0.753}\ (pH)^{-1.266}\ (O_3)^{1.265}\ (t)^{0.677}$$

$R^2 = 0.96$, F= 954, N = 176, $\alpha < 0.0001$

where

CT= (Concentration)(Time) (mg-min/L); $0.7 \leq CT \leq 155$

t = Time (min) ; $1 \leq t \leq 120$

pH; $6.5 \leq pH \leq 8.5$

DOC= Dissolved Organic Carbon (mg/L) ; $1.1 \leq DOC \leq 8.4$

O_3 = Transferred/Utilized Ozone (mg/L); $1.1 \leq O_3 \leq 10$

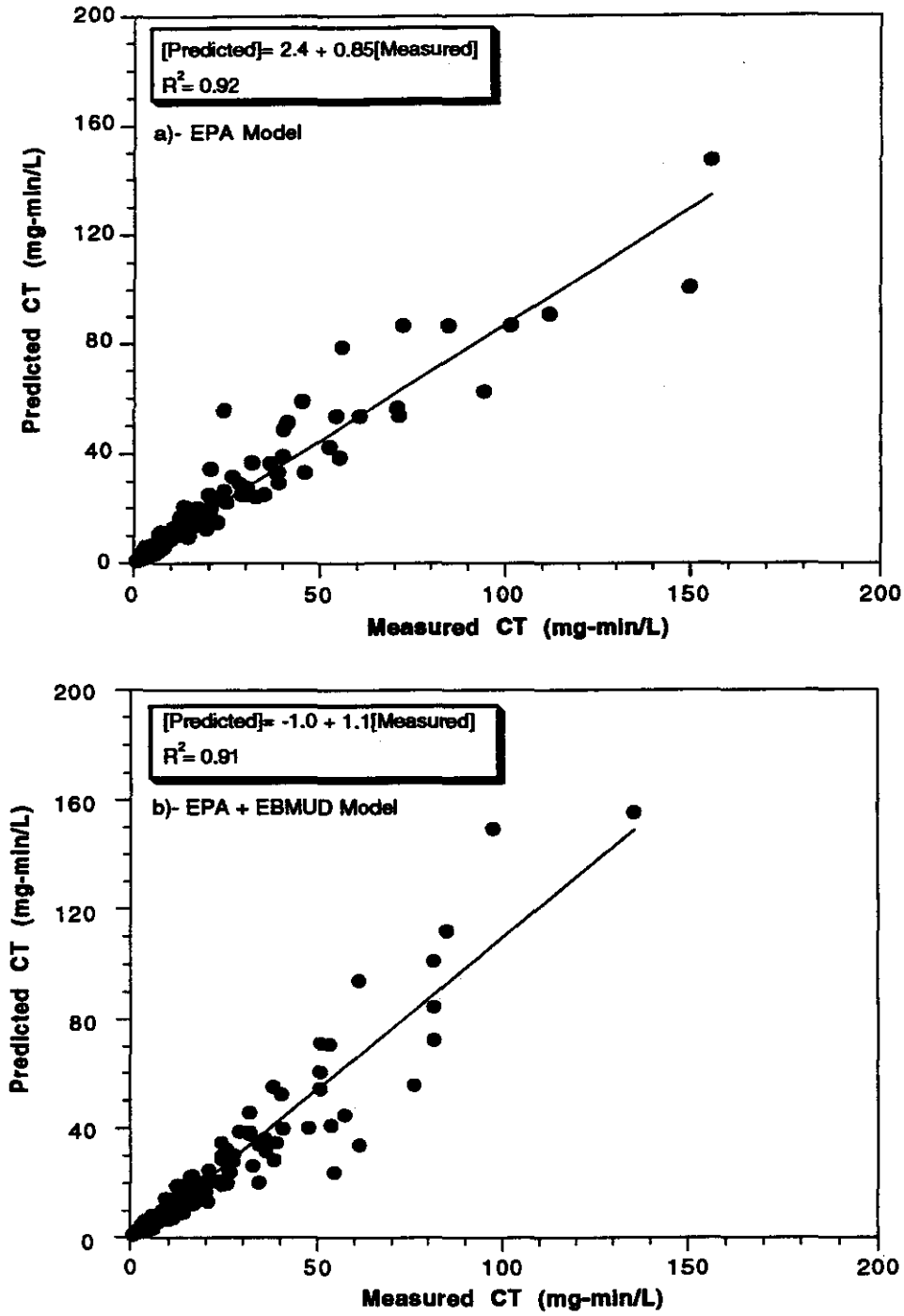

Figure 8.7. **Predicted versus Measured CT, True Batch-EPA, and True Batch EPA+EBMUD Models**

TABLE 8.4- PREDICTIVE MODELS FOR BROMATE FORMATION WITH CT

a- True Batch Model; EPA Data Only

(Source Waters: BGW, PBW, ISW, SPW, TYA, HMR)

$$[BrO_3] = 1.0 \times 10^{-6} (DOC)^{-0.368} (pH)^{6.185} (Br)^{0.793} (CT)^{0.553}$$

$R^2 = 0.7$, F= 66, N = 116, $\alpha < 0.0001$

b- True Batch Model; EPA+EBMUD Data

(Source Waters: BGW, PBW, ISW, SPW, TYA, HMR, EIS, ESL, EWC, EES)

$$[BrO_3] = 3.0 \times 10^{-7} (DOC)^{-0.211} (pH)^{6.818} (Br)^{0.684} (CT)^{0.603}$$

$R^2 = 0.7$, F= 100, N = 176, $\alpha < 0.0001$

where

BrO_3^- = Bromate (µg/L) ; $2 \leq [BrO_3^-] \leq 314$

Br^- = Bromide (µg/L) ; $70 \leq [Br^-] \leq 440$

t = Time (min) ; $1 \leq t \leq 120$

pH; $6.5 \leq pH \leq 8.5$

DOC= Dissolved Organic Carbon (mg/L) ; $1.1 \leq DOC \leq 8.4$

CT= (Concentration)(Time) (mg-min/L); $0.7 \leq CT \leq 155$

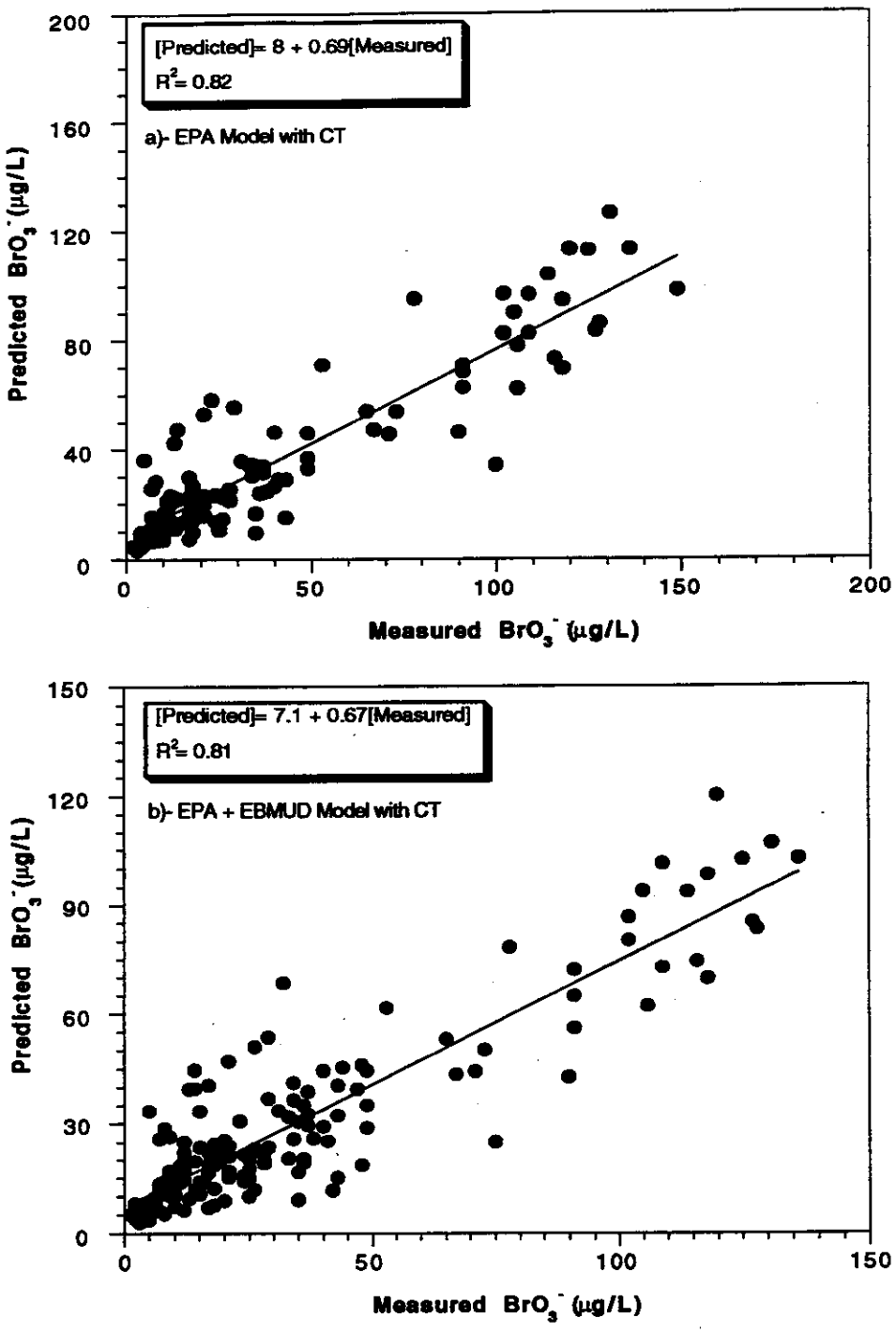

Figure 8.8. Predicted versus Measured Bromate Using True Batch-EPA, and True Batch EPA+EBMUD Models with CT

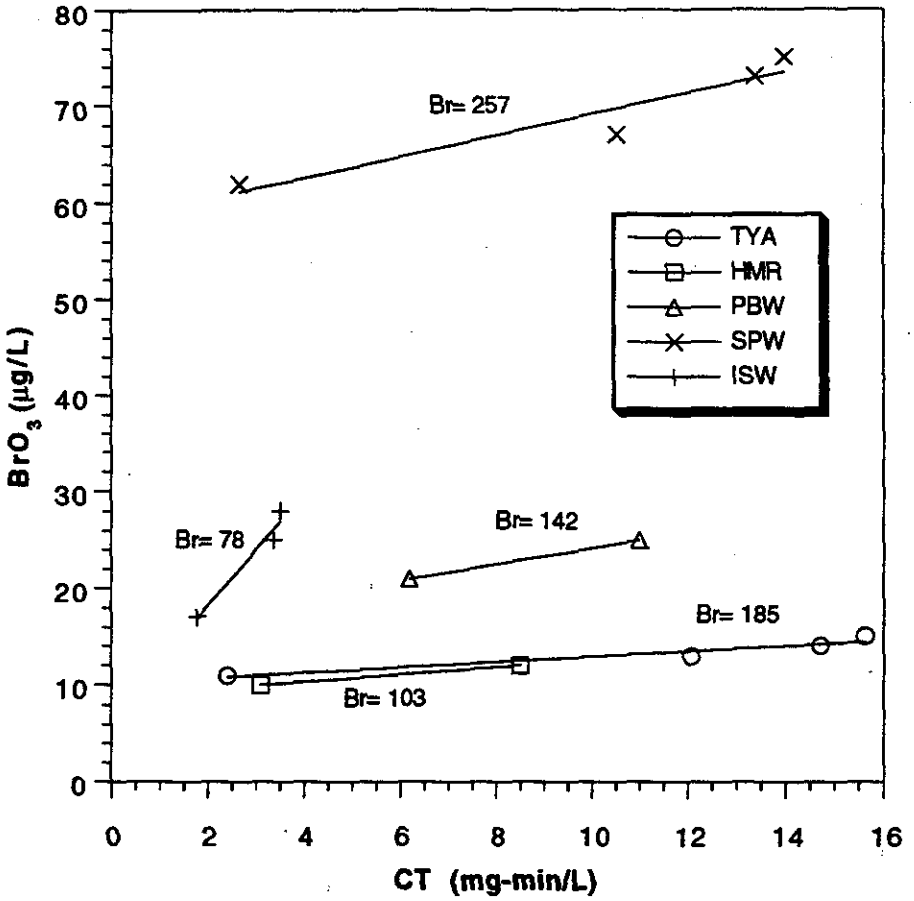

Figure 8.9. Bromate Formation as a Function of Ozone Exposure (C-T); Variable Bromide

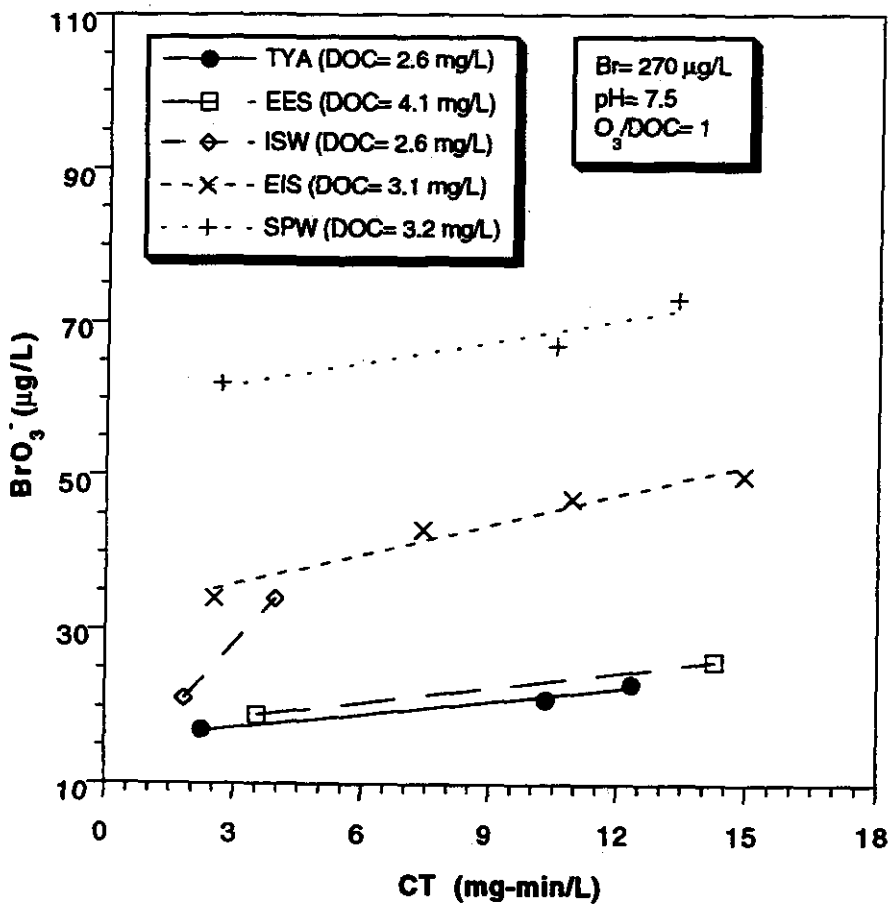

Figure 8.10. Bromate Formation as a Function of Ozone Exposure (C-T); Constant Bromide

TABLE 8.5- EXTERNAL VALIDATION OF MODELS WITH LITERATURE DATA

Water Source	Ref.	pH	Br (µg/L)	O3 (mg/L)	DOC (mg/L)	Measured BrO3(mg/L)	Predicted BrO3(µg/L) EPA	EPA+EBMUD
Utility #4	1	8.0	360	7.81	4.2	148	164	148
		7.0	360	2.35	4.2	8	16	11
		7.0	360	4.45	4.2	32	37	30
Utility #5	1	8.4	90	2.39	5.2	5	8	7
		7.4	90	4.63	5.2	8	12	10.5
Utility #23	1	7.3	400	1.98	3.3	10	23	16
Utility #24	1	7.2	260	0.42	0.6	15	17	11
		7.4	260	0.66	0.6	29	37	27
		8.2	260	0.41	0.6	14	33	21.5
Utility #27	1	8.1	30	9.8	4.5	10	25	29
Utility #30	1	7.3	30	5.1	4.5	6	6	6
Sacramento River Delta	2	7.3	30	9.7	4.5	14	14	16
		8.3	160	6.1	6.6	10	39	33
		6.8	60	6.6	3.7	7	13	14
		8.8	500	4.0	5.5	100	71	53
		8.8	500	4.0	5.5	121	88	65
		6.5	500	4.0	5.5	31	14	11
		6.5	500	4.0	5.5	37	17	13
		8.8	500	2	5.5	32	28	18
Colorado River	3	8.0	290	1	3.3	16	14	9
		8.0	290	2	3.3	28	36	25
		8.0	290	3	3.3	117	63	48
		8.0	290	4	3.3	122	93	76

1- James M. Montgomery Engineers, " Effects of Cagulation and Ozonation on the Formation of Disinfection By-Products", Prepared for AWWA, January 1992.

2- Siddiqui, M., Amy, G., Ozekin, K., Westerhoff, P., Miller, K., " The Role of Tracer Studies in Relating Laboratory and Pilot-Scale Ozonation Data", 11th Ozone World Congress Proceedings, San Francisco, 1993.

3- Krasner, S.W., Gramith, J.T., Coffey, B.M., Yates, R.S., " Impact of Water Quality and Operational Parameters on the Formation and Control of Bromate During Ozonation", International Water Supply Association Proceedings : Bromate and Water Treatment, Paris, November 22-24, 1993.

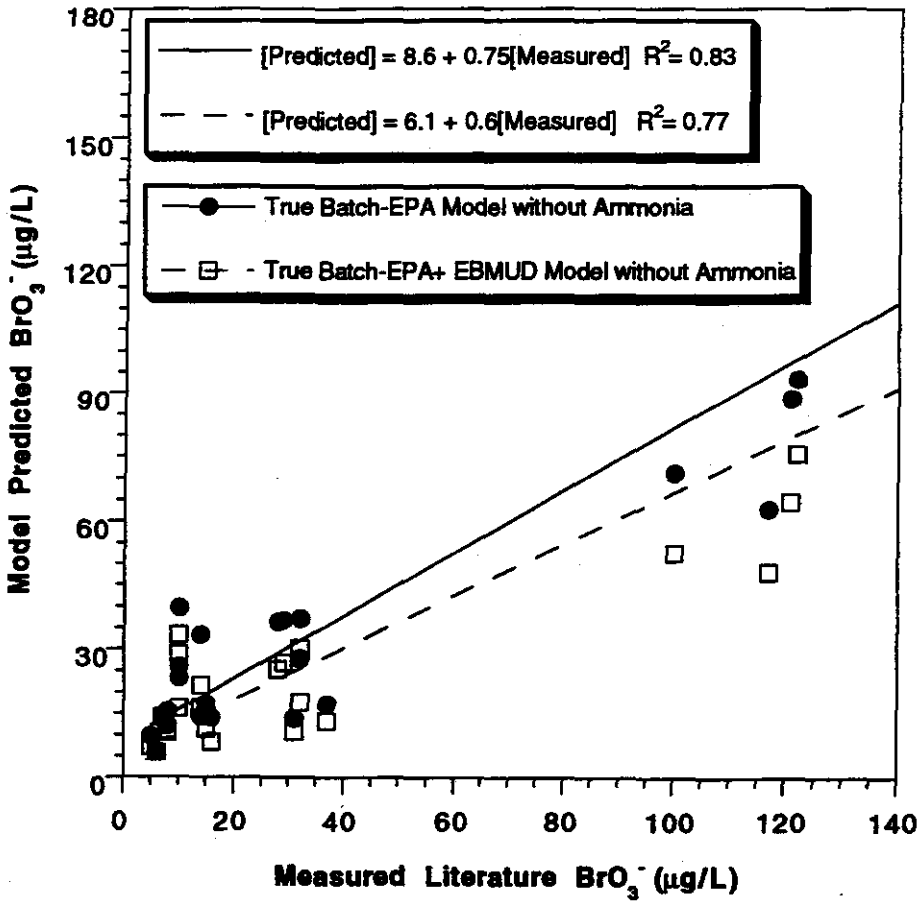

Figure 8.11. External Validation of Models with Literature Data (Data from Table 8.5)

(HRT); ozone doses are transferred doses; and the data reflect a mix of pre- and intermediate-O_3 tests. Figure 8.11 shows predicted values versus pilot (and continuous-flow bench) scale values for true-batch-EPA (without ammonia) and true-batch-EPA+EBMUD (without ammonia) models. These model predictions show some underprediction at higher values and some overprediction at low values, suggesting reasonably good predictions at intermediate values.

COMPARISON OF TRUE BATCH WITH SEMI-BATCH MODELS

It was previously stated that bromate formation is reactor specific, a premise that can be demonstrated by comparing the semi-batch and true-batch models under the same water quality and operational conditions. Figure 8.12 shows predictions of bromate for different source waters using semi-batch and true-batch-EPA models. These simulations show that the true batch model (and its mode of ozone application) results in greater predictions of bromate formation than the semi-batch model (and its mode of ozone application). The difference can range from as low as 30 % to as high as 100 %. One reason for this difference is that there is a higher driving force (higher DO_3) under true-batch mode of ozone application. Another possible reason is the presence of headspace in the semi-batch system, permitting transfer from the liquid to the gas phase after ozone application has ceased. The hydrodynamics of the reactor and associated mixing conditions are another possible reason for these differences. Still another reason is how reaction time is defined in modeling semi-batch data. The previous predictions applied to pilot-plant data are further revealing in that the true-batch models were reasonably capable of predicting bromate formation under continuous-flow pilot-plant conditions.

Thus, even at the laboratory scale, bromate formation is reactor specific. While the semi-batch mode of application more closely simulates a pilot- or full-scale reactor in terms of continuous ozonation, the DO_3 profile is much different; a continuous-flow system provides a steady state profile across the reactor. The true-batch mode of application results in a time-dependent DO_3 profile which is similar to the space-dependent profile observed in ozone contactors with a point of admission near the contactor entrance. We have found that true-batch models more accurately simulate pilot- and full-scale contactors. Such simulations were discussed in the previous section. Admittedly, part of the poor simulations of the semi-batch reactor may be attributed to its non-steady behavior and our assumptions on how to define the reaction time (defined as post-application herein).

EVALUATION OF CONTROL OPTIONS: MODEL SIMULATIONS

An important attribute of the bromate prediction models is that they allow

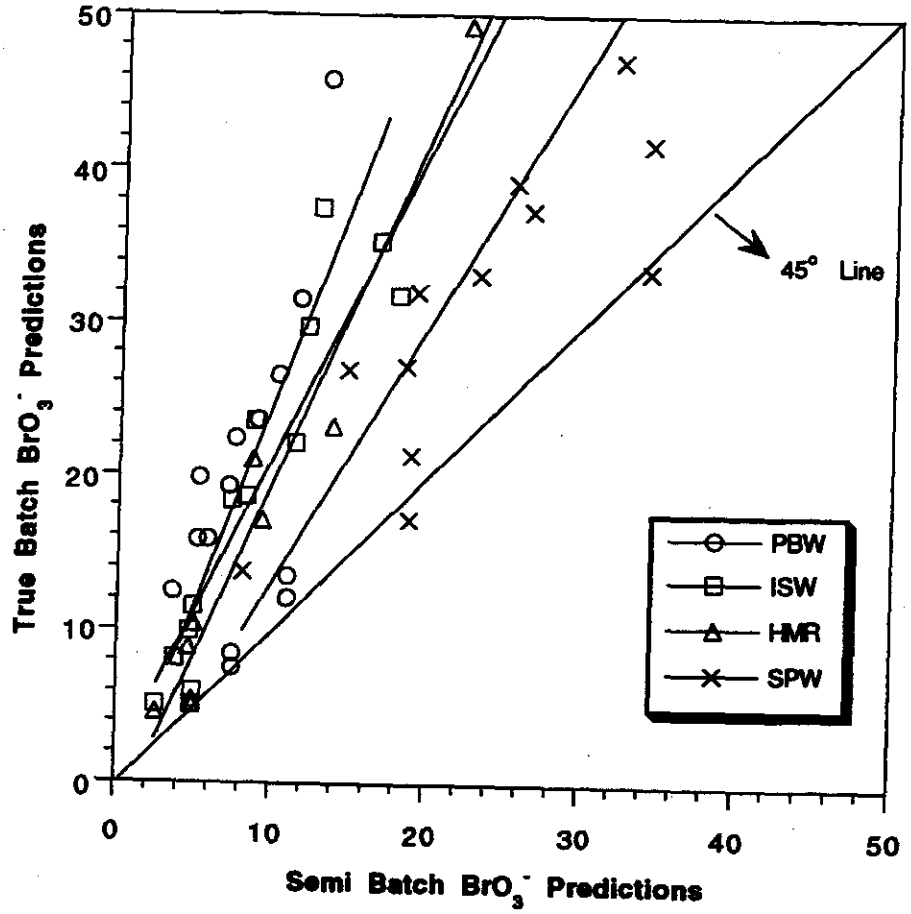

Figure 8.12. Predicted Bromate Using True Batch-EPA Model versus Semi Batch Model

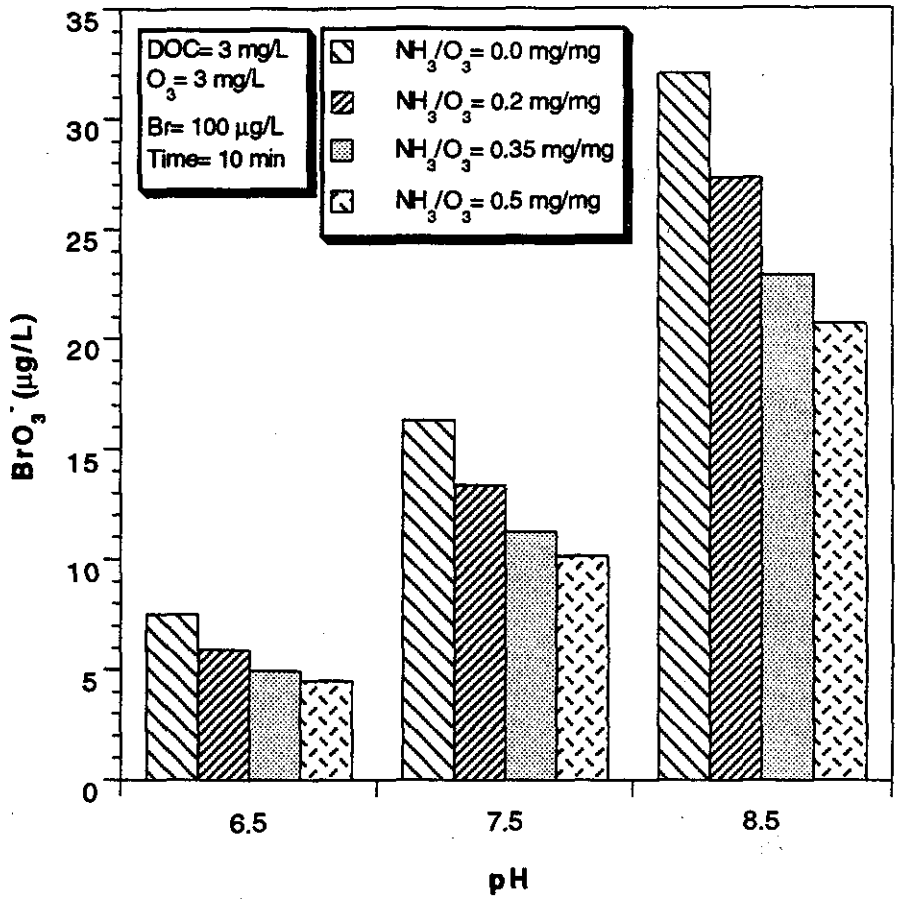

Figure 8.13. Bromate Control Options (Simulations of True Batch-EPA Model)

assessment of bromate control options, including pH depression and ammonia addition. Figure 8.13 shows such simulations based on a defined set of conditions. pH reduction from 8.5 to 7.5 to 6.5 is very influential; the major constraint to such an approach would be the amount of acid required, particularly for high alkalinity waters. Ammonia addition clearly has a lesser effect. These simulations are consistent with control option assessments performed by others, and the designation of pH depression as the best available technology (BAT).

ORGANO-Br FORMATION

In the presence of DOC and Br^-, ozonation of natural waters can lead to organo-Br by-products such as bromoform, bromoacetic acids, bromoacetones, and bromoacetonitriles. Bromoform, one of the brominated organic by-products, can form through reaction of HOBr, acting as a substitution agent, with DOC:

$$HOBr + DOC \rightarrow CHBr_3 \qquad (8.12)$$

It is evident from above reaction that bromoform formation is influenced by certain water quality and operational/treatment conditions such as pH and the presence of DOC. Figure 8.14 shows the effects of various parameters on bromoform formation. As can be seen from Figure 8.14, bromoform forms only in the case of a relatively high bromide concentration and application of relatively high ozone doses. Considering that the MCL for total THMs is 100 ug/L, with a proposal to lower the MCL to 80 ug/L, bromoform formation during ozonation will not be a significant problem for water utilities.

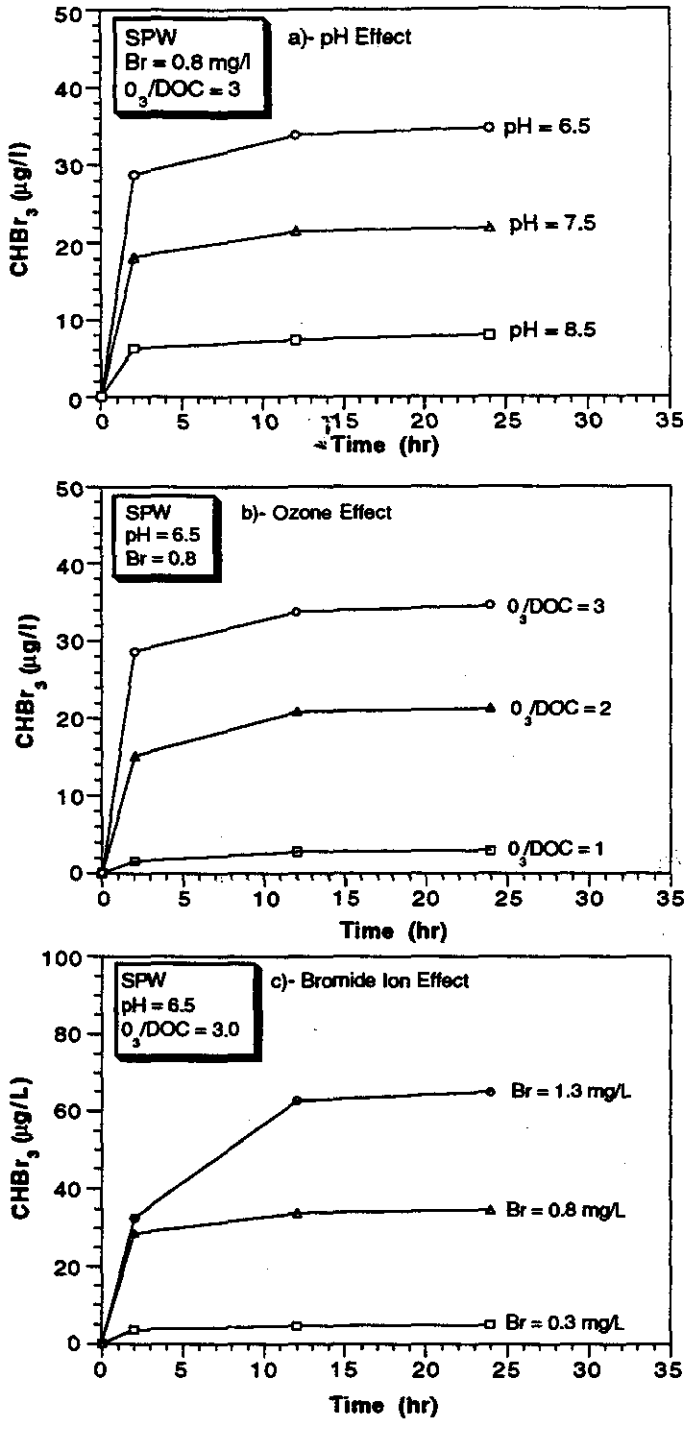

Figure 8.14. Individual Parameter Effects on Bromoform Formation (Semi Batch); Effects of pH, Ozone Dose, and Bromide Ion Concentration

SECTION 9

MODEL APPLICATIONS

The models developed herein can be used to assess the ability of water utilities to meet existing and future DBP regulations. These models have most relevance to inorganic ozonation by-products formed under pre-ozonation conditions, and to chlorination by-products formed either before or after significant DBP precursor removal has been accomplished.

CHLORINATION BY-PRODUCT AND CHLORINE DECAY MODELS

The chlorination by-product models can be used to assess both in-plant and distribution system formation of THMs, HAAs (HAA_6), and CH. (As mentioned previously, THAA models correspond to HAA_6; HAA_5 regulated under Stage 1 of the D/DBP Rule can be estimated by summation of predictions the five relevant individual HAA species). Water quality conditions such as DOC, pH, temperature, and bromide are needed as inputs to the models; such data then allow assessment of chlorination DBP formation as a function of reaction time. Within this context, time can reflect the hydraulic residence (HRT) of a chlorine contact basin or the average HRT of a distribution system.

The models can be used to assess pre-chlorination scenarios involving raw/untreated waters. Post-chlorination scenarios can be assessed using either raw/untreated water models, if little precursor removal has been achieved. Otherwise, either treated (coagulated) water models or reactivity-coefficient adjusted raw-water models can be employed (the latter recommended if temperature and pH variations are significant).

Chloramination scenarios involving the sequence of free chlorine followed by ammonia addition can be approximated by considering the lag time between addition of the respective chemicals; such an approximation would simply show DBPs formed in the presence of free chlorine before ammonia addition.

The effects of precursor removal by chemical coagulation can be assessed through use of the treated water models. One can either predict DBPs formed under a given degree of precursor removal, or can define the degree of precursor removal required to meet given DBP regulations. The impact of bromide ion on meeting regulations can also be assessed. If one makes the assumption that precursor reactivity (i.e., DBP/DOC) changes as a function of treatment type, one can also assess other precursor removal processes such GAC or membranes through use of the raw/untreated water models (i.e., ϕ_{GAC},

$\phi_{MEMBRANES}$). Otherwise, if one assumes comparable effects on reductions in precursor reactivity, the coagulated water models can be used to approximate the performance of these other precursor removal processes. Although it can be envisioned that there is a ϕ_{OZONE}, it is recommended that one should not one use the models to approximate post-chlorination by-products following an ozonation step, given the complexity of ozone effects on subsequent chlorine reactivity of NOM.

Through use of the chlorine decay models, one can assess CT requirements and CT conditions provided under various water quality conditions. Moreover, the chlorine decay models can be used to assess dosing requirements to ensure maintenance of distribution system residuals.

Another potential application is assessing impacts on DBP formation of the lead and copper rule through the pH parameter.

BROMATE AND OZONE DECAY MODELS

The bromate formation models presented herein can be used to approximate bromate formation under varying water quality (DOC, pH, Br^-) and treatment conditions (O_3 dose). The models can also be used to assess potential control strategies (pH depression, NH_3 addition). The major constraint to such use of these models is that bromate formation has been found to be largely reactor specific. It is the dissolved ozone time/space profile within a reactor which is most influential in determining the degree of bromate formation; these profiles are established through the mode of ozone application and contactor hydrodynamics (mixing). Given the two forms of models developed herein, true-batch and semi-batch, it is the former that comes closer to simulating continuous flow contactors, either at the pilot or full-scale.

The effects of DOC on bromate formation can be assessed to determine ozone point of application; either pre-O_3 before any DOC removal has been realized, or intermediate-O_3 after chemical coagulation has achieved some DOC removal. In applying the models to post-coagulated waters, one must assume (as an approximation) that the *character* of the DOC remaining after coagulation resembles that of the raw water. The effects of pH, either as a water quality condition or treatment option, can easily be assessed. Those models which include an ammonia term were developed to permit assessment of NH_3 addition. Ozone application strategies such as tapered ozonation can be assessed through stepwise application of the model.

The ozone decay models have relevance in both bromate minimization as well as CT aspects of ozone use. The models can be used to approximate contactor DO_3 residuals expected after a given HRT (or t_{10}).

REFERENCES

Amy, G.; Chadik, P. and Chowdhury, Z., "Developing Models for Predicting Trihalomethane Formation Potential and Kinetics", Journal AWWA, 79:7:89 (1987a).

Amy, G.; Minear, R., and Cooper, W., "Testing and Validation of Multiple Linear Regression Model For Trihalomethane Formation Potential", Water Research, 21:649 (1987b).

Amy, G., et al., "The Effect of Ozonation and Activated Carbon Adsorption on Trihalomethane Speciation", Water Research, 25:2:191 (1991).

Amy, G., et al., "Threshold Levels for Bromate Formation in Drinking Water", IWSA Proceedings: Bromate and Water Treatment, Paris (1993).

Amy, G., et al., "Bromide Occurence: Nationwide Bromide Survey", AWWARF Report (1994).

APHA, Standard Methods for the Examination of Water and Wastewater (1989).

Box, G., et al., Statistics For Experimenters, Wiley Interscience (1978).

Chadik, P., and Amy, G., "Coagulation and Adsorption of Aquatic Organic Matter and Humic Substances: An Analysis of Surrogate Parameters for Predicting Effects on Trihalomethane Formation Potential", Environmental Technology Letters, 87:8:261 (1987).

Chowdhury, Z.; Amy, G. & Siddiqui, M., "Modeling Effects of Bromide Ion Concentration on The Formation of Brominated Trihalomethanes", Proceedings. AWWA Conference (1991).

Engerholm, B., and Amy, G., "A Predicative Model for Chloroform Formation from Humic Acids", Journal AWWA 75:8:418 (1983).

Gordon, G., "The very Slow Decomposition of Aqueous Ozone in Highly Basic Solutions", Proceedings, 8th Ozone World Congress, IOA, Zurich, Switzerland (1987).

Gordon, G. Cooper, W., Rice, R., and Pacey, G., "Disinfectant Residual Measurement Methods", AWWARF, Research Report (1987).

Gould, J., Fitchhorn, L., and Urheim, E., "Formation of Brominated Trihalomethanes: Extent and Kinetics", Water Chlorination Environmental Impact and Health Effects/Vol. 4, pp. 297-310, Ann Arbor, MI: Ann Arbor Science Publishers, Inc. (1983).

Grasso, D., "Ozonation Dynamics in Water Treatment: Autocatalytic Decomposition, Mass Transfer and Impact on Particle Stability", Ph.D. Dissertation, The University of Michigan, Ann Arbor, Mich. (1987).

Haag, W., and Hoigne, J., "Ozonation of Bromide Containing Waters: Kinetics of Formation of Hypobromous Acid and Bromate", Envir. Sci. Technol., 17:261 (1983).

Hewes, C., et al., "Kinetics of Ozone Decomposition and Reaction with Organics in Water", A.I.Ch.E., 17:141 (1971).

Hoigne, J., and Bader, H., "Ozonation of Water: Selectivity and Rate of Oxidation of Solutes", Proceedings, 3rd IOA Congress, Paris, France (1977).

Hoigne, J., and Bader, H., "Rate Constants of Reactions of Ozone with Organic and Inorganic Compounds in Water: III: Inorganic Compounds and Radicals", Water Res., 19:993 (1985).

Krasner, S., et al., "The Occurrence Of Disinfection By-ProductsIn U.S. Drinking Water", Journal AWWA, 81: 8:41 (1989).

Krasner, S., et al., "Impact of Water Quality and Operational Parameters on the Formation and Control of Bromate During Ozonation", IWSA Proceedings: Bromate and Water Treatment, Paris (1993).

Lynn, S.W. "An Analytical Survey of Chloroform Formed from the Chlorination of Humic Substances", Ph.D. Dissertation, University of Massachusetts (1982).

Miller, J., and Uden, P., "Characterization of Nonvolatile Aqueous Chlorination Products of Humic Substances", Environ. Sci. Technol. 17:150 (1983).

Moomaw, C., Amy, G., Krasner, S., and Najm, I., "Predictive Models for Coagulation Efficiency in DBP Precursor Removal", Proceedings, AWWA Conference, pp. 221-233 (1993).

Montgomery Engineers, "Disinfection By-Products Database and Model Project", AWWA Project Final Report, James M. Montgomery, Consulting Engineers,Inc. (1991).

Montgomery Engineers, "Effect of Coagulation and Ozonation on the Formation of Disinfection By-Products", AWWA Project Final Report, James M. Montgomery, Consulting Engineers, Inc. (1992).

Oliver, B., and Lawrence, J., "Haloforms in Drinking Water: A Study of Precursors and Precursor Removal", Journal AWWA,. 71:161-163 (1979).

Oliver, B., et al., "Influence of Aquatic Humic Substance Properties on Trihalomethane Potential", Water Chlorination Environmental Impact and Health Effects Vol. 4:1, R.L. Jolley., Ann Arbor, MI: Ann Arbor Science Publishers, Inc., pp. 231-242 (1983).

Ozekin, K., "Modeling Bromate Formation during Ozonation and Assessing its Control", Ph.D. Dissertation, University of Colorado, Boulder (1994).

Qualls, R., and Johnson, D., "Kinetics of the Short-Term Consumption of Chlorine by Fulvic Acid", Environ. Sci. & Technol., 17:692 (1983).

Reckhow, D., and Singer, P., "Mechanisms of Organic Halide Formation During Fulvic Acid Chlorination and Implications with Respect to Preozonation", Water Chlorination: Environmental Impact and Health Effects, Vol. 5 , Lewis Publ., Chelsea, Mich. (1985).

Reckhow, D., and Singer, P., "The Removal of Organic Halide Precursors by Preozonation and Alum Coagulation", Journal AWWA, 76:4:151 (1984).

Rook, J., "Formation of Haloforms During Chlorination of Natural Waters", Water Treat. Exam. 23:234-243 (1974).

Roth, J., and Sullivan, D., "Solubility of Ozone in Water", Indus. Engrg. Chem.Fund., 20:137 (1981).

Siddiqui, M., and Amy, G., "Factors Affecting DBP Formation During Ozone-Bromide Reactions", Journal AWWA, 85:1:63 (1993).

Siddiqui, M., et al., "The Role of Tracer Studies in Relating Laboratory and Pilot Scale Ozonation Data", 11th Ozone World Congress, Volume 1: S-2-45

(1993).

Sotelo, J., et al., "Henry's Law Constant for the Ozone-Water System", Water Research, 23:1239 (1989).

Staehelin, J., et al., "Ozone Decomposition in Water Studied by Pulse Radialysis to OH and HO_4 as Chain Intermediates", Jour. Phys. Chem., 88:5999 (1984).

Tomiyasu, H., et al., "Kinetics and Mechanisms of Ozone Decomposition in Basic Aqueous Solution", Inorg. Chem., 24:2962 (1985).

von Gunten, U., and Hoigne, J., "Bromate Formation During Ozonation of Bromide Containing Waters", 11th Ozone World Congress, Volume 1: S-9-42 (1993).

Wang, H., "Empirically Based Kinetic Models for Predicting the Formation of Chlorination By-Products: Haloacetic Acids", M.S. Thesis, University of Colorado, Boulder (1994).

Weis, J., "Investigation on the Radical HO_2 in Solution", Trans. Faraday Soc., 31:668 (1935).

Zhu, H., "Modeling the Effects of Coagulation on Chlorination By-Product Formation", Ph.D. Dissertation, University of Colorado, Boulder (1995).

☆U.S. GOVERNMENT PRINTING OFFICE: 1999 - 750-101/00015

United States
Environmental Protection Agency
Technical Services Center
Cincinnati, OH 45268

Please make all necessary changes on the below label, detach or copy, and return to the address in the upper left-hand corner.

If you do not wish to receive these reports CHECK HERE ☐; detach, or copy this cover, and return to the address in the upper left-hand corner.

Official Business
Penalty for Private Use
$300

EPA 815-R-98-005